

RRS James Clark Ross JR206 Cruise Report



Volcanic and Continental Slope Processes,
South Georgia and South Sandwich Islands

RRS James Clark Ross JR206 Cruise Report
Volcanic and Continental Slope Processes, South Georgia and South
Sandwich Islands

P.T. Leat, A. J. Tate, T. J. Deen, S.J. Day & M.J Owen

British Antarctic Survey Cruise Report

Falkland Islands – South Georgia – South Sandwich Islands – Halley –
Montevideo

Report of *RRS James Clark Ross* cruise JR206, January-March 2010

BAS Archive Reference Number: ES6/1/2010/1

This report contains initial observations and conclusions. It is not to be cited without the written permission of the Director, British Antarctic Survey.

July 2010

Contents:

Summary

Objectives

Summary narrative for JR206/248

Personnel

Equipment Reports

1. EM120 Multibeam Echosounder
2. Expendable Bathy Thermographs (XBT)
3. TOPAS Subbottom Profiler
4. Neptune
5. Shipboard Three-Component Magnetometer
6. Dredges
7. Box Corer

Details of Surveys

1. Southern South Georgia continental margin
2. South Sandwich Islands
3. Weddell Sea

Summary

Acknowledgements

References

Appendix 1. EM120 log for cruise JR206

Appendix 2. Plotting cruise tracks on the Helmsman display

Appendix 3. XBT locations

Appendix 4. Table of TOPAS lines

Appendix 5. Details of Dredges

Appendix 6. Specimen Register for Dredges

Appendix 7. Proposed Feature Names

Front Page Image: Ice-covered cliffs at Harker Point, Bristol Island

Summary

RRS James Clark Ross cruise JR206 took place from 18th January 2010 to 13th March 2010. It was joined with cruise JR248 (retrieval of oceanographic moorings from the Antarctic margin in the Weddell Sea from 22nd to 25th February) and a logistics visit to Halley. A cruise track is shown in Figure 1. Six days were lost due to a medical evacuation near the start of the cruise which meant that some reevaluation of priorities took place. Surveys of the southern South Georgia margin and the South Sandwich arc were completed in good time, but time for the Weddell Sea work was lost.

Objectives

The main purpose of the cruise was to map the seafloor around the South Sandwich Islands and in parts of the southern continental margin of South Georgia and the continental margin at the mouth of the Thiel Trough in the Weddell Sea to provide a base map for future research in these areas, and in order to understand volcano and continental slope structure, instabilities, and sediment transport processes. The main focus was on mapping the structure of the submarine parts of the volcanoes of the South Sandwich volcanic arc, in order to understand their evolution and to assess hazards from volcano instability, such as debris avalanches and slumps. A secondary focus was on the southern continental margin of the South Georgia continent, where swath data collected on previous passages suggested it may be a site of slope instability. A third planned element, the investigation of the Weddell Sea continental margin around the north of the Thiel (Filchner) Trough was opportunistic, in that the science cruise was joined with a logistics trip to Halley. The Thiel Trough was one of the main dispersal routes for ice and sediment eroded from Antarctica during glacial periods. Yet little is known of the glacial history of the trough, and it was intended to attempt to identify locations of palaeo icestreams and moraines, if time and ice conditions allowed.

The South Sandwich Islands represent a major opportunity for multi-disciplinary research, including volcano evolution, magma generation in a simple intra-oceanic volcanic arc, volcano instability and tsunami generation, biodiversity and evolution in a remote archipelago, hydrothermal vent studies and associated deep sea high temperature biology. The islands are also a significant source of tephra in Antarctic ice cores. Mapping the essential volcanic and bathymetric features of the arc is an essential tool for progression in these areas.

Funding

The cruise was part of the Long-Term Monitoring and Survey (LTMS) Workpackage of the Environmental Change and Evolution Programme (BAS). Funding for participation of Simon Day and Matthew Owen was through a NERC-AFI-CGS grant [Instability of Submarine Volcanoes in the South Sandwich Arc CGS-11/58 (2009) to P.T. Leat, S. Day and M. Maslin].

Summary narrative for JR206/JR248

January to March 2010

The cruise track is shown in Figure 1. Note that the cruise incorporated cruise JR248, which involved recovery of moorings in the southern Weddell Sea, and a logistics visit to Halley to uplift personnel from the Halley VI rebuild.

The initial work along the southern margin of the South Georgia continent went well, in very favourable weather conditions, despite loss of TOPAS for several hours.

Arrival at the South Sandwich Islands was severely delayed by a medical evacuation, which entailed the ship breaking off the transit from South Georgia to the South Sandwich Islands to return to Stanley, Falkland Islands.

Once in the South Sandwich Islands work area, the work went very well, and swath mapping, dredging and TOPAS profiling went according to plan and on schedule in good weather conditions.

The moorings recovery for JR248 was completed on time, including CTD and moorings work in addition to the original plan.

Because of time lost to the medical evacuation, there was no time to do science work in the Thiel Trough area.

High winds at Halley slightly delayed operations there.

On the return trip to Montevideo, we passed back through the South Sandwich Islands, and were able to extend the swath coverage and do extra TOPAS lines on passage.

Date	Julian Day	Notes
18.01.10	18	Sailed from FIPASS, Falkland Islands 13.55 (Z). Lifeboat deployment and training.
19.01.10	19	Passage to southern South Georgia continental margin.
20.01.10	20	Started swath mapping for survey of southern South Georgia continental margin.
21.01.10	21	Swath mapping and TOPAS survey of southern South Georgia continental margin. TOPAS malfunctioned, and several hours lost trying to stabilize it.
22.01.10	22	Continued South Georgia continental margin.
23.01.10	23	Completed South Georgia continental margin. Started passage to northern South Sandwich Islands. Turned back to Falkland Islands for Medical Evacuation at 10.30 (Z).
24.01.10	24	Continued MEDIVAC passage to Falkland Islands.
25.01.10	25	Arrived Stanley Harbour 14.26 (Z) to complete MEDIVAC.

26.01.10	26	Sailed from FIPASS 14.56 (Z).
27.01.10	27	Passage towards South Georgia.
28.01.10	28	Passage towards South Georgia. Started TOPAS lines on passage to supplement survey of southern South Georgia continental margin.
29.01.10	29	Completed TOPAS passage line south of South Georgia, and continued passage to northern South Sandwich Islands
30.01.10	30	Three successful dredges and one TOPAS line on the Protector Shoal seamounts
31.01.10	31	Strong winds prevented work.
1.2.10	32	Hove to till 16.00 (Z). Continued swath mapping around Protector Shoal.
2.2.10	33	Three successful and one empty dredge on the Protector Shoal seamounts. Continued swath mapping of the Protector Shoal area.
3.2.10	34	Completed swath mapping of the Protector Shoal area. TOPAS lines west of Zavodovski. Started mapping Leskov.
4.2.10	35	Completed Leskov, Transit to Saunders Island area, and started swath mapping Saunders.
5.2.10	36	Mapped west and north of Saunders, including plateau north of the island.
6.2.10	37	Mapped east and south of Saunders. Started TOPAS lines on sediment waves east of Saunders.
7.2.10	38	Ran TOPAS lines on sediment waves east of Saunders, surveyed between Saunders and Montagu and to the west of Montagu.
8.2.10	39	Mapped around summit area of Montagu. Completed mapping between Saunders and Montagu.
9.2.10	40	Mapped south of Montagu and started TOPAS lines east of Montagu.
10.2.10	41	Completed TOPAS lines east of Montagu. Mapped around summit area of Bristol and the area north of Bristol.
11.2.10	42	Continued to map around Bristol.
12.2.10	43	Mapped around summit area of Southern Thule.
13.2.10	44	Investigated crater 'Resolution Caldera' to the east of Cook, ran TOPAS lines between Southern Thule and Bristol, and continued swath mapping around Southern Thule.
14.2.10	45	Completed swath map of Southern Thule.
15.2.10	46	Ran a swath from Southern Thule to the south of the Sandwich plate, and started to fill the southern part of the volcanic arc towards Kemp seamount.
16.2.10	47	Mapped the previously unknown 'Adventure' caldera east of Kemp seamount, and the seamounts northwest of Kemp.

17.2.10	48	Overnight mapped the eastern margin of the arc terrain and Nelson seamounts. Dredged the caldera east of Kemp, and ran a TOPAS line across sediment waves on its SW flank. Started the fill in the remaining area of the southern arc terrain.
18.2.10	49	Swath mapping of southern arc terrain.
19.2.10	50	Completed work on the South Sandwich arc. Started transit of Weddell Sea to moorings site for JR248.
20.2.10	51	Transit of Weddell Sea.
21.2.10	52	Transit of Weddell Sea.
22.2.10	53	Transit of Weddell Sea through mostly open ice. Swath and ADCP survey for JR248.
23.2.10	54	Started work on JR248 moorings.
24.2.10	55	Continued JR248 moorings.
25.2.10	56	Finished JR248 moorings.
26.2.10	57	Transit to Halley.
27.2.10	58	Arrived at Creek 3 at Halley. Bad weather forced move away from the sea ice in the evening.
28.2.10	59	Waited for weather to improve off Creek 3.
1.3.10	60	Waited for weather. Moored at Creek 3 in the evening.
2.3.10	61	Completed Halley relief. Started transit north.
3.3.10	62	Transit of Weddell Sea.
4.3.10	63	Transit of Weddell Sea.
5.3.10	64	Collected swath and TOPAS data on transit north through South Sandwich Islands.
6.3.10	65	Collected swath and TOPAS data on transit north through South Sandwich Islands.
7.3.10	66	Completed transit to east of South Sandwich Islands and started transit to Montevideo.
8-13.3.10		Transit to Montevideo.
13.3.10	72	Arrived Montevideo

Personnel

Officers and crew for JR206

BURGAN, Michael JS	Master
MARKHAM, Howard	Chief Officer
PAGE, Timothy S	Chief Officer
BEYNON, Euan D	2nd Officer
WYLES, Spencer Riches	3rd Officer
GLOISTEIN, Michael EP	ETO Comms
ANDERSON, Duncan E	Ch Engineer
ELLIOTT, Thomas R W	2nd Engineer
STEVENSON, James S	3rd Engineer
WILLETTS, John	4th Engineer
WALE, Gareth M	Deck Eng
MCMANMON, John P	ETO Engineer
TURNER, Richard J	Purser
PECK, David J	Bosun
BOWEN, Albert Martin	Bosun's Mate
CHAPPELL, Kelvin E	SG1
RAPER, Ian	SG1
DALE, George A	SG1
ESTIBEIRO, Anthony JJ	SG1
TRIGGS, David William	SG1
PHILLIPS, David A	SG1
REID, James Stephen	MG1
SUMMERS, Jeremy N R	MG1
HUNTLEY, Ashley Alan	Chief Cook
LEE, Jamie Edward	2nd Cook
JONES, Lee J	Sr Steward
GREENWOOD, Nicholas R	Steward
RAWORTH, Graham	Steward
WEIRS, Michael	Steward
GREGORY, Joanna Mary	Doctor

Scientific party

LEAT, Philip Timothy	BAS Geoscientist (PSO)
DEEN Tara Joy	BAS Geoscientist
TATE, Alexander James	BAS Geoscientist
KLEPACKI, Julian Z	BAS (Antarctic and Marine Engineering)
LENS, Peter C D	BAS (IT Support)
DAY, Simon John	University College London Geoscientist
OWEN, Matthew John	University College London Geoscientist
BEATON, John	Scottish Association for Marine Sciences (JR248 oceanographer)
CHAVANNE, Cedric P G	University of East Anglia (JR248 oceanographer)

Equipment Reports

The main equipment used was the EM120 multibeam echo sounder on the RRS *James Clark Ross*. We also dredged volcanic features to yield samples for geochemical analysis, and used sub-bottom profiling (TOPAS) to determine structures and sedimentation processes.

1. EM120 Multibeam Echosounder

The Simrad EM120 acquisition system performed well throughout the cruise with no major downtime. A log of EM120 operations during the cruise is presented in Appendix 1. The following paragraphs summarize operational parameters, observations and small issues that occurred from time to time for the benefit of future cruises.

The main survey locations of JR206 are areas of high relief that provide challenges for data acquisition. Survey planning prior to the event was possible for the deeper areas but it was not possible to predict the number of lines required to fill in the shallower seamount areas or those areas close to the islands themselves. As with the JR168 survey, the practice of circumnavigating the islands individually worked well. However in contrast to JR168, circumnavigations usually started at the shallowest point and worked out towards deeper water.

In terms of operational parameters, angular coverage was set to “manual” and beam spacing set to “equidistant”. Beam angles varied according to sea conditions and seabed morphology but were generally 60 – 65 degrees. Yaw stabilization was off. While this parameter (when on) provides a more even spacing of beams when changing heading it makes it very difficult to clean the data ping by ping as we did this cruise. All other parameters were left in their default settings. Sound velocity profiles were obtained from XBT data and were input into the acquisition software making use of a custom BAS script. To invoke the program, press the middle mouse button on a clear piece of the background desktop and select “Start SVP Upload Interface”. Overlap between swath lines was achieved using the Helmsman Display on the bridge and overlap was generally around 10 percent of swath width. As we had pre-existing areas of swath coverage, it was useful to provide polygons outlining these areas on both the Helmsman Display and the Microplot 7 navigational display. Appendix 2 describes the steps required to do this.

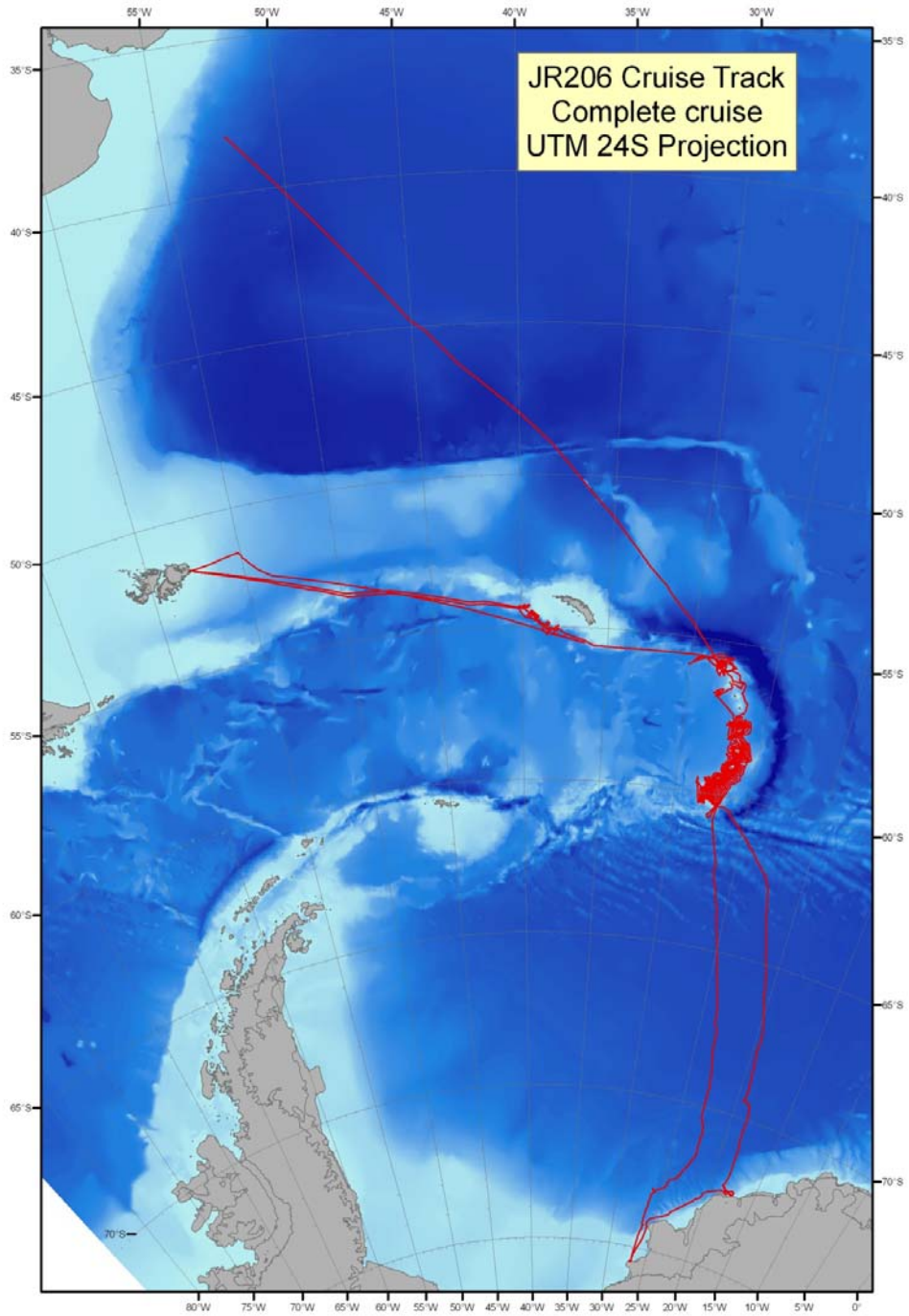


Figure 1. JR206 cruise track

The cruise was split up into 11 bathymetry surveys:

JR206_a was the initial transit between Stanley, FI and the South Georgia shelf area and then the subsequent transit from Stanley to South Georgia after the medevac (see JR206_c). Both transits were chosen to give extra opportunistic swath across the Scotia Sea.

JR206_b was a variety of small areas on the southern margin of South Georgia. These were primarily to fill in small gaps of coverage whilst undertaking a TOPAS survey of this area.

JR206_c was initially going to be the transit from the South Georgia area to the South Sandwich Islands. However, within the first few hours the ship returned to Stanley for a medevac. The transit covered limited unswathed areas but through necessity overlapped with a large amount of previously swathed areas.

JR206_d was the transit between the southern margin of South Georgia to the northern part of the South Sandwich Arc.

JR206_e was a collection of areas around the Protector Shoal area, Zavodovski Island and Leskov Island.

JR206_f was an extensive survey of Saunders and Montagu Islands from approximately 250m depth to around 2500m depth.

JR206_g was an extensive survey of Bristol and Southern Thule/Cook/Bellingshausen Islands from approximately 250m depth to around 2500m depth. It also included a shallow caldera between Cook and Bellingshausen Islands.

JR206_h was a survey of the Kemp and Nelson Seamounts and the shallow bank between them. It deliberately avoided the western extent of the Kemp edifice as this was previously surveyed on JR224. It included crossing the South Sandwich Trench.

JR206_i was the transit between the South Sandwich Arc after crossing the trench until reaching Halley and then transiting north back to the South Sandwich Trench. It includes swath along an AFI mooring line collected on behalf of JR248.

JR206_j was a transit line north along the South Sandwich Arc. It extended the swath already collected out to the east. It also included a shallow seamount to the west of Saunders Island that was not fully surveyed during the jr206_f survey.

JR206_k was the transit north from the northern end of the South Sandwich Trench to Montevideo.

Weather was rarely an issue for the operation of the EM120 throughout JR206. Poor data was acquired for a period of survey jr206_e (31st Jan – 1st Feb 2010) and for the last few hours of survey jr206_h. However all the main island surveys were completed in calm weather with the ability to swath on any given heading.

When surveying in steeply dipping shallow areas there was a tendency for the EM120 to lock onto false multiple returns on the upslope side of each ping. This was countered by forcing the depth to a value equal to the shallowest part of ping. As the EM120 does not return data from throughout the water column, if a false bottom is consistently found it leaves a large data gap. An example of this is shown in Figure 2 below showing six pings in

succession from the northern slope of Montagu Island. Ping numbers are 168-173 from bottom to top of the figure, the centre beam depth is ~420m and the slope is ~25 percent.

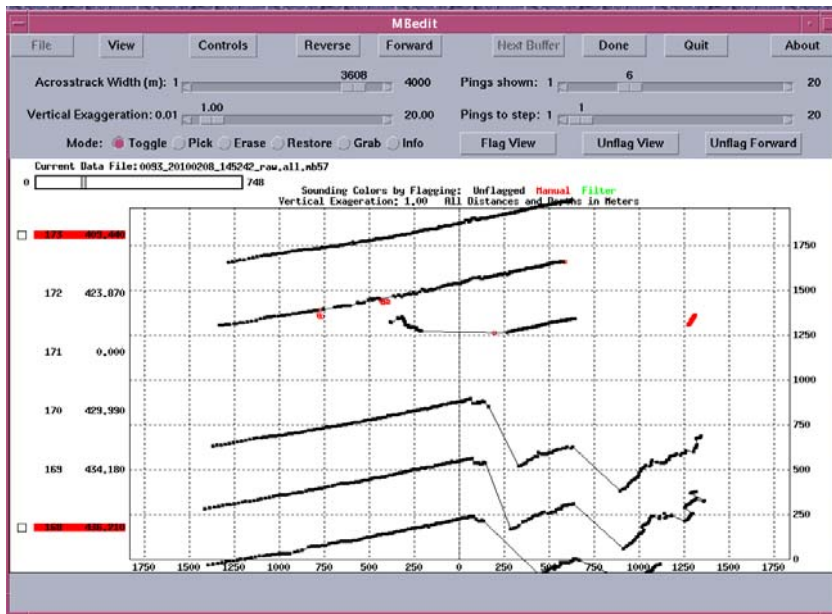


Figure 2. Display from mbedit.

The following steps were taken in this case.

- 1) Prior to ping 168, there had been several returns showing false multiples on the upslope side of the ping. It is always worth allowing a couple of bad returns to allow the EM120 to correct the error itself. However, this did not occur in this instance and the depth was forced to 300-350m (under the MBES window of the acquisition software). Several more pings (169-170) were received before this forcing takes effect.
- 2) Ping 171 shows that the upslope portion of the ping has been resolved again but to the detriment of the downslope portion which is not resolved.
- 3) Ping 172 shows the whole slope is now resolved although there is a tendency for the majority of the returns to be amplitude (displayed as blue in the EM120 ping window) related and the return can be quite noisy. Pings 171 and 172 show the downside of this method as it produces two suboptimal returns in order to regain the upslope component.
- 4) Ping 173 shows a normal return with both amplitude and phase returns. The process is then repeated when false multiples are evident again.

At various times the acquisition system appeared to freeze with no updates occurring in the profile window. Very occasionally this was due to an abnormally long wait time from either the EM120 or the EA600 (bridge single beam echosounder) before repinging. The more likely situation is that the EM120 locked onto noise near the hull (5-10m). This tends to happen in rougher weather or when surveying highly variable shallow bathymetry. Forcing the depth can help but sometimes stopping and restarting the EM120 is the best solution for this behaviour. There were also infrequent occurrences of a series of pings missing either

port or starboard beams. This rarely continued for more than 10 pings and in all instances corrected itself before intervention was necessary.

A previously known issue regarding the bottom detection range of the EA600 resurfaced on JR206. When the EA600 is controlled by the SSU (Simrad Synchronization Unit) it passively listens for the centre beam return of the EM120 and when it detects the seabed (i.e. displays a depth at the top of the screen) it awaits the next trigger. However, in rough weather or when the return is not clear, the EA600 may not record a depth and in this instance it will 'listen' through the entire length of its bottom detection range as set by the bridge officer on watch. In deep water, this is rarely an issue as the time taken to get a full ping return to the EM120 is always longer than the EA600 whatever the setting of the bottom detection range. However, in shallow water, the EA600 may take a significant time to give control back to the SSU if it is set to >1000m values. There were occasions on JR206 when the EM120 was ready to reping after a second but the EA600 was taking 4-5 seconds before giving back control. The only safe solution to this issue is for the officer on watch to change the EA600 bottom detection range to more closely match the actual depth. The EM120 operator has to be aware of this as the issue may not be immediately clear to the officer on watch as they could well have a readable echogram. If the SSU shows the EA600 is taking longer than the EM120, then it is almost certainly the EA600 bottom detection range that needs changing. For reference a red line on the SSU indicates an active listening period, while a green line indicates a waiting for next command period.

On several occasions the survey line number did not automatically change over after an hour. It was generally spotted after several hours and manually changed (stop and then start logging). There are recorded instances of this in several previous cruise reports but this is the first time it has been seen in a number of years. While it would not have gone unnoticed on JR206, it is an issue for opportunistic surveys where the lack of a dedicated swath operator could lead to survey files of hundreds of hours.

Data processing

Raw data were automatically copied from the em120 acquisition machine onto the Neptune workstation in one-hour files to the path:

```
/data/cruise/jcr/current/em120/raw/'survey name'
```

where current is a symbolic link to the leg id 20100118 (date the cruise started - YYYYMMDD)

Data were processed with MB System v5.1.0 and v.5.1.1 following the same general procedures detailed in the JR93, JR134 and JR168 cruise reports. MB can be setup by typing,

```
setup mb
```

```
setup gmt
```

GMT is needed for several of the MB System subroutines and is worth setting up at the same time. Type, `'man mbsystem'` for an overview of MB.

Copying the data and producing auxiliary files

The perl script `mbcopy_em120` was used to copy raw EM120 data into MB system format and produce auxiliary files. To run the script type,

```
setup gsd  
  
mbcopy_em120
```

from a Unix command line. You will be asked several questions regarding the raw data location, the desired location of the copied data and whether you want all the lines copied (type 'n' if you are actively acquiring data and the script will not copy the last hour file as it will not be complete). This information will be stored in a defaults file in your home directory and will not need to be re-typed until you change survey names. Note that the script will check for lines already copied and will ignore these. You can however, force the script to start at a predetermined line number if you do not want the earlier line numbers copied.

Cleaning the data

All of the data cleaning was done manually using the `mbedit` graphical interface. This allows the user to manually flag data in either a ping-by-ping view or as a waterfall view where n number of pings can be viewed together. Detailed editing was done using the ping-by-ping view for each hour file followed by a quick look using the waterfall view to check for any erroneous depth values missed.

Cleaning the data creates two additional files, a `.esf` file which holds the flagging information and a `.par` file which contains a whole variety of edits including cleaning and navigation fixes. Navigation data was not a problem during JR168 so did not need fixing.

Processing the data

The command `mbprocess` takes information from the `.par` file and processes the `.mb57` data to produce a final output file. If the input file is called `data.all.mb57`, the processed file becomes `data.allp.mb57`. `mbprocess` also creates additional auxiliary files (`.inf`, `.fnv`, `.fbt`). The command takes the form of:

```
mbprocess -Iraw_datalist -F-1
```

A text file containing the names of all the processed data can then be created (`proc_datalist` on this cruise, i.e. type, `'ls *.allp.raw.mb57 > proc_datalist'`). If at some point the user decides to go back and re-clean the data or edit the navigation for a single file, `mbprocess` can be run with the same command and it will process only the newly edited files.

To recap the processes and the files they create are:

Input	Process	Output
Data.all.raw	mbcopy	Data.all.raw.mb57
Data.all.raw.mb57	mbdatalist	Data.all.raw.mb57.inf
		Data.all.raw.mb57.fbt
		Data.all.raw.mb57.fnv
Note : The above two processes are combined in the script em120_mbcopy		
Data.all.raw.mb57	mbclean/mbedit	Data.all.raw.mb57.esf
		Data.all.raw.mb57.par
Data.all.raw.mb57	mbnavedit	Data.all.raw.mb57.nve
		Data.all.raw.mb57.par (modified)
Data.all.raw.mb57	mbprocess	Data.allp.raw.mb57
		Data.allp.raw.mb57.inf
		Data.allp.raw.mb57.fbt
		Data.allp.raw.mb57.fnv

Gridding the data

The command *mbgrid* with its associated options produces a user-defined grid for viewing the cleaned swath results. Data was output directly to ArcGIS ascii grids as ArcGIS was the primary software tool used to view the grids. One of the limitations of ArcGIS grids is the need for matching x and y grid resolution. Hence, it was necessary to use identical values in degrees (usually 0.001 or 0.002) that are unequal in distance, particularly at high latitudes. A grid resolution of 0.002 degrees is approximately equal to 62m (longitude) x 111m (latitude). The command and some of the more common options used are:

```
mbgrid -Iproc_datalist (can be ../ etc if in another directory)
-O'grid filename' (naming scheme - 'surveyname_resolution' e.g.
jr206_a_200m. A suffix is automatically added)
-R-29/-26/-57/-55 (bounding co-ords, min long/max long/min lat/max
lat. Note that MB v 5.1.1 will default to the maximum extent of the
input files. This is very useful for survey overviews. No -R flag is
needed in this case)
-E0.002/0.002/degrees! (grid resolution; 0.002 degrees in this case.
! forces the resolution by changing the extent slightly if
necessary.)
-G4 (Specifies an ArcGIS ascii grid output)
-A2 (produces a grid with bathymetry as negative values)
-F1 (type of filter used; 1=gaussian weighting, 2=median weighting)
-C5 (spline interpolation into data free areas, ~500m in this case
(grid resolution x 5)
-M (produces two further grids; one giving the number of beams
within each grid cell and the other giving the standard deviation of
those beams in each grid cell)
```

Ascii xyz files were also produced from the cleaned data using the command *mblist* and the following options

```
mblist -Iproc_datalist -F-1 -D2 > survey_name.mbxzy
```

-D2 is the output format (simply X,Y,Depth) and the output text file can be called anything you like. The file suffix 'mbxyz' was used to avoid confusion with Neptune 'xyz' files produced on previous cruises.

The mbxyz files can be used as an input to the GMT nearneighbor command or any other gridding software that accepts ascii xyz files.

Generated ascii grid files were converted into ArcGIS binary grids using the ArcGIS tool 'Ascii to raster'. They could then be viewed and manipulated using ArcGIS v9.3.1 and this proved a very useful tool for finding data spikes that needed further cleaning. This was done by both visual inspection of the bathymetric grid and identifying anomalies within the standard deviation grid. In general all survey files that caused standard deviations above 120m within a 0.002 degree grid cell were inspected again and cleaned if necessary. This provided a very robust way to identify spikes and false multiples that had not been seen at the cleaning stage. It was considered that standard deviations lower than 120m could be real in areas of high variability or more likely random noise in the outer beams that would average out in the grid itself.

File Structure

A common file structure was created to hold all the mb data located under

```
/data/cruise/jcr/20100118/work/mb/'survey_name'
```

Each survey_name (e.g. jr206_a) directory contains processing, grd and mbxyz subdirectories. The processing directory holds all the copied mb57 raw files, the edits and the processed mb57 files. The grd directory holds any GMT grids or ArcGIS ascii grids while the mbxyz directory holds the xyz text output.

Recommendation for MB system v5.1.1

In areas of great depth variation it was necessary to keep changing the horizontal scale and vertical exaggeration within the mbedit window. It would be desirable for the software to best fit the displayed pings to the window automatically. An option would allow the best fit of all beams or just those that are unflagged. It might also be possible to remove the first order trend from the data to allow easier viewing of the steep slopes encountered on JR206.

2. Expendable Bathy Thermographs (XBT)

XBTs were used where necessary throughout the cruise to provide the correct sound velocity profile for the EM120. In the main survey areas around the South Sandwich Islands there was very little difference in water column properties and only 6 XBTs were needed. As in previous cruises, we used archive XBT data collected on previous cruises when launching an XBT would have been impractical such as in rough weather. A full list of XBT locations deployed for this cruise can be found in Appendix 3.

3. TOPAS Sub-bottom Profiler System

Significant useful data were obtained using the TOPAS sub-bottom profiler system during the cruise, although in many areas strong reflectors close to the seabed restricted useful imaging to the top 20 – 30 ms TWTT of the sequence; the maximum depth of structures imaged was as much as 125 ms TWTT. Appendix 4 lists the TOPAS files.

Once acquired the TOPAS data was reviewed using the SIMRAD software TOPAS MMI 1.2. This package provides a useful reviewing tool, however, its functionality is fairly limited when considering interpretation and image output. In order to obtain a digital image of the line it is possible to print to file, however, the resolution is poor. In order to maximise the resolution whilst providing an overview of the TOPAS data a method was devised to produce mosaiced images of TOPAS lines. If attempting to export images from the TOPAS system it is vital not to zoom the image prior to printing as this will result in a lower resolution. The method is as follows:

- Replay TOPAS file and set the display parameters as desired.
- Set the view window to the upper 250 ms (e.g. 500 to 750) of the data. Click File > Print > Print Screen and set the printing limits to the same (e.g. 500 to 750). Then once presented with the print options select the PDF printer.
- Click Properties > Edit. This will allow you to change the pdf settings. On the first page increase the print resolution to 4000 dpi (maximum), then click the images tab. This will open a new page with the image downsampling and compression. For each of the options turn the settings to 'OFF'. This will maximise output resolution. You can then save your settings for future use.
- Continue and print. The resultant file should be of 1.84 MB size, this was found to be the maximum possible.
- Repeat this for each 250 ms section of the file. It was found useful to have a name of structure: [TOPAS line]_[File number of line]_[time range of file] (e.g. Line26_1_250-500.pdf).
- Once all images are exported it is possible to recombine them in a graphics package such as illustrator.
- Keeping a note of the total line length and vertical distance of the line it is also possible to scale the line to a known vertical exaggeration. If desired it is also possible to adjust the horizontal scale to ping rate changes.

3.a. TOPAS Sub-bottom Profiler System: $\pm 50V$ TOPAS PSU Error

Operation of the system was disrupted on several occasions, and the range of operating parameters severely restricted, by a fault associated with the charging of the profiler capacitors. Communications within the system also failed on one occasion, but that fault was rectified by shutting down and rebooting the Sun workstation used to control the

TOPAS system. The Power Supply Unit (PSU) error failure was much more serious and is therefore discussed in detail here.

Symptoms

The TOPAS was operated in chirp mode, appropriate to the 1000 - >2000 m water depth in which the work was taking place, without problem during the transit from the Falklands to South Georgia. At this time the system was being operated at the same time as the EM120 and ping intervals were accordingly large, in the range 4000 ms to over 10000 ms; chirp pulse duration was 15 ms, or less than 0.5% of the ping interval and power was set at 100%. At 11:11 UTC on 21st January, when the system was being operated on its own for the first time in the cruise, the ping rate was increased (to once every 1000 ms at 100% power) to optimise operation by increasing the effective lateral resolution of the profiles in areas of steep seabed terrain. After a short while, pinging was interrupted by the system and the user interface indicated a fault with the 50V power supply(s). This fault implies that the required 50V voltage level dropped sufficiently so as to reduce the amplifiers capacity to meet its configured requirements (ping rate/power output). The indicated fault manifested at minimum as 'missed' pings (typically 2 out of every 5) and at worst the 50V supply would automatically shut down. Resetting the system would briefly rectify the situation before 50V shutdown would occur again. On two occasions the 240V mains source fuse blew. Reducing the ping rate (to once every 2000 ms, so that the 15 ms chirp pulse duration was only 0.75% of the ping interval, as compared to the recommended maximum of 2% of ping interval) and the power output to 90% of maximum restored stability to the system but significantly reduced the quality of the data obtained.

Investigations

Previous cruise reports JR75, 77, 78, 104 and 142 had indicated the same problem. On those occasions no fault was found, other than on one occasion blown fuses on amplifier boards. The system was reported to revert back to normal operation independently.

The 50 volt power is supplied to the capacitor charging bank by four 50V power supplies and these were initially suspected as the source of the fault. JR206 investigations showed no blown fuses on any of the power supplies, nor on any of the 16 amplifier boards. Indication of the power supplies voltage (50V) was shown to be acceptable, i.e. above the fault level of 46-48 volts, even under load (transmission). Each 50V supply unit was in turn replaced with a spare unit. This made no difference to the problem when the system was operated at high ping rates; the TOPAS user interface still indicated a 50V fault and missing pings or shutting down of 50V supplies occurred after a short while in operation. In contrast, stability was consistently restored by operating the system at reduced power (90%) and reduced ping rate (maximum of 1 ping every 2 seconds).

When contacted, the TOPAS technical support engineer at Kongsberg stated that operation above 90% power did not improve results, and in some cases could prove detrimental and was ill advised. It was also stated that pulse length could contribute to the fault if too long, by stressing amplifier capabilities. It was advised that chirp pulse length be restricted to 15

ms or a small fraction of ping interval (see below). Also stated was the possibility of amplifier capacitor banks being degraded over time (the system on the JCR has been in use for some 10 years), resulting in an inability for the capacitors to be charged to the level required for operation at the transmission parameters used in high ping rate operation. It was suggested that insufficient capacitor charging could manifest itself as reduced voltage levels in the PSUs, and thus the fault indicated by the user interface.

Despite further investigation, no physical fault could be found with the system: no further blown fuses were found and all the 50V supply units were found to be functional. However, the electrolytic capacitor banks were not checked, as this requires specific instrumentation and was not possible with the equipment available on board.

Restricted operation of the TOPAS system.

The TOPAS system was not required from 23rd January to 29th January. During this time the spare 50V supplies fitted were removed and replaced with the original set. The system was used again for several periods later in the cruise operating at 90% power and in general with a 2 second ping interval and 15 ms chirp pulse length, without further problems. It was also found that increasing both the ping interval and the pulse length, for example to 4 seconds and 30 or 35 ms respectively (thus keeping the pulse length / ping interval ratio well below 1%), was a possible alternative mode of operation: this was used in some specific cases where increased depth of acoustic penetration below the seabed was required and the loss of horizontal resolution implied by the reduced ping rate was acceptable.

During the 28th of February when waiting to take on passengers at Halley the opportunity was taken to test the operation of the TOPAS system.

The system was tested at ping intervals of 0.5, 1.0, 2.0 and 4.0 seconds and at different duty cycles (chirp pulse length divided by ping interval). The aim being to find at what point the system fails and, by inference, at what level the system is stable. During the course of these tests the system failed frequently after periods of between three and ten minutes. Once estimated stable parameters were obtained these were then tested for periods of over an hour.

It was found that a 1% duty cycle could be operated at 90% power and a 2% duty cycle at 50% power. 1.5% duty cycle seemed stable at 60% power. For instance if a ping interval of 1.0 s is desired the chirp pulse maybe not greater than 10 ms if the system is operated at 90% power (as may be required in deep water). However, if the power is reduced to 50% then the chirp pulse length may be increased to 20 ms at a 1.0 s ping interval. Overall, however, restriction of TOPAS operation to source parameter ranges that were well below the design rated limits, broadly by a factor of 2, was felt to be unsatisfactory.

Recommendations

For the present, when pinging more frequently than one every 4000 ms, the TOPAS system should only be used at 90% power or less and with the restrictions on pulse length and ping interval noted above. However, in view of the impact of these restrictions upon the quality

of data obtained with the system during JR206, and the definite possibility that the problem will worsen as the system ages, it is strongly recommended that service and testing of the TOPAS by Kongsberg be carried out at the next available period, with particular attention being paid to the capacitor banks.

4. Neptune

Neptune was used throughout the cruise for underway visualisation of swath bathymetry data. Neptune reads all files in a current survey except for the one currently being written to. To look at the most recent data, logging on the EM120 system was stopped and restarted to close the active file. It is important to remember that the Neptune system does not access the raw swath data on the EM120 system directly, but reads a copy which is automatically created every 10 minutes. Consequently it may not be possible to read the most recent swath file until 10 minutes after it has been written.

No problems were encountered with the Neptune system.

5. Shipboard Three-Component Magnetometer

The Shipboard Three-Component Magnetometer (STCM) acquired data continuously throughout the cruise. No problems were observed. Data are collected and included in the Seatex data logging stream. The system records time, latitude, longitude, x, y and z components of the magnetic field and a calculated total field.

5.1. Extracting data from the Seatex data streams

Data are extracted from the streamstate files using the rvs software (on the unix system, type `setup rvs`). RVS will default to reading the current cruise on the ship; in Cambridge it will prompt you to choose a suitable cruise from those available. To see what data streams are available in rvs, once it has been set up, type `lookc`. Typing in the command `var`, followed by any of the data streams listed (i.e., `var bestnav`) will give a list of the variables available for that data stream. Data are extracted using the command `listit`, with a command of the following format:

```
listit -sYYDDHHMM -eYYDDHHMM -i60 stream var1 [var2...]
```

Where `-s` is the start time for the stream, `-e` is the end time for the stream (omit to obtain the entire stream), `-i` dictates the sampling interval in seconds, `stream` is the data stream required and `var` indicates the required variables. For example, to obtain the navigation data from the stream `bestnav` at 10 minute intervals, type the command:

```
listit -i600 bestnav lat lon >latlon.asc
```

6. Dredges

Dredges were conducted over the stern of the ship using a dredge consisting of a chain bag and attached bucket, with an acoustic pinger attached 200 m up the dredge cable to monitor dredge position relative to the seabed. Some problems were initially encountered in operation of the pinger because of a lack of user documentation on board. A minor (but welcome!) problem resulting from the wide variety of rock types collected at Protector Shoal was a shortage of sample bags in which to separately store different rock types: various waterproof sample containers were found on board, but in future it would be better to plan for success in dredging sites that may contain a wide variety of rock types (such as the volcanoclastic sites at Protector Shoal), and begin with a larger supply of sample bags including smaller bags for individual distinctive clasts.

7. Box Corer

The box corer was not used because of the cancellation of the scheduled work in the Thiel (Filchner) Trough area.

Details of Surveys

1. Southern South Georgia continental margin

The South Georgia continental block (or micro-continent?) is located at a compressional bend at the strike – slip plate boundary between the South American Plate and the Scotia Sea Plate (Cunningham et al., 1998). The sedimentary basins on the southern margin of the block, although originally formed by Scotia Sea extension, may therefore be experiencing active transpressional deformation. A recent study based upon compilations of bathymetric data from the shallow shelf (Graham et al. 2008) indicates that during glacial maximum conditions a local ice cap may have extended out to the margins of the South Georgia continental shelf. If correct, this would have a strong effect upon sedimentation in the basins to the south; such as an overall very high sediment input rate and the development of glaciogenic debris flows comparable to those developed on passive continental margins (for example, the Barents Sea margin; Dowdeswell et al. 2002). The combination of active transpressional tectonics and glacial influence is unusual and the South Georgia region offers an opportunity to examine the interaction of the two in the patterns of sedimentation and slope instability within the marginal basins along the south side of the South Georgia micro-continent.

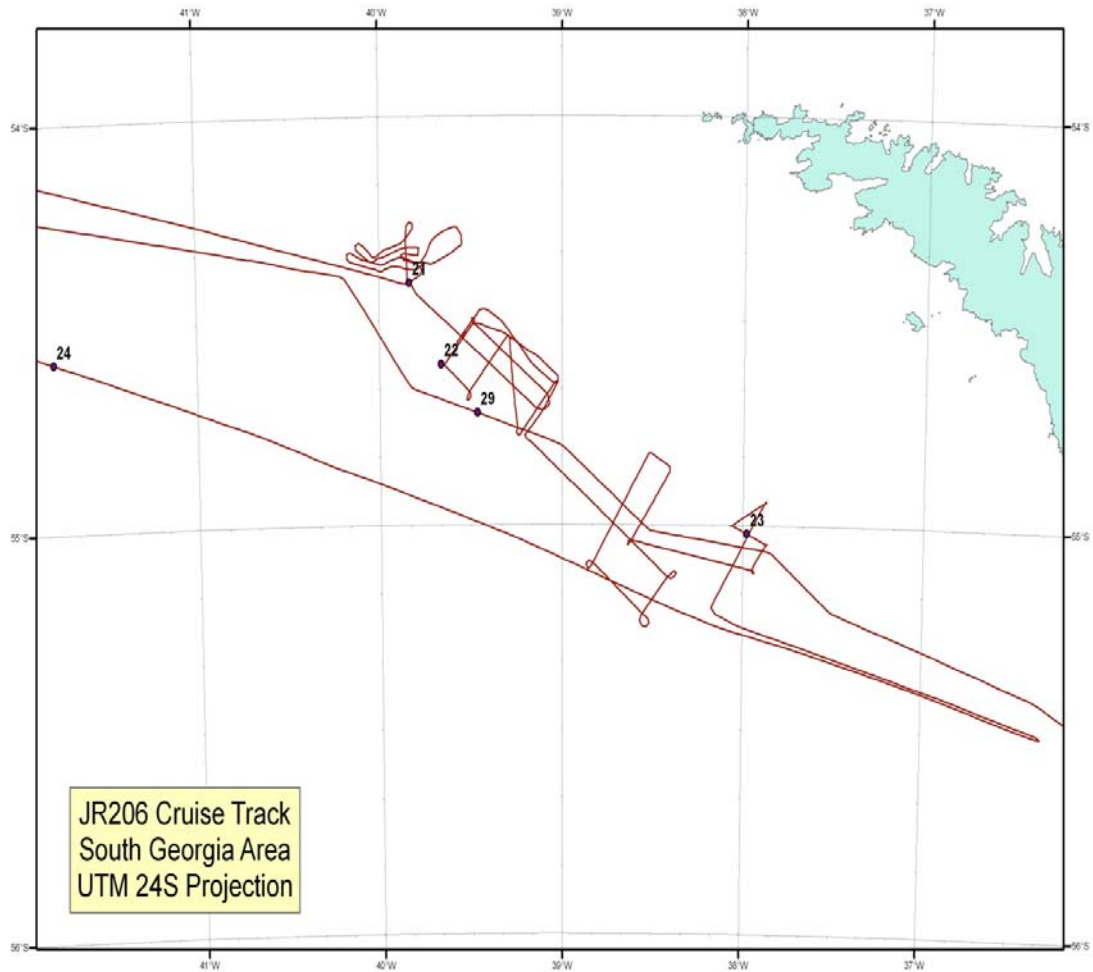


Figure 3. Cruise track for JR206, southern continental margin of South Georgia.

The objectives of the work along the South Georgia continental margin were therefore to map out the bathymetry of the main marginal basin using the EM120 system; use this bathymetry to define sites of sediment input, slope instability features, and the structure of the basin including active fault scarps; and then use the TOPAS profiler system to investigate patterns of recent sedimentation and how they relate to the bathymetric features.

1.1. Bathymetric mapping.

Multibeam sonar swath mapping between previous swaths of data, collected on passages along the south side of the South Georgia micro-continent margin, produced a complete bathymetric map of the elongate, broadly WNW-ESE trending basin around 150 km long and 50 km wide, between approximately 54.3° S, 39.7° W and 55.3° S, 38.0° W. The cruise track is shown in Figure 3, and bathymetric data are presented in Figure 4, along with the positions of the TOPAS profiler lines discussed in section 1.2 below.

Note on name: Endurance Basin

We propose to name this feature Endurance Basin, after the ship used by the explorer Ernest Shackleton. South Georgia was the ship's last port of call before it was lost off the Antarctic Peninsula. Later ships of the same name have been used for extensive survey and research work around South Georgia.

The northern margin of the Endurance Basin is formed by a series of steep slopes and intervening troughs rising some 3000 m to the shelf edge. Individual slope segments trend slightly oblique to the basin and are linked by SE-facing ramps and slopes. These features were interpreted as a left-stepping *en echelon* array of oblique, left-lateral strike-slip fault scarps with intervening elongate highs and small basins. Where they intersect the basin floor some of the main faults curve into subtle N-S trending scarps and ridges (interpreted as reverse faults and compressional fault arrays) that divide the basin into at least three sub-basins with near flat floors and slightly different seafloor depths. A number of large landslide scars were identified cutting the steep northern margin of the basin, but no associated debris deposits or slide blocks were identified on the basin floor from the bathymetric data, suggesting that the scars are relatively old and deposits from them are buried beneath basin-floor sediments.

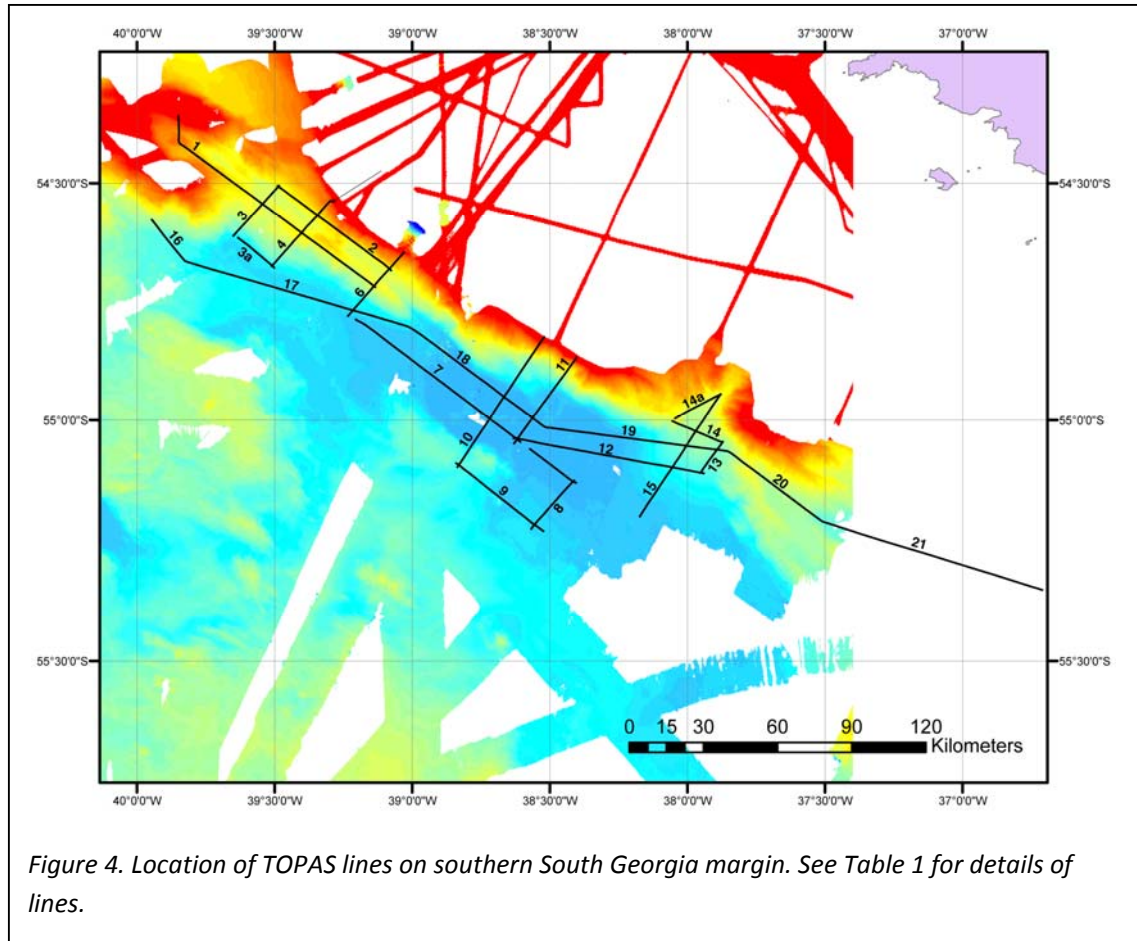
The southern margin of the basin consists of a series of *en echelon* scarps up to a few hundreds of metres high, that are also left-stepping and linked by E-W trending scarps. The latter are interpreted as normal faults, being orthogonal to the basin-crossing compressional ridges. The WNW end of the mapped basin steps south-westward into further, slightly shallower water depth basins; the eastern end is bounded by a scarp and fan (with an area of at least 420 km²) system at the mouth of a canyon cutting the micro-continent margin. The canyon coincides with the only shelf trough, interpreted as the pathway of an ice stream, to be identified on the south side of the micro-continent by Graham et al. (2008). The northwestern side of the fan is cut by a channel and canyon system inferred to be the currently or most recently active sediment pathway from the shelf to the basin, whereas the crest of the fan is occupied by a topographically subdued channel system that is inferred to have been abandoned. This geometry is consistent with the left-lateral geometry of strike-slip faulting along the margin, as South Georgia and the shelf trough are moving NW with respect to the basin and the fan.

1.2. Sub-bottom profiling.

A total of 647 km of TOPAS sub-bottom profile lines were obtained in the basin and on the adjacent slopes (see Table 1 for details). Their positions are indicated in Figure 4. Broadly, the lines can be grouped into:

a). Long lines along the axis of the basin. These include lines 7 and 12; and lines 16-20 which together form a single stepped line and were obtained during the eastward transit through the basin to the South Sandwich Islands on 28th-29th January following the medevac return to Port Stanley.

b). Three groups of shorter lines whose positions are indicated in Figure 4. The latter include: short lines along or across faults and small troughs around the periphery of the basin; lines orientated transverse to the main basin, in its central part (lines 8, 10 and 11); and lines crossing the submarine canyon and fan system at the southeastern end of the basin.



TOPAS line number	Brief line description	Time start of line	Vessel speed (kts)	Ping interval (ms)	Start frequency Hz/ Stop frequency Hz/ Chirp pulse length (ms)	Length (km)
JR206_TOPAS_01		21/01/2010 10:21:23	10	External	1500/5000/15	64.218
JR206_TOPAS_02	Run with EM120	21/01/2010 14:13:04	10	External	1500/5000/15	33.444
JR206_TOPAS_03	Perpendicular to western fault system	21/01/2010 16:15:09	6	1250-2000	1500/5000/15	16.478
JR206_TOPAS_03a	Recorded in transit to line 4	22/01/2010 00:11:59	6	2000	1500/5000/15	11.063
JR206_TOPAS_04	Perpendicular to western fault system	22/01/2010 01:43:25	6	2000	1500/5000/15	21.085
JR206_TOPAS_06		22/01/2010 05:06:27	6	2000	1500/5000/15	20.245
JR206_TOPAS_07	Parallel to margin through basin	22/01/2010 07:57:47	10	7000	1500/5000/15	61.598
JR206_TOPAS_08		22/01/2010 11:47:47	10	7000	1500/5000/15	14.964
JR206_TOPAS_09	Run with EM120	22/01/2010 13:04:16	10	7000	1500/5000/15	25.682
JR206_TOPAS_10	Across basin, intersects margin in heavily scarred area	22/01/2010 14:44:57	10 – 6	7000-2000	1500/5000/15	36.392
JR206_TOPAS_11		22/01/2010 17:43:27	6 – 10	2000	1500/5000/15	24.911
JR206_TOPAS_12	Across basin and onto trough-mouth fan	22/01/2010 19:35:59	10	2000	1500/5000/15	44.791
JR206_TOPAS_13	Up fan slope	22/01/2010 22:31:08	6	2000	1500/5000/15	8.663
JR206_TOPAS_14	Across upper fan	22/01/2010 23:27:45	6	2000	1500/5000/15	12.954
JR206_TOPAS_14a	Transit to line 15	23/01/2010 00:50:07	10	2000	1500/5000/15	12.236
JR206_TOPAS_15	Down strike of fan	23/01/2010 01:44:40	6 – 10	2000	1500/5000/15	33.997
JR206_TOPAS_16	Down slope into basin	28/01/2010 22:00:18	10	2000	1500/5000/15	12.967
JR206_TOPAS_17	Cross basin, proximal to western faulted area	28/01/2010 22:41:56	10	2000	1500/5000/15	54.860
JR206_TOPAS_18	Cross basin	29/01/2010 01:34:07	10	2000	1500/5000/15	33.949
JR206_TOPAS_19	Across basin and onto trough-mouth fan	29/01/2010 03:30:32	10	2000	1500/5000/15	42.746
JR206_TOPAS_20	Down slope from saddle to eastern basin	29/01/2010 05:47:14	10	2000	1500/5000/15	26.976
JR206_TOPAS_21	Run with EM120 across eastern basin	29/01/2010 07:09:21	12	External	1500/5000/15	53.188
Total line length (km):						667.407

Table 1. South Georgia southern margin TOPAS line summary.

Of these various TOPAS lines, the most successful were those running along the axis of the basin and across the southern margins; the steep slopes on the northern side, coupled with very limited acoustic penetration, meant that results from lines 1 and 2, and those parts of the basin-crossing lines that crossed these slopes, were of limited value. Furthermore, it proved difficult to place the along-profile lines to consistently run along the narrow, irregular troughs that trend along this slope. In contrast, the lines along the basin axis, across the basin floor, and on the southern margin produced excellent results, with exceptionally good acoustic penetration of up to 125 ms in well-stratified units in the westernmost sub-basins. Intraformational deformation and possible slumping was identified in some of these well-stratified units. In view of the ongoing active faulting evident at sub-basin margins, in particular from surface-rupturing faults cutting sediment sequences at the foot of the main scarps and in the transverse ridges, this sediment deformation is likely to be associated with seismic activity. Further east (in the sub-basin closest to the fan system), in contrast, acoustically transparent units were identified that thicken into the sub-basin centre; whilst thick units with uneven tops occur in the profiles closest to the fan. These are interpreted, respectively, as ponded turbidites and debris flows sourced from the fan system. All of these units are overlain by laterally continuous stratified units at the sea bed, suggesting a recent decline in sedimentation rates and energies.

Strikingly, the various units below the drape sequences pinch out at or near the foot of the fault scarps and ridges bounding the sub-basin, suggesting strong control of sediment movement by these structures and a resulting restriction of a clear glaciated margin signature to those parts of the basin with an uninterrupted sediment pathway to the fan and canyon system. Conversely, the ponding of sediments from the fan system in the southeastern most sub-basin means that this sub-basin may preserve continuous sediment sequences derived from the fan system and therefore preserve a long record of the history of glaciation on the South Georgia microcontinent, in particular of the proposed ice cap that is inferred to have covered the entire continental shelf of the microcontinent during glacial maxima (Graham et al. 2008).

2. South Sandwich Islands

Mapping of the northern part of the South Sandwich arc with multibeam swath bathymetry had been largely completed from Protector Shoal to Candlemas Island in an earlier cruise in 2007 (Tate & Leat 2007). The principal objective was therefore to complete the coverage in the northern part of the arc, and to extend coverage into the central and southern parts of the arc. Additional objectives were to dredge sites of submarine volcanism of particular interest, and to investigate the internal geometries of sedimentary and mass transport structures on the flanks of the volcanic islands and seamounts with the TOPAS system. A subject of particular interest was the nature and significance of slope-transverse (contour parallel) undulations evident around the islands covered by the 2007 survey work: it was not clear from that work whether these features were a type of slump structure, erosional features or depositional structures of the sediment wave type (Lee et al., 2002). Sediment

waves are normally associated with non-volcanic depositional systems such as deep sea fans and contourite fields, but are also associated with down-slope sediment transport on the submarine slopes of volcanic islands (Silver et al., 2005; Hoffmann et al. 2010). Similar structures have also been identified around submarine calderas and associated with downslope flow after eruption column collapse in large-volume explosive eruptions (Wright et al. 2006). Figure 6 shows the cruise track. A summary of TOPAS lines is presented in Table 2 and positions of TOPAS lines are indicated in Figures 7-9 and 12, 13 and 15.

TOPAS line number	Brief line description	Time start of line	Vessel speed (kts)	Ping interval	Start frequency Hz/ Stop frequency Hz/ Chirp pulse length (ms)	Length (km)
JR206_TOPAS_22	Dredge site 193	30/01/2010 11:54:22	10	External	1500/5000/15	7.151
JR206_TOPAS_23	Dredge site 194	30/01/2010 16:06:36	10	External	1500/5000/15	4.201
JR206_TOPAS_23a	Across possible slump on northwest aspect of Protector Shoal	30/01/2010 21:29:33	10	5000	1500/5000/15	14.096
JR206_TOPAS_24	Downslope along Protector Shoal slump feature	30/01/2010 22:25:54	6	1500	1500/5000/15	20.205
JR206_TOPAS_25	Across Protector Shoal slump feature	02/02/2010 15:39:39	11	1500	1500/5000/15	22.282
JR206_TOPAS_26	Dredge site 199	02/02/2010 21:46:22	-	2000	1500/5000/15	1.014
JR206_TOPAS_27	Downslope through Zavodovski sediment waves	03/02/2010 12:35:09	10	2000	1500/5000/15	39.328
JR206_TOPAS_28	Traverses slope at distal end of Zavodovski sediment waves	03/02/2010 15:20:10	10	2000	1500/5000/15	21.743
JR206_TOPAS_29	Upslope through Zavodovski sediment waves	03/02/2010 16:38:59	10	2000	1500/5000/15	30.966
JR206_TOPAS_30	Up stepped channel upslope from sediment waves	03/02/2010 18:23:33	10	2000	1500/5000/15	11.173
JR206_TOPAS_31	Saunders -Downslope through gully	07/02/2010 01:03:53	8	2000	1500/5000/15	25.431
JR206_TOPAS_32	Saunders - Upslope across broad ridge	07/02/2010 03:29:32	8	2000	1500/5000/15	29.410
JR206_TOPAS_33	Saunders -Downslope through gully	07/02/2010 06:12:49	8	2000	1500/5000/15	21.463
JR206_TOPAS_34	Across basin to east of Montagu	07/02/2010 17:44:53	11	External – 10000	1500/5000/35	37.511
JR206_TOPAS_35	Montagu - Downslope along ridge neighbouring line 36	09/02/2010 18:33:41	10	2000	1500/5000/15	19.547

JR206_TOPAS_36	Montagu - Upslope within gully neighbouring line 35	09/02/2010 20:18:32	10	2000	1500/5000/15	20.654
JR206_TOPAS_37	Montagu - Downslope through sediment waves	09/02/2010 21:31:38	10	2000	1500/5000/15	25.598
JR206_TOPAS_38	Montagu - Across fan structure at base of sediment waves	09/02/2010 23:10:24	10	2000	1500/5000/15	12.465
JR206_TOPAS_39	Montagu - Upslope through sediment waves	10/02/2010 00:07:12	10	2000	1500/5000/15	8.731
JR206_TOPAS_40	Montagu - Crosses gully upslope from fan structure	10/02/2010 00:47:50	10	2000	1500/5000/15	13.162
JR206_TOPAS_41	Montagu - Upslope on same route as line 37 with settings for greater sediment penetration	10/02/2010 01:50:30	8	4000	1500/5000/30	17.280
JR206_TOPAS_42	Montagu - Run with EM120, crosses gullies on upper slope	10/02/2010 03:15:34	8	External	1500/5000/15	10.351
JR206_TOPAS_43	Downslope through sediment waves ending in basin to southeast of Montagu	10/02/2010 04:40:26	10	2000	1500/5000/15	26.832
JR206_TOPAS_44	Bristol - Run with EM120, across glaciogenic or volcanoclastic debris fan structure	11/02/2010 19:27:46	10	External	1500/5000/35	11.214
JR206_TOPAS_45		11/02/2010 21:07:22	10	External	1500/5000/35	25.211
JR206_TOPAS_46	Downslope through sediment waves south of Bellinghausen	13/02/2010 16:23:29	8	2000	1500/5000/15	11.170
JR206_TOPAS_47	Bellinghausen -Across sediment wave glaciogenic / volcanoclastic fan boundary	13/02/2010 21:53:03	10	2000	1500/5000/15	21.468
JR206_TOPAS_48	Same route as line 47 with settings for greater sediment penetration	13/02/2010 23:11:03	6	4000	1500/5000/35	17.338
JR206_TOPAS_49	Run with EM120, across basins and sediment waves south of Southern Thule	14/02/2010 17:05:22	10	External	0/3500/35	30.123
JR206_TOPAS_50	Run with EM120, within sediment waves south of Southern Thule	14/02/2010 18:45:23	10	External	0/3500/35	6.029
JR206_TOPAS_51	Run with EM120, across basins and ridges east of	15/02/2010 12:59:09	10	6000	1500/5000/15	75.797

Vysokaya bank							
JR206_TOPAS_52	Crosses bathymetric high on route to dredge site 200	17/02/2010 13:00:01	10	2000	1500/5000/15	9.250	
JR206_TOPAS_53	Recorded on approach to dredge site 201	17/02/2010 16:33:36	10 – 0.1	2000 – 4000	1500/5000/15	4.445	
JR206_TOPAS_54	Recorded on dredge site 201	17/02/2010 17:30:31	1 – 0.1	4000	1500/5000/15	0.273	
JR206_TOPAS_55	Crosses caldera and downslope through sediment waves	17/02/2010 19:53:13	8	2000	1500/5000/15	17.613	
JR206_TOPAS_56	Down slope through sediment waves	17/02/2010 21:06:10	8	2000	1500/5000/15	13.921	
JR206_TOPAS_57	Run with EM120, crosses boundary between tilted structure and sediment waves	18/02/2010 17:16:22	11	External	1500/5000/15	21.915	
JR206_TOPAS_58	Run with EM120 to east of arc	06/03/2010 01:36:08	11	External	1500/5000/30	305.891	
JR206_TOPAS_59	Run south of Saunders	06/03/2010 16:54:27	8	1500	1500/5000/15	30.389	
JR206_TOPAS_60	Across slope to Humpback seamount	06/03/2010 18:19:52	8	1500	1500/5000/15	27.449	
JR206_TOPAS_61	Northeast from Humpback seamount	06/03/2010 23:18:52	8	1500	1500/5000/15	39.309	
						1109.397	

Total:

Table 2. South Sandwich TOPAS line summary.

2.1. Protector Shoal area

The area was known to contain at least seven seamounts from previous survey (Tate & Leat 2007). The northern part of the area was unsurveyed.

We completed swath survey of the Protector Shoal area, defining a large plateau ‘Nimrod Bank’ forming the northern part of the volcanic area, and a previously known (Leat et al., 2010) line of seamounts ‘Protector Seamounts’. Nimrod Bank is ringed by seamounts of various sizes on its southern and western sides, whilst it is cut by broadly NE- trending faults on its northern and eastern sides. We also completed survey of the area between Protector Shoal and approximately the 3000 m contour, defining the position of numerous faults to the north and east of the plateau in particular. These faults enclose or nearly enclose small basins to the north and east of the plateau area.

Note on names: Protector Seamounts

We propose to name the seamounts after British ships involved in Antarctic exploration and research, particularly work in the South Sandwich Islands and Scotia sea region more generally. We propose to name Protector Seamounts for the whole seamount group.

Proposed names for individual seamounts replace the PS1-PS7 numerical sequence used by Leat et al. (2010) as follows (see also Appendix 7):

PS1	Tula Seamount
PS2	Bisco Seamount
PS3	[no proposed name as this is a small feature]
PS4	Protector Seamount, with Protector Shoal retained for summit
PS5	Endurance Seamount
PS6	JCR Seamount
PS7	Quest Seamount

Other proposed names are as follows

Seamount west of PS7	Scoresby Seamount
Large bank north of PS4	Nimrod Bank

2.1.1. Dredges

Seven dredges (DR193-DR199) were completed in the area (Figure 5; Appendix 5). Six of the dredges, DR193 to DR198, were from major seamounts in the central part of the Protector Shoal area. All of these produced a successful haul of notably varied volcanic rocks, with different varieties of silicic pumice and denser volcanic rocks being prominent. In some cases the chain dredge bag contained a poor haul (perhaps because relatively fragile pumice clasts were shattered and lost through the chain mesh) and more of the collected material came from the solid-walled bucket dragged behind the chain bag.

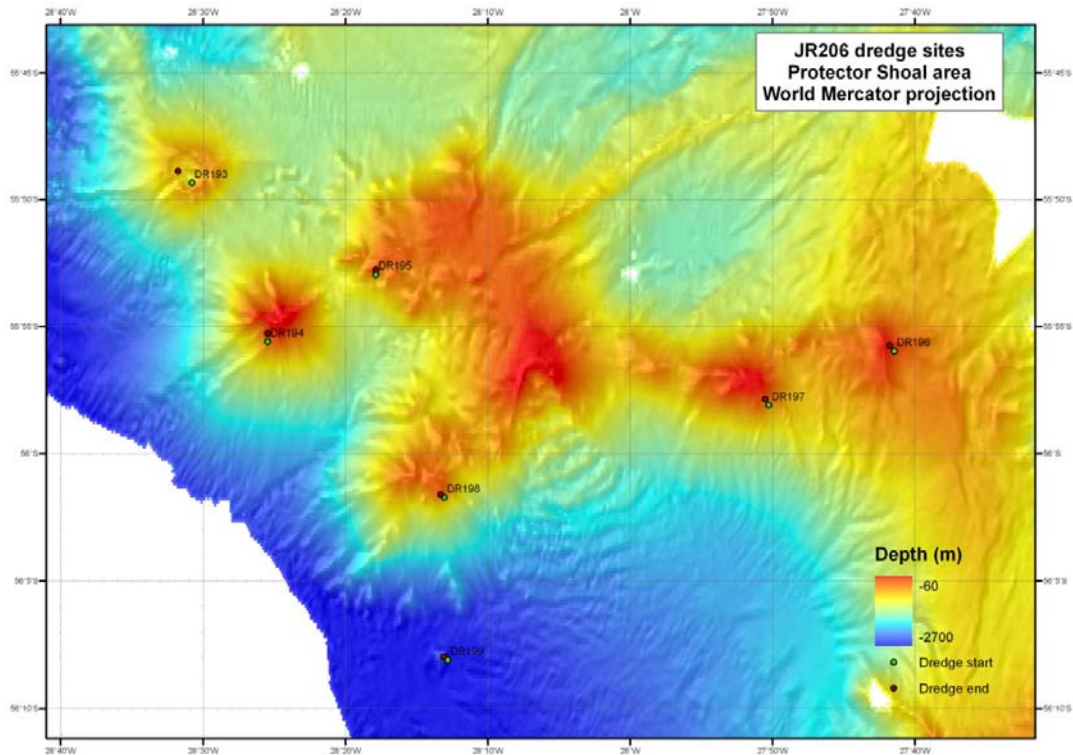


Figure 5. Dredge sites in the Protector Shoal area.

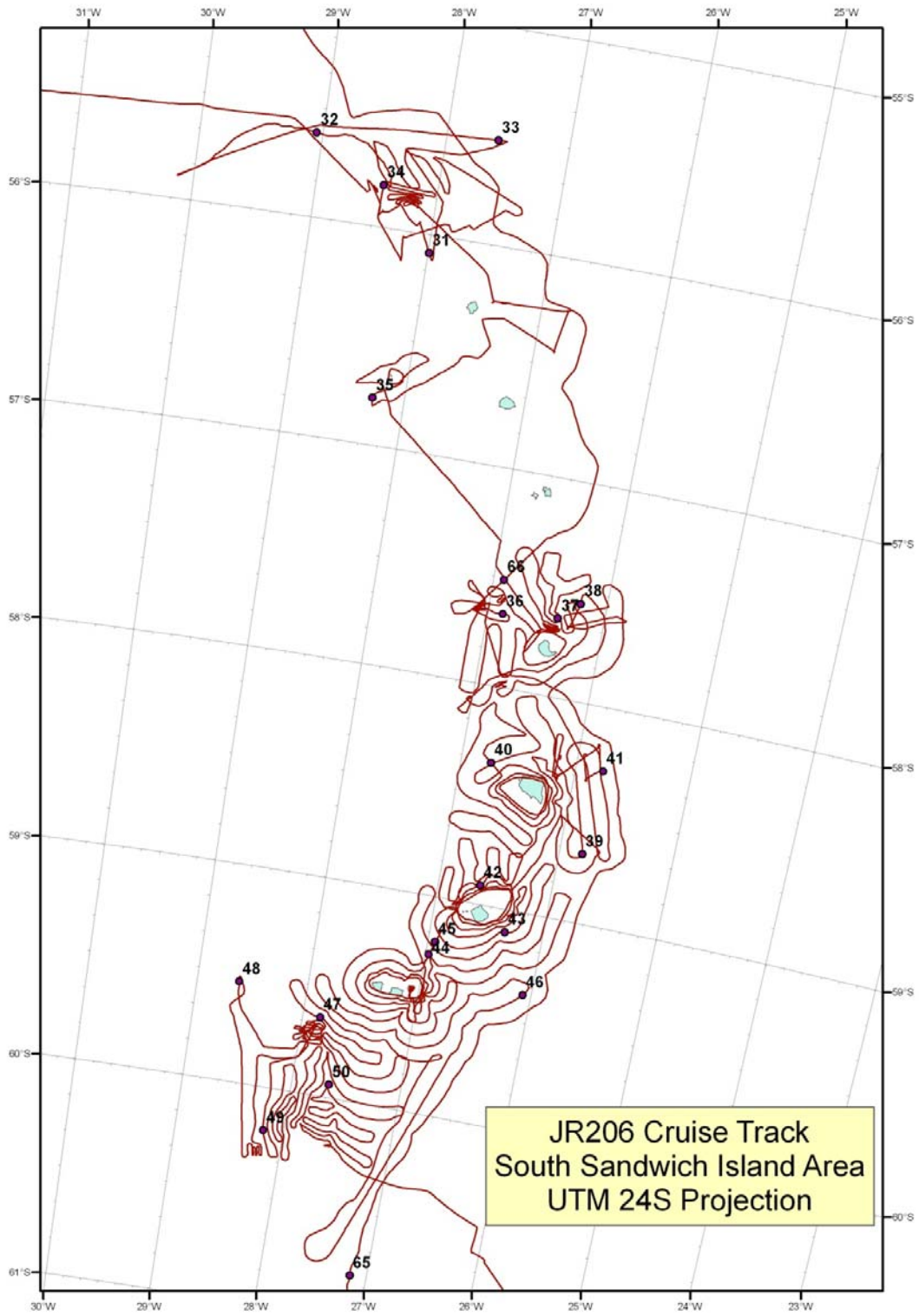


Figure 6. JR206 cruise track, South Sandwich arc.

Some of the dredge hauls were dominated by notably fresh rocks whilst others (especially from the eastern dredge sites) were mainly composed of intensely seawater – weathered [31]

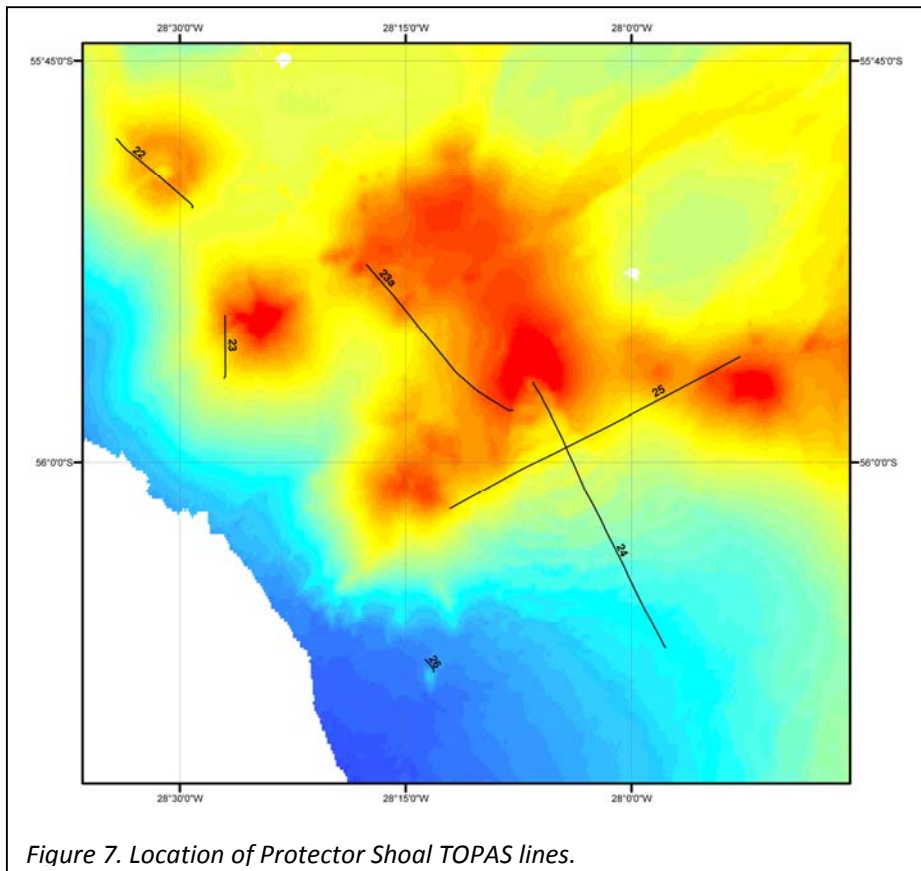
pumice with thick black (likely, manganiferous) encrustations. The fresher dredge hauls also tended to be more monolithologic and to contain few if any glacial dropstones, implying that these were from sites of recent volcanic activity. Almost all the sampled material (other than glacial dropstones) appeared to be volcanoclastic in nature, consistent with the low cable tensions observed as the dredge was hauled across the seafloor: there were no abrupt increases and decreases in tension such as are observed when dredges snag on submarine lava flows. The final and most time-consuming dredge, DR 199, was from one of a group of small volcanic cone-like features south of Protector Seamounts in 2525 m of water. This dredge contained only sticky, cohesive marine mud and three drop stones; this implies that the dredge did not penetrate through thick drape over the feature, which is therefore thought to be relatively old.

Discussion: dredge sites

The success of the dredges from the Protector Seamounts indicates that location of dredge sites on likely explosive volcanic vents or other volcanoclastic features is an effective strategy for sampling multiple lithologies in single dredges (note also that although the dredging process destroys all stratigraphic information, the wide variation in alteration state of the samples collected indicates that it will be possible to reconstruct an inferred relative age sequence of the samples using the variation in intensity of seawater alteration). In contrast, the failure of DR199 highlights the benefits that would be gained from prior backscatter sonar imaging of potential dredge sites, as backscatter intensity data would have made it immediately evident that the site was covered in a fine-grained drape. TOPAS profiles were run across some of the dredge lines on the Protector Seamounts and in the absence of a backscatter system the TOPAS system would in some cases be useful as a means of checking for the presence of thick (> 5 metres or so) drape on dredge sites; but this still leaves open the problem of sites with drape that is too thin to resolve with TOPAS but too thick and cohesive to be penetrated by the dredge.

2.1.2. TOPAS subbottom profiler lines

In addition to short lines over some of the dredge sites (Lines 22, 23, 23A), TOPAS lines were run along the length and across the slump feature on Protector Seamount (PS4). Line 24 ran from within the collapse scar on the south side of seamount PS4 toward the southeast, along the direction of transport of the slump. Data obtained defined clear downslope variation from large back-rotated slump blocks at the top to smaller, more subdued features at the base. Line 25 ran across the slump in its middle section and defined the margins and the lateral continuity of slump blocks.

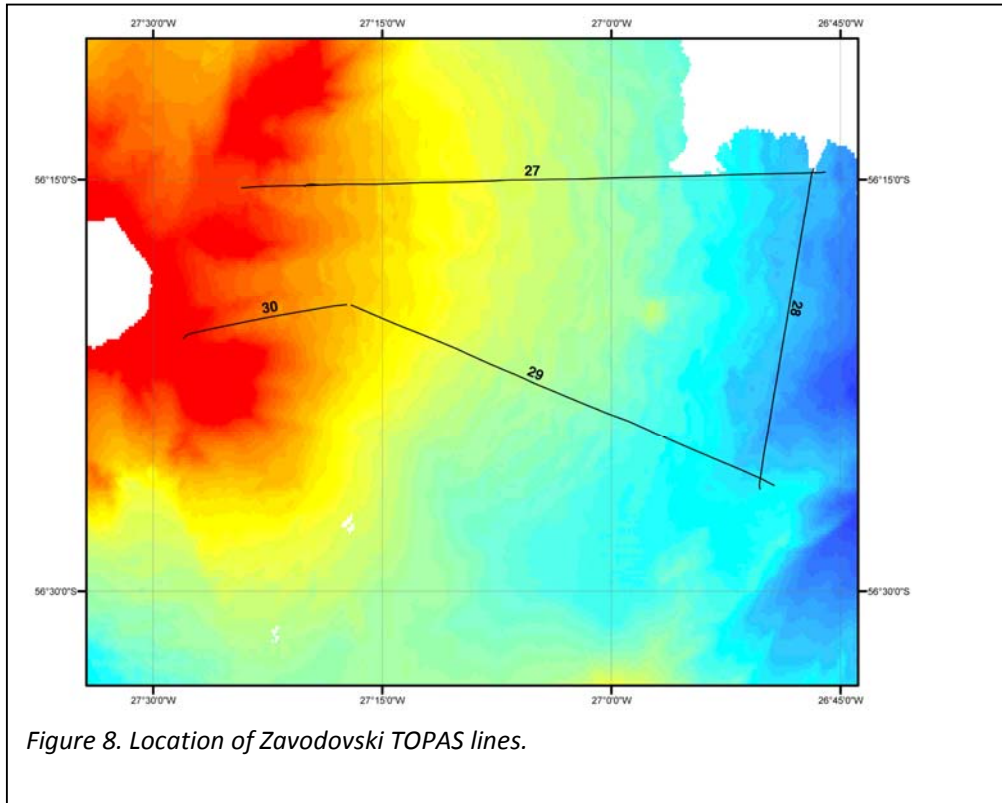


2.2. Zavodovski

Zavodovski was previously well-surveyed by swath bathymetry (Tate & Leat 2007), and few further swath bathymetry data were added during the cruise. TOPAS subbottom profiler lines were run to the east of the volcano (Fig. 8).

2.2.1. TOPAS subbottom profiler lines

TOPAS lines (27, 28, 29, 30) were run to the east of Zavodoski to profile the internal structure of slope-parallel seabed undulations. These were previously thought to be possible erosional features, or very thin-skinned, laterally extensive slumps, or downslope-directed sediment waves. Lines 27, 29 and 30 (the last two together forming a kinked line) ran down and up the slope, whereas 28 ran parallel to the slope and thus the trend of the features. Acoustic penetration of the features was limited owing to the development of a highly reflective unit at c. 10 to 25 ms two-way-travel-time (TWTT) below the seabed, but downslope progradation of reflectors in the top layer indicated sediment wave formation and progradation, whereas no features indicative of large-scale slump movement or erosional formation were found except for near the island at the western end of Line 30, where there is possible slumping and erosion in the chute that feeds the area downslope. Amplitudes of the undulations were up to 100 m at the top of the wave field but decreased downslope to 50 m or less; these values are typical of sediment wave fields around volcanoes (Hoffmann et al. 2010).



2.3. Leskov

Leskov was previously unsurveyed by swath bathymetry. It is situated some 55 km to the west of the main volcanic arc, in a rear-arc position. The island is 900 m across, and rises to 190 m, and the coastline entirely consists of cliffs (Holdgate & Baker 1979). The subaerial island dominantly consists of one or two eroded andesite lava flows. There is no record of volcanic eruptions. Bathymetrically, Leskov is connected to the Zavodovski edifice by a prominent northeast-southwest trending ridge with a distinct rise to form a seamount in the centre of the ridge. The Admiralty chart shows the Leskov edifice rising steeply from depths of around 2400-3000 m, with a continuation of the ridge rising to 1108 m southwest of the island.

We surveyed the area around Leskov and the ridge that connects it to Zavodovski with swath bathymetry. The data show that Leskov Island is the summit of a simple conical volcano, which rises from a base level of about 3000 m. There is a second volcanic cone on the southwest flank of the main cone. The secondary cone rises to about 1200 m and appears to occupy the upper slopes of a scar left by a lateral collapse landslide which was directed toward the southwest. The scar appears to extend down to the base of the Leskov edifice and is as much as 10 km across: it is unusually large for an arc volcano lateral collapse, perhaps as a result of failure occurring on weak marine sediments below the base of the volcanic edifice. The geometry also implies a southwestward migration of volcanic activity at Leskov, through time.

Note on names: Leskov Seamounts

We propose to name the Seamount chain trending NE toward Zavodoski and SW from Leskov Island Leskov Seamounts. We propose to name the prominent seamount west of Leskov Vostok Seamount, and the one on the ridge to the east as Mirnyi Seamount (Fig. A7.2). Vostok and Mirnyi were the two ships of the Russian expedition led by Bellingshausen that discovered the northern islands in the South Sandwich arc.

2.4. Saunders

The Saunders edifice is previously unsurveyed by swath bathymetry. The 8.3 x 5 km island rises to 991 m at Mount Michael. The island consist of the central cone of Mount Michael, which is ice-covered and has a summit crater, and low areas to the north (Blackstone Plain) and southeast (Ashen Hills) (Holdgate & Baker 1979). Blackstone Plain consists of recent lava flows that have surrounded a former sea stack at Yellowstone Crags. Ashen Hills consist of scoria and ash deposits forming degraded tephra cones. The northeast coast of the island is occupied by a ca. 6 km wide bay, Cordelia Bay, which is shallow and has numerous reefs and sea stacks forming Brothers Rocks some 2 km offshore. The Admiralty chart indicates that Saunders is the most extensive edifice of the South Sandwich group, with large submarine plateau areas to the north, northeast and southwest of the island. It also shows a series of apparent ridges projecting north, northwest and south west from the island.

We surveyed the Saunders edifice by swath bathymetry to a depth of around 2500 m. The data reveal that there is no significant shallow plateau to the south of the island. Moreover, whilst there is a submerged, gently inclined plateau with deeply incised margins to the north of the island this is smaller than indicated on the Admiralty chart. The plateau north of Saunders Island is resolved into two parts, a shallow (~160-270 m) bank up to 6 km from the coast ('Harper Bank'), and a deeper (~740-1035 m), larger bank ('Saunders Bank') that extends to 23 km from the coast.

The swath bathymetric data indicates that the Admiralty chart data does not resolve two lines of seamounts adjacent to but distinct from the Saunders edifice, but amalgamates them into the plateau. These seamounts form two WSW – trending groups, one north of the Saunders edifice and the other to the southwest; individual seamounts are broadly conical, either circular in plan or elongate along the overall WSW trend. These are large volcanic edifices in their own right, rising from as much as 3000 m base depth to (in the case of 'Humpback Seamount', the westernmost feature of the northern line) within 100 m of the sea surface. At least one west-directed lateral collapse scar, albeit largely infilled by later volcanic activity, may be present. The direction of this scar, towards another seamount, suggests that the latter is younger and that, as at Leskov, westward to southwestward migration of volcanic activity may have taken place.

Note on names: Saunders Seamounts, Harper Bank and Saunders Bank

We propose to name the five seamounts around Saunders Island as a group, after species of whales whose ranges include the South Sandwich Islands region, as follows:

Northern Chain, from NE to SW: Minkie Seamount, Orca Seamount, Humpback Seamount.

Southern Chain, from NE to SW: Fin Seamount, Southern Right Seamount (Fig. A7.3).

We propose to name the Shallow (~160-270 m) bank immediately north of Saunders Island Harper Bank, following the name of the northern point of Saunders Island, which is Harper Point. We propose to name the deeper (~740-1035 m) bank to the north Saunders Bank (Fig. A7.3).

The eastern side of the Saunders edifice, in contrast, is intensely gullied with irregular ridges extending to the northeast in particular. Sediment wave-like fields fill the troughs between the ridges and extend further downslope to the east and the limit of the mapped area, except in the far northeast (furthest from the island) where the gullies are empty, with more V-shaped profiles. A small field of similar features occurs to the west and northwest of Saunders Island, but as around the islands to the north they are much less strongly developed to the west than to the east. This may reflect eastward transport of sediment from the island, controlled by prevailing winds and currents. The strongly incised nature of the slopes and 'Saunders Bank' east and north of Saunders suggests that they are older, consistent with the evidence for migration of volcanic activity to the south and west provided by the seamounts noted above.

2.4.1. TOPAS subbottom profiler lines

TOPAS lines around Saunders were run in two groups, one during the main survey of the islands and the second during the transit north, which took a dogleg around Saunders in order to complete mapping of the summit of 'Humpback Seamount' to the west of the island.

TOPAS lines 31 to 33 (Figure 9) were run to profile features of the wave field to the northeast of Saunders Island. In this area the waves are organized into broadly bilaterally symmetric areas, with arcuate slope-parallel waves to either side of a downslope-directed trough which itself has wave-like features in its floor. This geometry suggests formation of the arcuate waves by overbank deposition from sediment flows centred upon the axial trough. As with the Zavodovski lines, acoustic penetration of the structures was limited owing to the development of the highly reflective unit at 10 to 25 ms depth (and parts of the internal structure obscured by diffractions from the cusped surface profiles of the waves), but in the downslope part of Line 33 in particular, multiple downslope-prograding units were resolved below the reflective unit within the downslope side of each wave, indicating that these are depositional sediment waves. Amplitudes of the wave features were in the range 40 to 70 metres, and increased downslope rather than upslope.

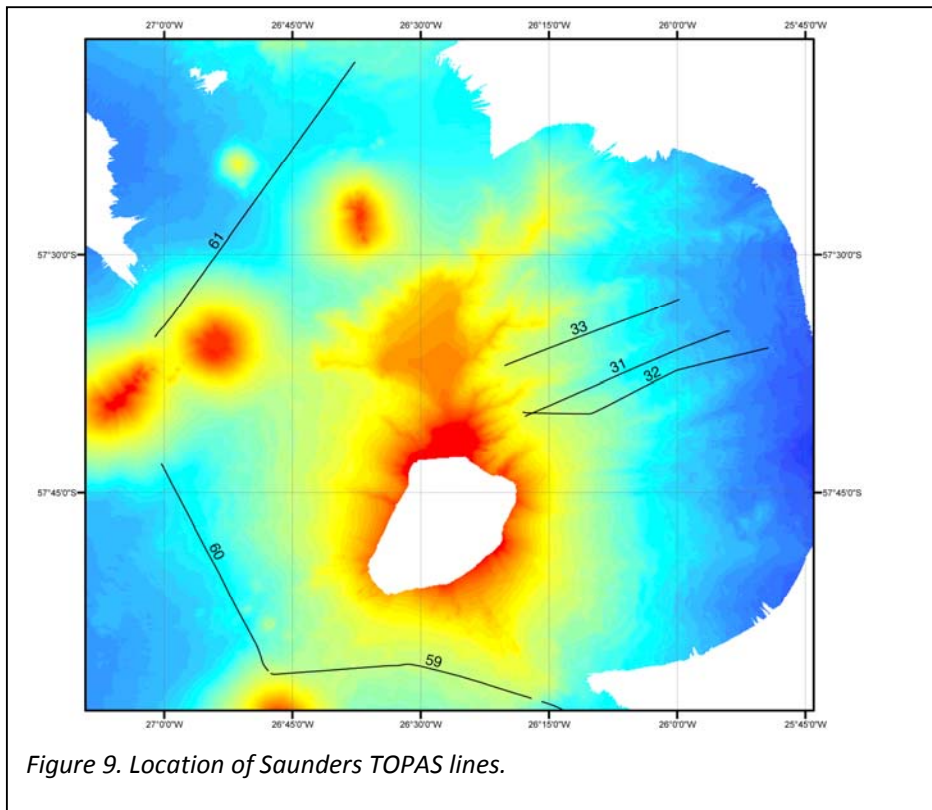


Figure 9. Location of Saunders TOPAS lines.

TOPAS lines 59 to 61 include sections of sediment wave fields originating from Montagu and Candlemas Islands, but are dealt with here because the main features of interest are associated with the parts of the lines closer to Saunders Island. Lines 59 and 60 both run approximately parallel to wave crests in their respective sediment wave fields, and show marked progradation in the upper stratified unit along wave crests: the direction of propagation may be either lateral (lengthening the wave crests over time) or downslope. The waves pass laterally into slope areas with only diffuse, diffractive returns and so the age relationships of the sediment wave fields to seamounts (particularly the young seamounts west of Saunders) are not clear. Line 61 includes a large section across the flat saddle between Saunders and Candlemas. The profile along this part of the line includes both upper low-reflectivity (to c. 10 ms TWTT in the eastern part of the section) and lower high-reflectivity units, and both are well-stratified. The upper units is mainly plane-stratified but onlaps to the west, whilst the lower unit shows evidence of internal deformation and possible slumping; cross-bedding may be present locally in the lowest parts of the imaged profile, at c. 25 ms TWTT. The presence of the upper and lower units, of low and high reflectivity respectively, matches the sequences in the sediment wave fields elsewhere in the arc and indicates that the pair of units may be of regional stratigraphic significance (see also section 2.9).

2.5. Montagu

The Montagu edifice was previously unsurveyed by swath bathymetry apart from a single track on JR149 that passed to the east and north of the island. The island is about 12 km

across (Patrick et al. 2005), who noted that the map in Holdgate & Baker (1979) inaccurately suggests a larger size. Most of the island is occupied by an ice cone that reaches an altitude of 1372 m at Mount Belinda, a small summit volcanic cone. Much of the coast of the island is formed by ice cliffs, although the north coast is dominated by rock cliffs up to 600 m high; similar but lower rock cliffs occur along the west coast as well. The southeast end of the island is formed by a satellite cone, Mount Oceanite, that is some 900 m high and steep-sided. Its east-facing flank is formed by the headwall of a small collapse scar. Patrick et al. (2005) interpreted the ice dome as an ice-filled caldera some 6 km across occupying the central part of the island. The most recent eruption, largely observed through visible-light, infra-red and radar satellite data with infrequent observations from ships and only one landing on the island during the activity, lasted from autumn 2001 until late 2007 or early 2008 (Patrick et al. (2005) and Global Volcanism Program reports summarized in Global Volcanism Program (2010)). The eruption consisted of small-scale explosive activity at the summit and effusion of a number of lava flows one of which reached the sea and produced a small lava delta on the north coast of the island.

2.5.1 Subaerial slopes of Montagu.

We approached Montagu from the north and then circled the island in exceptionally clear weather, allowing visual inspection of the island. Whilst the summit cone of Mount Belinda was largely obscured by cloud (a few brief sightings confirmed that there is now no sign of volcanic activity, although parts of the summit were free of snow which might be a result of continued localised ground heating), the coastal cliffs and numerous glaciers were clearly visible up to as much as 1000 m elevation above sea level.

The recent lava was clearly visible within a gully from the edge of the plateau to the sea. Steam was rising from five ice-free patches along the lava, indicating that significant heat sources were still present. There were no other signs of continuing eruptions.

Discussion: Calderas and rock cliffs at Montagu:

The ice cover in the centre of the island may have subsided. The extent of ice cover along the north coast is less than is shown in the map produced by Holdgate & Baker (1979), although their map of Montagu was clearly not intended to be accurate. It is possible that ice has retreated on the north coast and within the caldera, possibly as a result of melting due to the eruption. The crags forming the north coast also form a line of inward-facing cliffs (Figure 10). The inward-facing cliffs are readily interpreted as the topographic rim of a caldera, providing new evidence in support of the interpretation of Patrick et al. (2005).

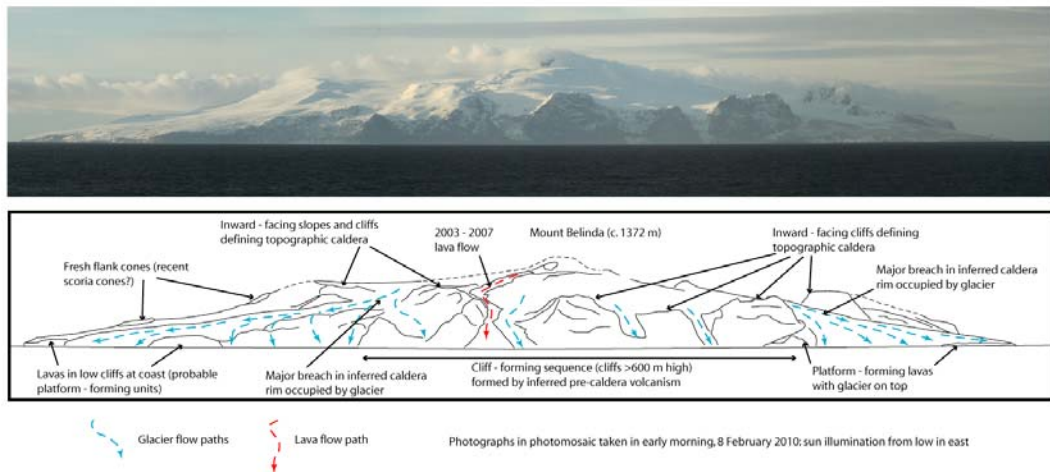


Figure 10. Photomosaic and line interpretation of Montagu Island, viewed from the north.

Post-caldera-formation ponding of lava flows in the centre of the island may have produced a hiatus in activity at the coast, allowing a period of continuous erosion that produced the spectacular, high rock cliffs. These cliffs expose sequences of lavas and pyroclastic rocks, cut by numerous dykes, with numerous unconformities (Figure 11). The pyroclastic rocks are dominantly yellow-brown weathering, well-bedded units that are likely to be hydromagmatic deposits. Red-weathering deposits, interpreted as scoria, are a minor component. Most of the major major unconformities visible in the cliffs are U-shaped in profile, and were likely produced by glacial erosion, and subsequent in-filling. A laterally extensive, inward-facing unconformity with some hundreds of metres of vertical relief indicates extensive dissection, and may be an older caldera wall, with flat-lying or inward-sloping lavas present above the unconformity, particularly towards its western end, representing caldera fill sequences (Figure 10).

In contrast to the high rock cliffs, low coastal platforms formed by lava flows occur at a number of points around the island, most notably at the northwest (Borley Point) where a glacier largely covers a platform that is some 3 km wide but with cliffs that rise only a few tens of metres above sea level at most, exposing one or more flat-lying lava flows. The limited coastal erosion of this platform, despite its position on the windward side of the island, and an analogy with the post-glacial platform-forming lavas found on many oceanic island volcanoes (Carracedo et al. 1999), suggests that it is a young lava delta that prograded on to the shallow shelf adjacent to the island, and that Montagu Island has experienced a number of recent eruptions, in addition to the 2001-2007 eruption. Other recent eruptions with lava flows directed to the northeast of the island are indicated by a similar low coastal platform under the glaciers there, but this platform is markedly more incised by the glaciers than the Borley Point platform.

Photomosaic and interpretation of cliffs on the north side of Montagu Island. Estimated height of cliffs 500 - 600 meters; length of coastline shown is about 4 kilometers.

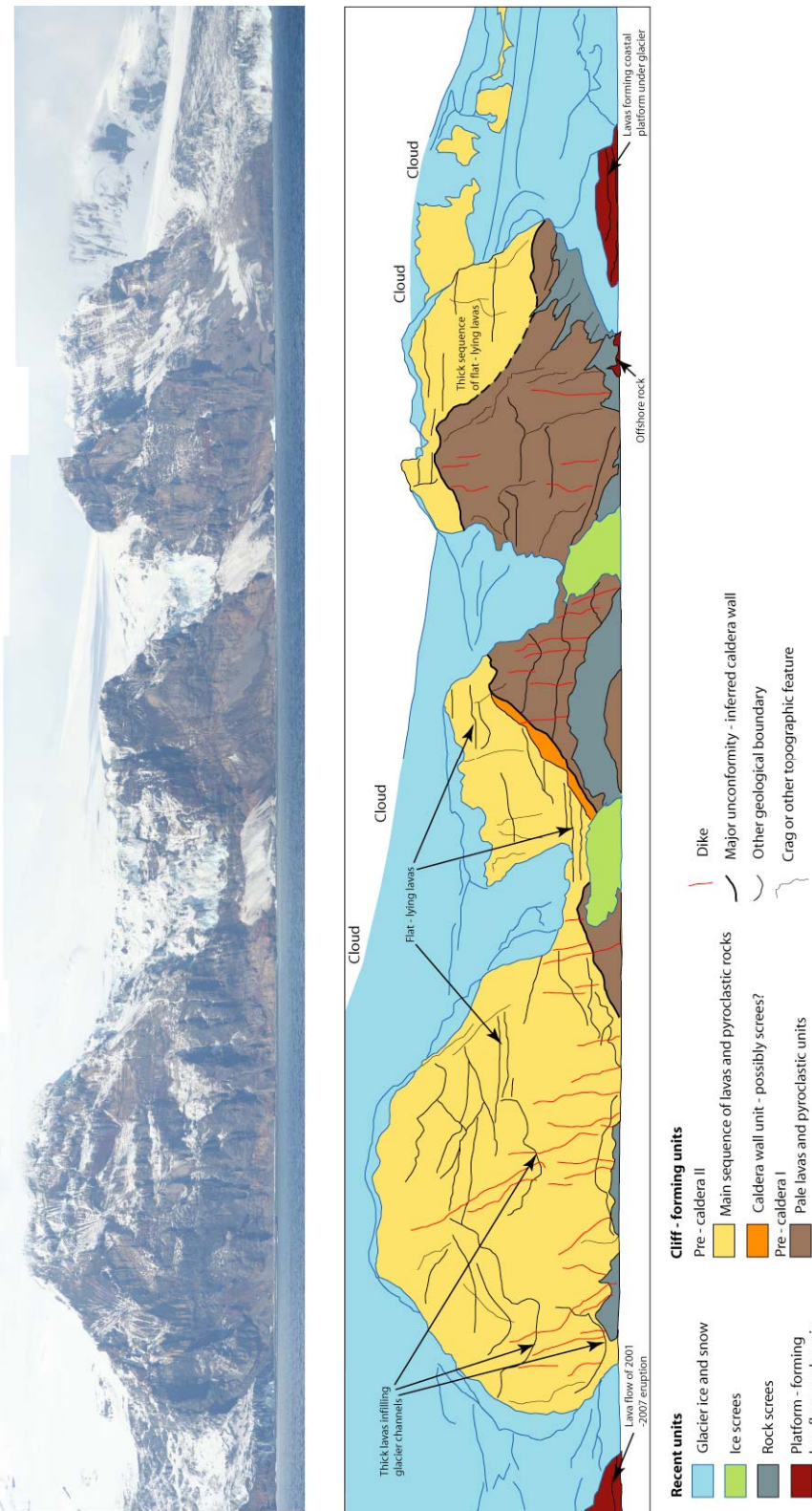


Figure 11. Photomosaic and interpretation of the high cliffs on the north coast of Montagu Island.

2.5.2. Submarine slopes of Montagu – bathymetric data

The Admiralty chart indicates a roughly conical shape to the underwater edifice, with no evident secondary seamounts or ridges. There is no indication in the chart of a significant shallow platform in any direction from the island, although a nearshore shallow zone around the islands was evident from a large number of stranded icebergs on the west side in particular.

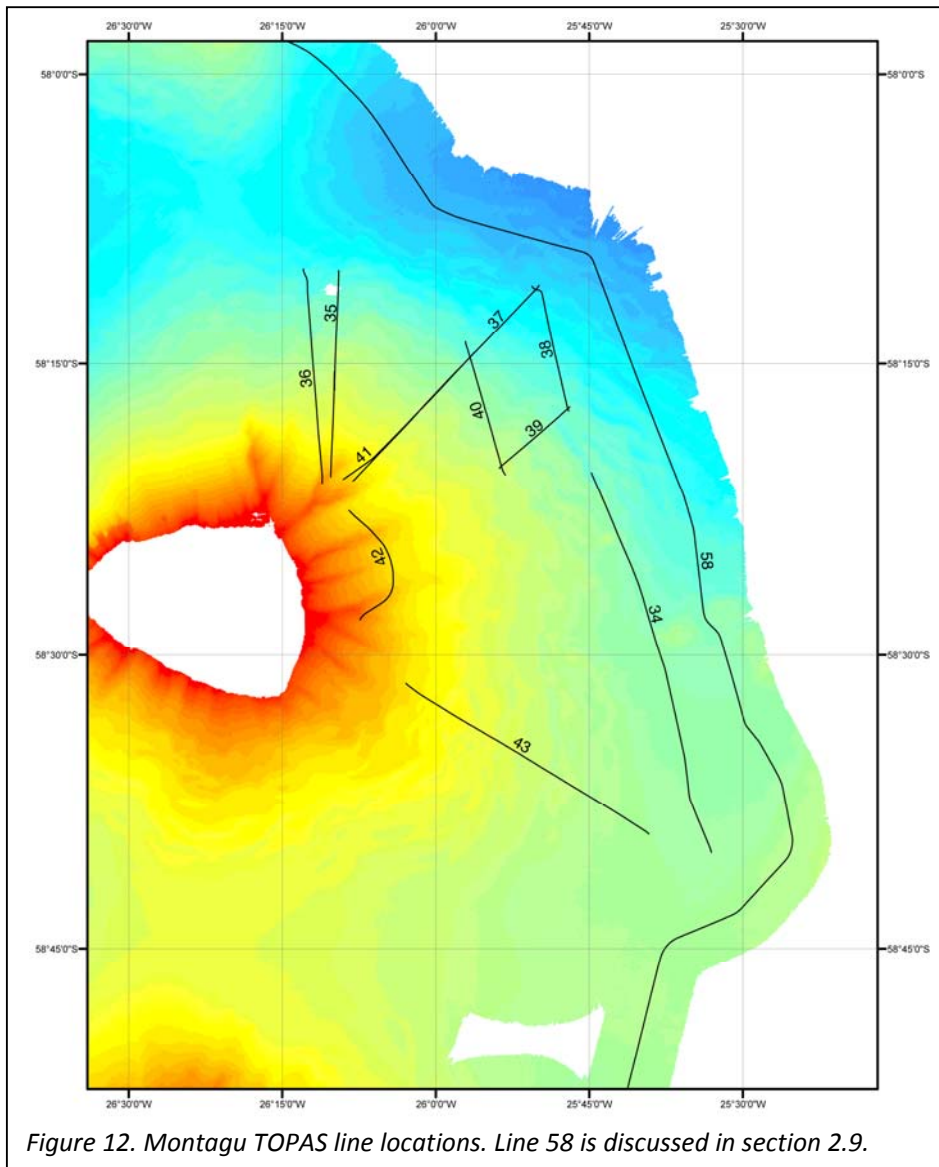
The swath mapping of Montagu revealed well-developed and often large-amplitude sediment wave type features on the slopes around the island, forming a series of lobes centred upon flat-floored to grooved channels or chutes. The positions of these chutes may loosely correlate with the main areas of glacier outflow from the centre of the island, most notably in the case of a prominent group of chutes off the northeastern point. The chutes die out downslope at around 2000 m water depth with distinct irregular rises beyond. Other chutes and wave fields are located off the east, south and southwest of the island. In contrast, the wave fields are less well developed offshore from the northern shore where the cliffs largely block glacier outflow; and are not developed at all offshore of Borley Point, despite the large glacier that emerges there.

Discussion: Borley Point

The slopes offshore from the edge of the shelf near Borley Point (northwest corner of Montagu) are steep, with a distinct downslope-trending topographic fabric and no sediment waves. Similar slopes have been found west of Candlemas Island (Leat et al. 2010). One possible interpretation is that debris flows generated by repeated collapses of the front of the lava delta that forms Borley Point have covered any earlier sediment wave type features in this area, which would again imply that the lava delta and the eruptions that formed it are recent. Alternatively, sediment from this glacier may have been transported to the east along the shelf by prevailing currents, being deposited on the slope to the northeast of the island rather than off Borley Point.

2.5.3 TOPAS profiling around Montagu Island

Montagu Island was subjected to a detailed TOPAS survey during which time some 192 km of lines were run (see Figure 11 for locations). The slopes of the underwater volcano are characterised by a combination of relatively high amplitude sediment waves parallel to slope and pronounced canyon-like trough structures running downslope. All the sediment waves are characterized by low-reflectivity uppermost units and high reflectivity at 10 to 25 ms depth; acoustic penetration is again limited, but possible downslope progradation of the uppermost units over the wave crests was observed in lines 37 and 43 in particular. Large sediment waves with amplitudes of over 150 metres were crossed in lines 36 and 43; the latter profile in particular is characterized by a marked downslope decrease in wave amplitude to only about 70 m. The waves are markedly asymmetric, with near-flat tops and steep downslope faces: this may be due to slump-like deformation of the sediment waves as they accumulate (Hoffmann et al. 2010).



The group of lines from 37 to 41 cover a striking trough and sediment wave system, with arcs of sediment waves extending out from the lower two-thirds of the trough in a geometry that suggests formation of the sediment waves by overbank flows that spilled out from the trough. The upslope transition from sediment waves to smoother slope is sharp, but the upslope areas Lines 37 and 41 follow the same route though with different chirp settings: an attempt to gain greater insight to the wave structure by increasing the chirp pulse length from 15 to 30 ms, this resulted in increased penetration from ~ 20 to ~ 40 ms (corresponding to 16 to 33 m assuming sound velocity of 1650 m/s^{-1}). However, little additional structure was observed as the lower part of the high-reflectivity unit passes down into a diffuse high-reflectivity zone. The downslope part of trough itself was crossed obliquely by lines 38 and 40: here it has a relatively subdued topographic expression but is characterized by a zone of diffuse diffractive reflectors, suggesting a rough seabed in the direction of traverse; the bathymetric data suggest a marked downslope fabric.

Finally, Line 34 and the along-arc Line 58 to the east of Montagu cross the lower ends of the sediment wave fields where they divide around bathymetric highs to the east (see section 2.9).

2.6. Bristol

Bristol Island is approximately square in plan, with a maximum dimension of 14 km in the east-west direction. It is almost entirely ice covered, and most of the coast consists of ice cliffs. The summit is at Mount Darnley, 1097 high, south of its centre. There is a group of prominent sea stacks to the west of the island, the largest of which is Freezland Rock, which is 305 m high, the others being Grindle Rock and Wilson Rock. The island is almost entirely inaccessible, has only been visited at a few points, and is geologically poorly known. A well-observed eruption occurred at the summit area in 1956 and was characterized by strombolian-like activity. A prominent, laterally very continuous black tephra layer is visible in the ice cliffs at the seaward ends of the glaciers. This may be a deposit from the 1956 eruption, if so, suggesting a more violent explosive phase at some point in the eruption. Holdgate & Baker (1979) describe steaming pits and fissures in the glacier ice cover at the western tip of the island, observed in 1962-3; but these may have developed over subglacial lava flows rather than marking the sites of eruptive vents.

The Admiralty chart indicates that Bristol is a relatively simple cone, similar to that of Montagu, rising from about 2000 m from the east and west, and about 1600 m to the north and southwest, where ridges connect to the neighbouring islands. There is no indication of any satellite seamounts on the Admiralty chart, but it does indicate a significant shallow shelf to the northwest and west of the island. There is no previous bathymetric survey of the edifice.

The new multibeam data confirm that Bristol has a relatively simple cone shape. A wide shallow shelf area exists to the west of the island, the shelf continuing to Freezland Rock, Grindle Rock and Wilson Rock. Numerous grounded icebergs occupied this area when we visited. A smaller shelf spur occurs northwest of the island. There is a prominent smooth-floored embayment to the south of the island, bounded to its east by a narrow high ridge with a steep western face that defines part of a possible sector scar. It is possible that the part of the edifice with Freezland Rock at its summit postdates and occupies the collapse embayment. On the lower slope of the edifice to the west of Freezland Rock is an area of rugged topography, associated with a small seamount, which is interpreted as a recent field of lava flows. Sediment wave fields are well developed east of the island, but mostly absent in the west. The sediment waves are broadly radial, and not associated with large troughs or canyons. Their development to the east is consistent with their source sediments being moved to the east of the shallow shelf by prevailing shallow currents.

2.6.1 TOPAS profiling around Bristol Island

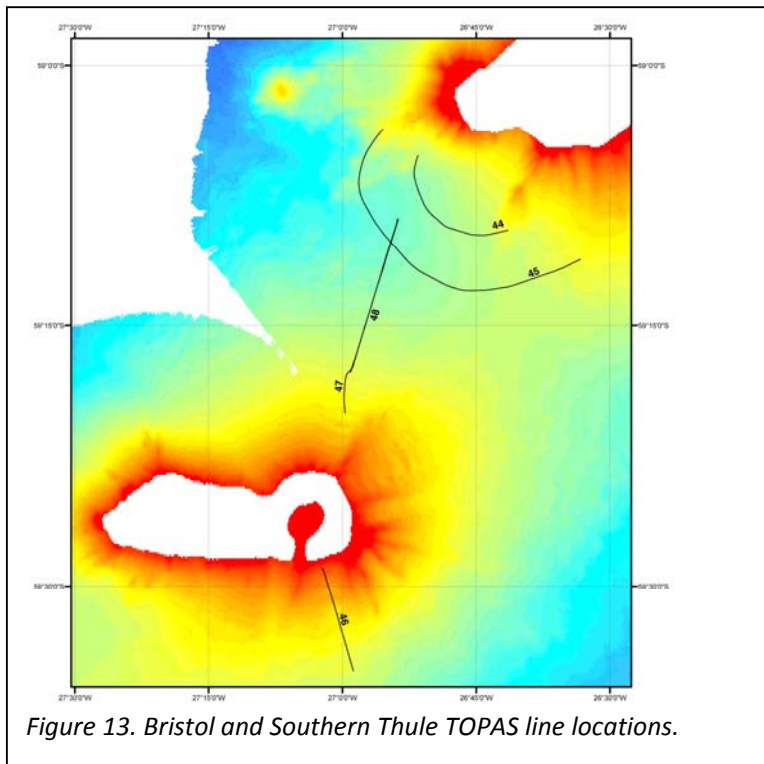


Figure 13. Bristol and Southern Thule TOPAS line locations.

Two TOPAS lines (44 and 45) were run with the EM120 across a distinctive smooth-surfaced fan structure that descends from the trough between Freezland Rock and the glacier-covered western end of Bristol Island itself (Figure 13). Unusually, the sequence profiled in the fan is acoustically homogenous, being weakly stratified and of high reflectivity throughout; the lack of a low-reflectivity upper unit suggests that it formed in a single recent event or episode of deposition. The fan may be of glaciogenic origin, in view of the extensive development of glaciers on the west side of the island, but an alternative possibility is that it developed downslope of a lava delta (comparable to the possible origin of the slope below Borley Point on Montagu Island). Such a lava delta might have formed as recently as the 1956 eruption, although there is no record of lava reaching the sea during that eruption (Holdgate & Baker 1979). Two further lines (47 and 48) were run between the Southern Thule and Bristol groups: these are discussed in the Southern Thule section.

2.7. Southern Thule

Southern Thule is relatively well-described in the literature (Holdgate & Baker 1979; Smellie et al. 1998; Leat et al. 2003; Allen & Smellie 2008). It consists of three islands, Thule, Cook and Bellingshausen. Thule is the in the west of the group, is ice covered, 5.4 m across and rises to 725 m above sea level. Cook is the largest of the group, at 6 km across and 1067 m high, and is also ice-covered. Bellingshausen is 1.7 km long, rises to 253 m and is largely ice-free. Cook and Thule islands are separated by Douglas Strait, which is underlain by a circular crater (see below). Bellingshausen Island is a recently active volcanic cone, and is persistently fumarolically active. When we sailed past the island on 12th and 13th February 2010 there was steam rising from the western side of the main crater and from the sea cliffs on the seaward side of a septum of rock, between the crater and the ocean, that runs to the

south of Jagged Point; the latter is an eastern promontory of the island comprising an eroded pyroclastic cone. There is evidence of recent volcanic activity at the summit cone of Thule (Allen & Smellie 2008). No volcanic or hydrothermal activity has been recorded on Cook Island.

The Admiralty chart indicates that Southern Thule is a single edifice rising steeply from a base around 1400-1800 m. There is no indication of a wide shelf, except to the east of Cook Island, where an apparently circular shelf some 10 km across, with Bellingshausen Island occupying its northern rim, is indicated. Previous bathymetric coverage of the area is patchy. In 1997, HMS *Endurance* surveyed Douglas Strait between Cook and Thule islands, and an area immediately to the north of this using its survey boat, and the area south of Douglas Strait using single beam echo sounder on the ship. This established that Douglas Strait is a steep-walled caldera with a floor ca. 620 m below sea level (Smellie et al. 1998). Douglas Strait caldera was resurveyed during JR149 by multibeam swath bathymetry (Allen & Smellie 2008).

The new multibeam data show that Southern Thule forms an elongate ellipsoidal structure aligned east-west in plan view. There are no wide shallow shelves. A small ridge trending SW from the edifice may be recent lavas, similar to those west of Bristol. Sediment wave fields are well-developed toward the eastern end of the group of islands, with three large fans directed to the NW, NE and SE. These are consistent with the sediment wave fields being sources from sediment moving downslope from the shallow shelf after being transported along the shelf from the western end of the group.

2.7.1. Resolution Caldera

Note on name: Resolution Caldera

This is the proposed name for the newly-discovered submarine crater immediately east of Cook Island. Resolution Point is the nearest feature on the coast of Cook Island to the west of the crater. The name commemorates Cook's ship on the voyage during which the islands were first sighted.

The area shown on the Admiralty Chart as a circular submarine structure east of Cook Island was investigated. The central area of this structure is a depression centred to the SSE of Bellingshausen Island. The notably flat floor of the depression is c. 276 m below sea level and the margins were mapped to the west and south, where steep walls rise to <150 m. To the east, the chart shows reefs rising to as shallow as 35 m. To the north, the depression is bounded by Bellingshausen Island. The depression therefore appears to be roughly circular in plan, and some 3-4 km across (Figure 14). It is interpreted as a volcanic crater, here called Resolution Caldera, and is most likely, in view of its size, a collapse caldera. Resolution Caldera is approximately the same size as, although shallower than, Douglas Strait crater, which is also a collapse caldera. The two calderas are aligned with the Thule-Cook axis of Southern Thule.

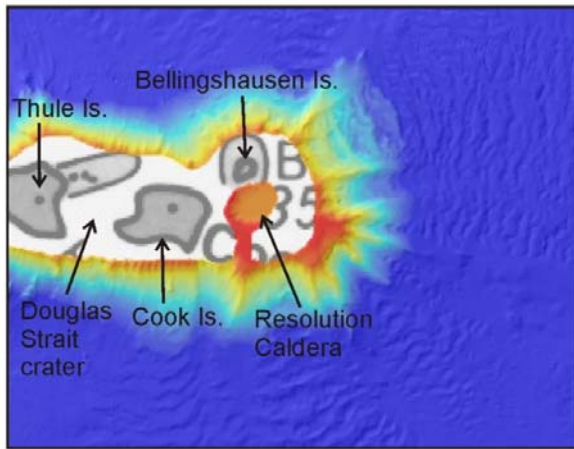


Figure 14. New bathymetric map of Southern Thule, showing the newly mapped and named Resolution Caldera. The swath data are superimposed on an Admiralty chart, showing the approximate relative positions of the islands of Southern Thule.

2.7.2. TOPAS profiling around the Southern Thule group

Three TOPAS lines were run in the immediate vicinity of the Southern Thule group (see Figure 13, section 2.6, for locations). The most noteworthy of these are lines 47 and 48 which follow the same course under different chirp settings, and so provide different degrees of sediment penetration and signal resolution. These lines cross the boundary between the sediment waves sourced from the eastern end of the Southern Thule group and the smooth-surfaced fan sourced from Bristol and as such provide data on the relative ages and interactions of the two types of sedimentation. Initial study of the results indicates that the fan deposits overlie the downslope end of the sediment wave field in the saddle between the two volcanoes: the indicated younger age for the fan is consistent with the idea that it may be a very young feature produced by collapse of relatively recent lava deltas, as the ongoing glaciation and coastal erosion in both island groups would be expected to lead to a more complex interfingering relationship if both fan and sediment wave field were linked to glacial erosion of both islands.

2.8. The southern submarine arc volcanoes: Vysokaya Bank, Kemp and Nelson seamounts.

Note on names: Vysokaya Bank, Kemp Seamount, Adventure Seamount and Caldera, Nelson Seamount.

Vysokaya Bank is a recently approved official name for the relatively shallow area forming the southernmost, submarine part of the main South Sandwich arc SE of the Southern Thule edifice and around Kemp seamount. Kemp Seamount and Nelson Seamount are unofficial names, of long usage, for individual seamounts in the southern part of the arc (Barker 1995; Leat et al. 2004). They are named after the authors of the report of the 1939 RRS *Discovery* survey of the South Sandwich Islands (Kemp & Nelson 1931). Kemp Seamount is situated within Vysokaya Bank, and we use the term to mean the well-defined and long-recognised

seamount located by RRS *Discovery* in 1985 and sampled by dredge DR.112 during that cruise (Hamilton 1989; Leat et al. 2004). We propose the name Adventure Seamount for the newly discovered seamount, mapped for the first time on JR206, east of Kemp Seamount. This seamount has a clearly defined summit crater that was evidently caused by collapse. We name this crater Adventure Caldera (Figure A7.4). Adventure was the small stores ship that accompanied the Resolution during the first part of Cook's voyage around the southern ocean, during which the southern South Sandwich Islands were first discovered. Nelson seamount is to the south of Vysokaya Bank, forming the extreme southern volcano of the arc. Nelson Seamount located by RRS *Discovery* in 1985 and sampled by dredge DR.111 during that cruise (Hamilton 1989; Leat et al. 2004).

This is a complex area where several terrains meet at the southern edge of the Sandwich plate. Vysokaya Bank, which includes Kemp Seamount, and is regarded as representing the southernmost major volcano of the South Sandwich arc. Nelson seamount is in an anomalous position, being south of the main arc of volcanoes. To the west, the East Scotia Ridge spreading centre converges with the south end of the arc at segment E10. To the east of E10, the transform margin at the south end of the arc meets the trench at another triple junction. The area is entirely below sea level, and was previously mostly unsurveyed, although some areas have been investigated. Dredges were made of Kemp and Nelson seamounts in 1985, and were described by Hamilton (1989). The area around the southern plate margin was investigated using GLORIA data, which has been used in descriptions of the tectonics of the area (Larter et al., 2003 and references therein). The MR1 multibeam and sidescan sonar survey of JR09A of the East Scotia Ridge (Livermore et al. 1997; Fretzdorff et al. 2002) extended to the western edge of the southern arc, and included the west flank of Nelson seamount. Dredges from the area were geochemically analysed by Leat et al. (2004), who interpreted basalts and basaltic andesites from Kemp Seamount (DR.112) as part of the main volcanic arc, and showed that dacites from Nelson Seamount (DR.111) are anomalous, and interpreted their magmas to contain a high component of subducted sediment, and linked this to the plate-edge position of the seamount.

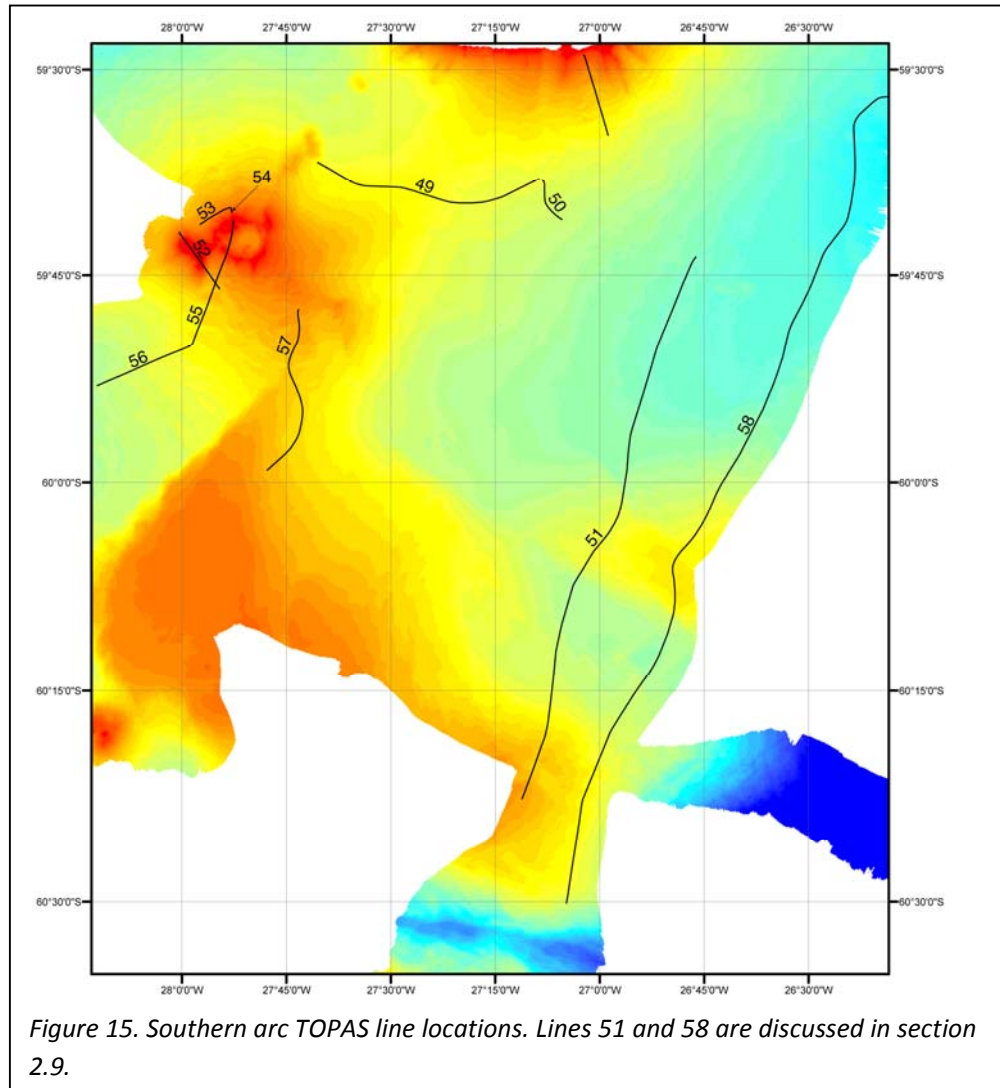
Previous bathymetric coverage of the area is patchy. JR149 crossed the area and collected passage data. JR224 surveyed the Kemp seamount and the area immediately to the west, where a caldera was discovered (not to be confused with 'Adventure Caldera', which is further east).

We mapped Vysokaya Bank from the south of the Southern Thule edifice to the SW, except for Kemp Seamount and the crater to the west of it, which had been previously mapped. The shallowest summit of Vysokaya Bank is revealed as a seamount, herein named 'Adventure Seamount', with a circular central crater 5 km in diameter. The crater of Adventure has a generally flat floor at ~750 m below sea level, and a rim that rises to 180 to 380 m below sea level. The rim and walls of the crater are well-preserved, and a smaller 0.7 km diameter crater was mapped on its northern rim; two other, smaller cones with summit craters may also be present on this rim. The Adventure Caldera is interpreted as a relatively young collapse caldera. The volcanoes Adventure, Kemp seamount and the crater to the

west of Kemp form an E-W volcanic line that parallels that formed by Resolution Caldera, Cook Island, Douglas Strait crater and Thule Island in the Southern Thule group, implying similar structural and magmatic control. Sediment wave fields extend to the NW, east and SW of Adventure Caldera.

Nelson Seamount is revealed as a steep-sided cone rising to 198 m below sea level, within a group of smaller seamounts.

2.8.1. TOPAS sub-bottom profiling within the southern arc



A number of TOPAS lines were run within the southern portion of the arc. The majority of these lines were recorded at relatively high vessel speed and at a long ping rate interval as the TOPAS system was run alongside the EM120 system.

Lines 55 and 56 were run as dedicated TOPAS lines with high ping rate, down a sediment wave field that descends from the Adventure Caldera and is deflected west along the NW side of a large bank to the south (section 2.9). This field is characterized by a very much more rapid downslope decrease in sediment wave amplitude than most other sediment

wave fields profiled, from over 200 m amplitudes at 1000 to 1500 m water depth to less than 60 m amplitudes at around 1800 m water depth. Furthermore, the sediment wave field is of comparable area to those found around the islands to the north, whereas the potential source has a much smaller area. These differences suggest that the Adventure sediment waves may have a different origin from those around the islands to the north. In view of the presence of the summit caldera, one possibility is that they are the products of a large explosive eruption as proposed for similar wave-like features around submarine calderas of the Kermadec arc (Wright et al. 2006). However, the seamount is likely to have been emergent during glacial sea level low stands, suggesting that coastal erosion to form clastic sediments may also have been a possible sediment source.

2.8.2. Dredge samples from eastern end of Kemp seamount group

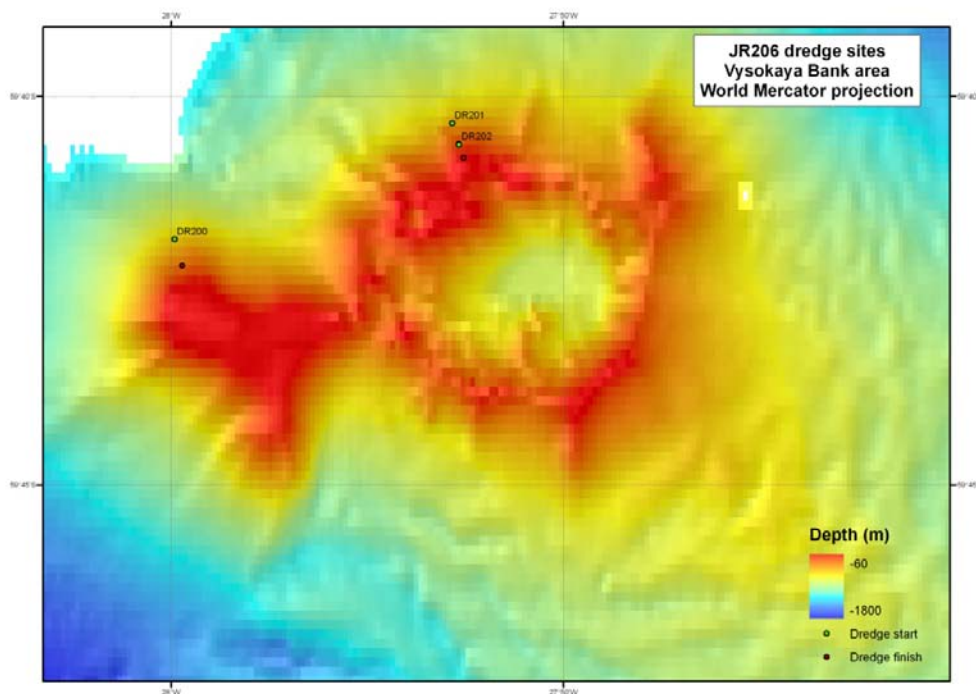


Figure 16. Dredge sites on Adventure Seamount (Vysokaya Bank), near Adventure Caldera which is the prominent depression in the centre of the diagram.

Dredges 200 through 202 were conducted on the western and northern sides of Adventure Seamount (Figure 16). Dredge 200 was located on the northern side of a plateau that projects to the west from Adventure Caldera. The plateau may form a relatively old part of the volcano. Dredges 201 and 202 were on the northern outer slope of Adventure Seamount. Two dredges were carried out at the latter site because the first encountered a snag that led to snapping of the first weak link and the haul was restricted to a small number of clasts in the dredge bucket. Whilst the dredges were dominated by pyroclastic, mainly scoriaceous, rocks that are believed to be of relatively evolved compositions on first examination, pumiceous clasts comparable to those found in the Protector Seamounts area were notably absent. This suggests that the caldera edifice has been draped by the products

of post-caldera eruptions from the small cones and craters (at least three) that occur on the rim of the caldera.

2.9. Tectonic structures and sedimentation south and east of the volcanic arc

Bathymetric mapping during JR206 was extended to areas south and east of the southern half of the arc in order to consider the relationships of the arc volcanism to the southern boundary of the Sandwich plate. This area is bounded by the southernmost segment (E10) of the East Scotia spreading centre to the west, the transform plate boundary between the Sandwich plate and the Antarctic plate to the south, and the subduction zone between the Sandwich plate and the South America plate to the east. Two triple junctions are present, and the plate geometry is notably unstable. We therefore anticipated that this would be an area of complex deformation. We also sought to investigate the relationship of the arc, and sedimentation from the arc volcanoes, to the little-mapped fore-arc rise that separates the southern half of the arc from the trench but dies out to the northeast of Montagu Island.

2.9.1. Bathymetric mapping results

A large bank (Bank B; see Figure A7.4) was mapped between 59°52'S and 60°20'S. The bank forms an escarpment, with a steep west flank and gentle east flank. The summit area is flat and extensive, rising to ca. 650 m below sea level.

The northwest and southwest scarps are irregular and scalloped, with no evidence of deformation cutting sediments at the scarp bases, suggesting that they are now inactive structures. The feature is interpreted as a rotated fault block related to the initial rifting to form the East Scotia Sea spreading centre. The rifted crust may have been pre-existing arc terrain or continental crust.

Discussion box: Faults within Bank B.

Faults to the east of Bank B were partly mapped and may form an east-west trending, left-stepping *en echelon* array of oblique slip faults with a scissors-type geometry (the direction of downthrow reverses along the length of each fault segment). Minor, more north-south trending fault scarps cut the top surfaces of the uplifted fault blocks and well-defined troughs at the bases of the main fault scarps are interpreted as the surface expressions of antithetic extensional faults (see also discussion of TOPAS lines 51 and 58, below). These features imply that the *en echelon* structures are still active and have a right-lateral transtensional geometry. Movement on them may relate to the right-lateral transform plate boundary to the south.

Also present on the gentle east slope of the main bank is an area of symmetrical undulations, with crests trending broadly north-south. These may be sediment waves, and if so may be contourites related to regional westerly deep currents as there is no local sediment source or marked slope.

To the north of Bank B and east of the arc, the transition to the outer arc high is marked by a nearly flat plain, punctuated by a series of steep-sided irregular highs with east-west trends, and gentle slopes up toward the fore-arc high. The highs have irregular scalloped margins, suggesting old inactive fault scarps.

2.9.2. TOPAS profiles

Two long TOPAS profiles were obtained by running the TOPAS system along with EM120 during two broadly north-south mapping swaths: these are lines 51 and 58 (Figures 12 and 15). Both cross the *en echelon* fault system in the south, whilst line 58 extends north past all the southern islands as far Montagu. Despite the need to run the TOPAS at low ping rate during EM120 operations, useful results were obtained over areas of flat to gently inclined seabed. These include the bases of the *en echelon* fault scarps, where the troughs at the scarp bases were found to be bounded by faults cutting right up through the sediment sequences to the seabed, confirming that this is an active fault system; slump features were also present deeper in the profiled sections, again indicating recent activity on the faults.

Further north, Line 58 shows the transition from the flat plain, which includes the distal end of the sediment wave fields descending from Bristol and Montagu islands, to the margins of the fore-arc rise, in an area from 59°0'S to 58°27'S. The rise is draped in a well-stratified sediment sequence which was well imaged to depths of 35 ms TWTT with the transition from upper low-reflectivity to lower high-reflectivity units well developed at around 15 ms TWTT. The upper unit is largely planar-stratified; north-directed onlap is evident toward the base of the imaged sequence on the south side of the rise whilst the lower unit shows evidence of disturbance and slumping further north.

Overall, these two TOPAS profiles confirm that the east-west trending *en echelon* fault system to the south of the arc is active, but also show that there is little deformation ongoing in the area between the southern half of the arc and the western margin of the fore-arc rise; this does not however exclude the possibility of active deformation further to the east.

2.10. Summary of overall trends and processes

Discussion

Overall, results from JR206 combined with those from JR168 (Tate & Leat 2007; Leat et al. 2010) indicate that the South Sandwich arc consists of four main sections characterized by different combinations of style of volcanism, orientation of tectonic and volcanic features, and bathymetry.

Protector Seamounts area (northern seamounts). This consists of a broadly E-W trending group of relatively small, polygenetic (stratovolcano) seamounts, some with distinct summit craters or lateral collapse structures, located around a central plateau at < 1000 m water

depth with an area to the north and east cut by mainly NE-trending fault scarps. Dredge samples collected on JR206 indicate a broadly rhyolitic to dacitic compositional range for these seamounts, consistent with limited previous sampling (Leat et al. 2007).

Northern volcanic islands (Zavodovski to Saunders). These volcanoes rise from ca. 3000 m water depth, the islands are relatively small and there is also a number of discrete seamounts. The island volcanic edifices are mainly of basaltic and basaltic andesite composition (from previous studies), although andesites and dacites form the recent Lucifer Hill volcano on Candlemas Island, and andesite occurs on Leskov Island. The submarine volcanoes are associated with distinctive gullied and eroded terrains, which tend to be on their eastern sides. Extensive sediment wave fields occur on the eastern sides of Zavodovski and Saunders, with only limited sediment wave field development to the west. Sediment wave amplitudes in these fields are typically 50 to 100 metres. Three distinct NE to SW-trending chains of seamounts (one of which is emergent to form the island of Leskov) are situated to the west of the islands and appear morphologically young, suggesting relative westward migration of the volcanism with time. Little or no faulting is evident around or between these islands.

Southern volcanic islands (Montagu, Bristol and the Southern Thule). These islands are larger than the northern islands and rise from a broad ridge at about 2000 m water depth. These islands lie to the west of the outer or fore-arc rise that is present in the southern part of the arc. Calderas are present in all except Bristol, whose interior structure is poorly known. Onshore studies indicate that dacites are locally present and may be spatially associated with calderas. The volcanic edifices (including submarine flank vents) tend to be E-W elongated (or aligned in an east-west chain, in the case of the Southern Thule group). Apparently recent satellite lavas and cones occur west of the islands, but apart from that, there is known no clear age trend. Large sediment wave fields are present around all of these islands, perhaps associated with intense glacial as well as coastal erosion; a tendency to greater sediment wave development on their eastern sides is present but less pronounced than around the northern islands. Maximum sediment wave amplitudes exceed 200 metres around Montagu but are generally around 100 m. Little or no faulting is evident around or between these islands.

Southern seamounts (Kemp, Nelson and newly discovered features). Vysokaya Bank has an east-west alignment, and two calderas are present. This bank resembles southern Thule. Previous dredging shows the presence of dacitic rocks on Nelson. Sediment waves are present, with amplitudes up to 200 metres around the newly-discovered Adventure seamount caldera, but showing rapid downslope decrease in amplitude and other anomalous features. Fault scarps with various orientations (mainly E-W to NW-trending) and a large tilted submarine plateau are present in this southernmost part of the arc.

This distribution of structural and volcanic features is broadly symmetrical north to south, with the Protector Seamounts area having some similarities with the southern seamounts, and contrasting with the central areas. This may reflect transitions to more strike-slip or

transform plate boundaries at either end of the arc. The greater edifice base depths to the north of the central part of the arc coincides with a number of other features: the north end of the fore-arc ridge; the north end of more recent rifting to form the back-arc; possibly the northern limit of older crustal components, exemplified by the tilted Bank B south of Kemp, and the fore-arc highs. There is also a northward transition from E-W to NE-SW to structural trends in the arc. It is possible that the northern half of the arc is undergoing higher rates of extension, although the crust in the southern part of the arc may also be thicker and structurally more heterogeneous. At the south end of the arc, the Sandwich plate abuts the transform plate boundary between the South American and Antarctic plates, which may generate less extension than in the north, where the South American plate is tearing as it enters the subduction zone.

JR206 results show that there are fewer lateral collapse features in the South Sandwich arc than in intra-oceanic volcanic arcs elsewhere, such as the Lesser Antilles and the Bismarck arc (Silver et al., 2009). Those lateral collapse structures that were identified are mainly on the flanks of seamounts and the just-emergent island of Leskov. In contrast, the sediment wave fields first identified around islands in the north of the volcanic arc (Leat & Tate, 2007) were found to be very abundant and very well developed, especially on the eastern sides of the islands. This asymmetry suggests that the sediment wave fields are fed by sediment transported along the coasts of the islands and in shallow water by currents driven by the prevailing westerly winds. High sediment fluxes are likely responsible for the very well developed features of the sediment wave fields, and to reflect high rates of coastal and glacial erosion on the islands in the prevailing cold and stormy climate.

An alternative interpretation, that the sediment wave fields are the products of eruption column collapse producing dense submarine sediment flows during violent explosive eruptions (Wright et al., 2006), may apply to the anomalous sediment waves around the submarine Adventure Caldera. However, this interpretation seems unlikely in the case of the majority of the sediment wave fields because of their asymmetric distribution, the lack of other evidence for large-volume eruptions on islands without calderas (for example, Saunders, Candlemas and Zavodovski, all of which have well-developed sediment wave fields), and the presence in the majority of the sediment wave fields (with the exception, again, of the Adventure sediment wave fields) of the region-wide contrast between upper low reflectivity and lower high reflectivity units in the TOPAS profiles.

The low abundance of lateral collapse structures on the flanks of the emergent islands and the high abundance of sediment wave fields may be linked, as high rates of erosion of the upper parts of the edifices and transport of the resulting sediment to the lower flanks in the sediment wave systems will tend to reduce overall slope angles and to stabilize the edifices against catastrophic slope failures. At the other end of what may be a spectrum of island arc systems, in the Bismarck volcanic arc sediment wave systems are mainly found around caldera volcanoes and offshore from major river systems (Hoffmann et al., 2010) and are almost entirely absent around the steep-sided stratovolcano type of volcanic island. Many such islands in the Bismarck arc do have one or more lateral collapse debris avalanche

deposits (Silver et al., 2009). Located in the semi-enclosed Bismarck Sea and on the equator (and so are not affected by tropical cyclone storm systems), the Bismarck arc stratovolcanoes experience low rates of coastal erosion (and by implication, offshore sediment transport) by comparison with the South Sandwich Islands, leading to the intriguing possibility of a regional climate control upon volcanic island erosion and mass wasting mechanisms.

Acknowledgements

We are grateful to Captain Burgan and officers and crew of the RRS James Clarke Ross for their tremendous help in carrying out this science cruise.

We are grateful to the Antarctic Funding Initiative (AFI) of NERC for making the participation of Simon Day and Matt Owen possible.

References

- Allen, C.S. & Smellie, J.L., 2008. Volcanic features and the hydrological setting of Southern Thule, South Sandwich Islands. *Antarctic Science*, 20, 301-308.
- Barker, P.F., 1995. Tectonic framework of the East Scotia Sea. In: Taylor, B. (ed.) *Backarc Basins: Tectonics and Magmatism*. Plenum Press, New York, 281-314.
- Carracedo, J.-C., Day, S.J., Guillou, H. & Gravestock, P., 1999. The later stages of the volcanic and structural evolution of La Palma, Canary Islands: The Cumbre Nueva giant collapse and the Cumbre Vieja volcano. *Geological Society of America Bulletin* 111, 755 – 768.
- Cunningham, A.P., Barker, P.F. & Tomlinson J.S., 1998. Tectonics and sedimentary environment of the North Scotia Ridge region revealed by side-scan sonar. *Journal of the Geological Society, London*, 155, 941-956.
- Dowdeswell, J.A., O Cofaigh, C., Taylor, J., Kenyon, N.H., Mienert, J. & Wilken, M., 2002. On the architecture of high-latitude continental margins: the influence of ice sheet and sea-ice processes in the Polar North Atlantic. In: Dowdeswell, J.A. & O Cofaigh, C. (eds.) *Glacier-Influenced Sedimentation on High Latitude Continental Margins*. Geological Society, London Special Publication 203, 33-54.
- Fretzdorff, S., Livermore, R.A., Devey, C.W., Leat, P.T. & Stoffers, P., 2002. Petrogenesis of the back-arc East Scotia Ridge, South Atlantic Ocean. *Journal of Petrology*, 43, 1435-1467.
- Global Volcanism Program, 2010. Index of Monthly Activity Reports for Montagu Island. http://www.volcano.si.edu/world/volcano.cfm?vnum=1900-081&volpage=var#bgvn_3307 Date accessed: 7 February 2010.
- Graham, A.G.C., Fretwell, P.T., Larter, R.D., Hodgson, D.A., Wilson, C.K., Tate, A.J. & Morris, P., 2008. A new bathymetric compilation highlighting extensive paleo-ice sheet drainage

on the continental shelf, South Georgia, sub-Antarctica. *Geochemistry, Geophysics, Geosystems* 9(7) Q07011, doi:10.1029/2008GC001993

Hamilton, I.W., 1989. Geophysical investigations of subduction related processes in the Scotia Sea, Ph.D. thesis, University of Birmingham.

Hoffmann, G., Silver, E., Day, S., Morgan, E., Driscoll, N. & Orange, D., 2008. Sediment waves in the Bismarck Volcanic Arc, Papua New Guinea. *Geological Society of America Special Paper* 436, 91 – 126.

Hoffmann, G., Silver, E., Day, S.J., Driscoll, N. & Orange, D., 2010. Deformation versus deposition of sediment waves in the Bismarck Sea, Papua New Guinea, in: Shipp, R.C., Weimer, P. & Posamentier, H.W. (Eds.), *Mass Transport Deposits in Deepwater Settings*, SEPM (Society for Sedimentary Geology), Tulsa, Special Publications, 95, in press.

Holdgate, M.W. & Baker, P.E., 1979. The South Sandwich Islands: I. General Description. *British Antarctic Survey Scientific Reports*, No. 91.

Kemp, S.W. & Nelson, A.L., 1931. The South Sandwich Islands. *Discovery Reports*, 3, 133-198.

Larter, R.D., Vanneste, L.E., Morris, P., & Smyth, D.K., 2003. Tectonic evolution and structure of the South Sandwich arc, in: R.D. Larter, P.T. Leat (Eds.), *Intra-Oceanic Subduction Systems: Tectonic and Magmatic Processes*, Geological Society, London Special Publication, 219, 255– 284.

Leat, P.T., Pearce, J.A., Barker, P.F., Millar, I.L., Barry, T.L. & Larter R.D., 2004. Magma genesis and mantle flow at a subducting slab edge: the South Sandwich arc-basin system. *Earth and Planetary Science Letters*, 227, 17-35.

Leat, P.T., Larter R.D. & Millar I.L., 2007. Silicic magmas of Protector Shoal, South Sandwich arc: indicators of generation of primitive continental crust in an island arc. *Geological Magazine*, 144, 179-190.

Leat, P.T., Tate, A.J., Tappin, D.R., Day, S.J. & Owen, M.J., 2010. Growth and mass wasting of volcanic centres in the northern South Sandwich arc, south Atlantic, revealed by new multibeam mapping. *Marine Geology*, doi:10.1016/j.margeo.2010.05.001.

Lee, H.J., Syvitski, J.P.M., Parker, G., Orange, D., Locat, J., Hutton, E.W.H. & Imran, J., 2002. Distinguishing sediment waves from slope failure deposits: field examples, including the 'Humboldt slide', and modeling results. *Marine Geology*, 192, 79-104.

Livermore, R., Cunningham, A., Vanneste, L. & Larter, R., 1997. Subduction influence on magma supply at the East Scotia Ridge. *Earth and Planetary Science Letters*, 150, 261-275.

Patrick, M.R., Smellie, J.L., Harris, A.J.L., Wright, R., Dean, K., Izbekov, P., Garbeil, H. & Pilger, E., 2005. First recorded eruption of Mount Belinda volcano (Montagu Island), South Sandwich Islands. *Bulletin of Volcanology* 67, 415-422.

Silver, E., Day, S.J., Ward, S.N., Hoffmann, G., Llanes-Estrada, P., Lyons, A., Driscoll, N., Perembo, R., John, S., Saunders, S., Taranu, F., Anton, L., Abiari, I., Appelgate, B., Engels,

- J., Smith, J. & Taglioides, J., 2005. Stratovolcano lateral collapses in the Bismarck volcanic arc, R/V Kilo Moana KM0419 Cruise Report.
- Smellie, J.L., Morris, P., Leat, P.T., Turner, D.B. & Houghton, D., 1998. Submarine caldera and other volcanic observations in Southern Thule, South Sandwich Islands. *Antarctic Science*, 10, 171-172.
- Tate, A.J. & Leat, P.T., 2007. RRS James Clark Ross JR168 Cruise Report, Swath Bathymetry South Sandwich Islands, British Antarctic Survey Report ES6/1/2007/1.
- Wright, I.C., Worthington, T.J. & Gamble, J.A., 2006. New multibeam mapping and geochemistry of the 30°-35° S sector, and overview, of the southern Kermadec arc volcanism. *Journal of Volcanology and Geothermal Research*, 149, 263-296.

Appendix 1. EM120 log for cruise JR206.

Time	Latitude	Longitude	Depth - EM120	Wind Speed	Heading	Comment	User
18/01/2010 13:55	- 51.6897	-57.825		1.98	217.82	Depart FIPASS	ajtate
18/01/2010 17:50	- 51.7227	-57.499		20.86	111.93	EM120 on in 100m water depth using XBT profile jr73_02.asvp, a nearby xbt with similar water temp/salinity.	ajtate
18/01/2010 18:08	- 51.7459	-57.401	174.31	21.77	109.73	EM120 started logging to survey jr206_a. Beams at 60 degrees.	ajtate
18/01/2010 18:43	- 51.7875	-57.215	303.73	25.26	108.95	EM120 line increment for test purposes.	ajtate
18/01/2010 20:12	- 51.8871	-56.774	633.55	21.01	109.26	Deployed xbt 1	ajtate
18/01/2010 20:23	- 51.8963	-56.735	626.45	21.49	108.35	Yaw stabilization turned to off from filtered heading.	ajtate
18/01/2010 20:24	- 51.8974	-56.729	627.07	22.2	108.27	jr206_xbt1.asvp loaded into EM120.	ajtate
19/01/2010 12:49	- 53.0927	-51.339	2600.39	17.89	113.84	Deployed xbt 2.	ajtate
19/01/2010 13:00	- 53.1017	-51.301	2612.34	18.25	110.53	jr206_xbt2.asvp uploaded to EM120 logging to line 22	ajtate
19/01/2010 14:39	- 53.2191	-50.761	1790.24	15.98	109.37	SSU now controlling TOPAS - swath artifacts now much reduced.	ajtate
20/01/2010 11:40	- 54.0004	-43.889	3099.25	14.42	104.76	Deployed xbt 3.	ajtate
20/01/2010 12:02	- 54.0134	-43.799	3078.92	18.04	105.49	jr206_xbt3.asvp loaded into EM120 logging to line 46.	ajtate
20/01/2010 22:30	- 54.3564	-40.279	1518.69	6.35	104.58	Survey jr206_a stopped. Survey jr206_b started.	ajtate
21/01/2010 03:24	- 54.3482	-39.852		7.76	120.06	pulled port beam in to 60 degrees	tde
21/01/2010 03:36	- 54.3576	-39.8	544.19	4.07	95.96	Port and starboard beams brought in to 55 degrees	tde
21/01/2010 03:52	- 54.3618	-39.725		8.86	103.82	Port and starboard beams brought in to 45 degrees	tde
21/01/2010 04:07	- 54.3502	-39.661		9.07	70.42	Ship turned, bad data cleared. Poor data quality probably due to swell direction. Swath beams taken back out to 65 degrees.	tde
21/01/2010 10:07	- 54.3135	-39.854	1045.28	13.62	179.44	Swath logging turned off as crossing previously swathed area.	tde
21/01/2010 10:14	- 54.3369	-39.852	518.85	12.86	177.73	Swath logging commenced after very noisy patch to line 13.	tde
21/01/2010 16:00	- 54.5057	-39.49	2268.62	20.73	307.54	Swath turned off.	tde
21/01/2010 18:12	- 55.0515	-38.593	3883.47	9.82	128.29	Swath on and logging to line 19, survey jr206_b.	tde
21/01/2010 20:20	- 54.6465	-39.022	1260.88	22.09	20.46	Swath stopped logging.	tde

21/01/2010 20:23	- 54.6411	-39.021	1492.24	21.12	351.21	Swath turned off.	tde
22/01/2010 10:34	- 55.0515	-38.593	3883.47	9.82	128.29	Swath logging on, logging to line 22, survey jr206_b.	tde
22/01/2010 12:00	- 55.1453	-38.444	3873.82	8.17	235.22	Deployed xbt 4.	tde
22/01/2010 12:13	- 55.1668	-38.477	5285.66	8.1	225.71	jr206_xbt4.asvp loaded into EM120 logging to line 24, survey jr206_b.	tde
22/01/2010 15:21	- 55.0149	-38.739	3883.7	7.16	29.32	Swath off. End of survey jr206_b.	tde
23/01/2010 04:38	- 55.2091	-38.174	3772.47	16.08	160.39	Swath on. Start of survey jr206_c.	tde
23/01/2010 22:14	- 54.7095	-41.053	3470.9	21.4	284.79	jr206_xbt3.asvp loaded into EM120 logging to line 20, survey jr206_c.	tde
24/01/2010 14:05	- 53.5882	-47.332	3639.05	17.13	289.18	jr206_xbt2.asvp loaded into EM120 logging to line 39, survey jr206_c.	tde
25/01/2010 06:31	- 52.3401	-53.79	2122.26	36.23	298.45	Swath off due to bad weather approaching Falklands.	tde
25/01/2010 19:26	- 51.6877	-57.833	139.44	19.13	305.75	Arrive Stanley Harbour.	tde
26/01/2010 14:56	- 51.6919	-57.821	139.44	29.56	103.69	Left FIPASS	tde
26/01/2010 16:39	- 51.7635	-57.398	185.64	32.23	114.64	Swath on and logging to line 57, survey jr206_a. (Can delete small line 1 at this time only a few pings.) Using jr73_02.asvp for velocity profile as per Jday18.	tde
26/01/2010 18:32	- 51.8909	-56.855	488.7	28.34	114.29	jr206_xbt1.asvp loaded into EM120 logging to line 59.	tde
27/01/2010 18:31	- 53.5628	-49.259	3398.62	20.25	93.21	jr206_xbt2.asvp loaded into EM120 logging to line 83, survey jr206_a. Shag Rocks Passage.	tde
28/01/2010 13:16	- 54.2189	-42.764	3020.07	16.32	92.32	jr206_xbt3.asvp loaded into EM120 logging to line 102, survey jr206_a. South of Shag Rocks Passage.	tde
28/01/2010 17:14	- 54.2804	-41.416	2460.49	21.08	97.26	Swath off.	tde
28/01/2010 17:37	- 54.2923	-41.293	2469.43	20.82	98.37	Swath on, logging to line 107, survey jr206_a.	tde
28/01/2010 21:58	- 54.5687	-39.958	4114.54	31.62	141.15	Swath off. Last line logged 112.	tde
29/01/2010 07:12	-55.214	-37.493	3232.06	27.66	107.93	Swath on, logging to line 1, survey jr206_d.	tde
29/01/2010 11:04	- 55.4196	-36.34	1784.46	29.57	117.66	jr206_xbt4.asvp loaded into EM120 logging to line 5, survey jr206_d. Southern end of South Georgia.	tde
30/01/2010 07:02	-55.566	-29.895	4108.04	18.72	89.54	Stop logging to jr206_d. Start logging to jr206_e.	tde
30/01/2010 09:25	- 55.6307	-29.086	3059.88	12.85	133.09	Deploy XBT 5.	tde
30/01/2010 11:01	- 55.8105	-28.664	2143.82	13.71	126.79	jr206_xbt5.asvp loaded into EM120 logging to line 5, survey jr206_e	tde
30/01/2010 12:15	- 55.8304	-28.506	787.65	16.94	134.01	EM120 interface froze as zooming in on survey display during line 6. Pinging continues on SSU.	tde

30/01/2010 12:30	-55.827	-28.499	691.22	12.75	335.94	Swath back on after freezing. Logging to line 7, survey jr206_e.	tde
30/01/2010 13:02	- 55.8225	-28.513	949	11.26	290.13	Swath off for dredge.	tde
30/01/2010 14:40	- 55.8147	-28.529	860.83	11.6	329.46	Swath on somewhere around here for transit.	tde
30/01/2010 16:20	- 55.9482	-28.45	1210.62	19.14	244.04	Swath off for test CTD station.	tde
30/01/2010 19:18	- 55.9305	-28.391	1212.65	25.25	70.42	Swath on and logging to line 10, survey jr206_e. Noisy turning onto line.	tde
30/01/2010 19:43	- 55.8921	-28.296	5.85	23.82	348.43	EM120 interface freezing.	tde
30/01/2010 19:47	- 55.8888	-28.297	839.54	22.46	342.38	EM120 interface freezing issues clear up without explanation.	tde
30/01/2010 19:57	- 55.8828	-28.298	642.55	27.55	359.44	Swath off at dredge site.	tde
30/01/2010 21:10	- 55.8796	-28.298	432.53	16.31	331.03	Swath on.	tde
30/01/2010 22:00	- 55.9532	-28.176	647.04	18.29	133.14	Swath on, logging to line 15, survey jr206_e.	tde
30/01/2010 22:18	- 55.9514	-28.107	526.17	22.66	67.98	Swath off.	tde
31/01/2010 00:26	- 56.1124	-27.956	5.98	24.96	358.56	Swath on, logging to line 16. Survey 206_e.	tde
31/01/2010 09:24	- 55.7845	-28.395	6.44	37.24	341.71	Swath off due to bad weather. Line 24, Survey jr206_e.	tde
31/01/2010 09:48	- 55.7566	-28.4	1394.23	36.63	320.01	Swath on, logging to line 25, survey jr206_e.	tde
31/01/2010 12:03	-55.684	-28.522	2262.36	37.53	290.94	Beams brought in to 62 degrees.	tde
31/01/2010 12:20	-55.678	-28.534	6.32	36.74	292.29	Swath ping display freezes.	tde
31/01/2010 12:30	- 55.6743	-28.54	2222.37	39.47	297.08	Swath beams brought in to 45 degrees.	tde
31/01/2010 12:35	- 55.6727	-28.543	2214.23	45.44	293.84	EM120 stopped and restarted as consistently not finding bottom.	tde
31/01/2010 13:40	- 55.6479	-28.584	2505.61	36.16	281.3	Swath beams out to 55 degrees.	tde
31/01/2010 19:35	- 55.6068	-28.84	3	47.6	258.11	Logging stopped - too rough.	tde
31/01/2010 19:44	- 55.6082	-28.846	2738.05	46.86	256.78	Swath on and logging.	tde
31/01/2010 22:04	- 55.6208	-28.971	3097.72	36.14	255.73	Swath off.	tde
01/02/2010 10:14	-55.689	-29.704	3439.97	26.86	238.14	Start logging swath though still hove to, as outside previously swathed area.	tde
01/02/2010 16:00	- 55.8917	-30.134	3616.75	18.07	63.57	Turn NE and return to survey area after being hove to into weather. Beams back to 65 degrees.	tde
01/02/2010 18:00	- 55.6695	-29.409	4038.96	16.39	66.74	Swath off as repeating earlier lines. Line 47, survey jr206_e.	tde
01/02/2010 19:17	- 55.5749	-28.958	2871.52	13.1	88.69	Swath on, logging to line 48, survey jr206_e. Beams to 63 degrees.	tde

02/02/2010 10:41	- 55.9163	-27.606	782.33	24.13	233.68	Swath off as on existing lines. Line 63, survey jr206_e.	tde
02/02/2010 14:20	-55.966	-27.841	548.32	19.26	298.96	Swath on, logging to line 64, survey jr206_e.	tde
02/02/2010 14:42	- 55.9644	-27.842	478.95	19.26	308.64	Swath off.	tde
02/02/2010 14:53	- 55.9644	-27.842	479.58	19.34	297.55	Swath on.	tde
02/02/2010 15:35	- 55.9346	-27.87	578.99	19.46	319.82	Swath off.	tde
02/02/2010 18:34	- 56.0552	-28.223	1476.09	17.04	175.09	Swath on, logging to line 67, survey jr206_e.	tde
02/02/2010 18:59	- 56.1383	-28.213	2553.86	23.31	312.3	Swath off.	tde
02/02/2010 22:28	- 56.0497	-28.332	1857.1	24.07	322.73	Swath on.	tde
03/02/2010 09:27	- 55.8826	-28.14	457.41	20.93	102.54	Swath off. Line 79, survey jr206_e.	tde
03/02/2010 19:04	- 56.3583	-27.462	229.94	19.28	154.31	Swath on, logging to line 80, survey jr206_e.	tde
03/02/2010 19:20	- 56.4064	-27.415	521.44	21.75	152.11	Processing note: most of first 10 mins is rubbish going over shallow 120-190 m shelf. Be aware of realistic fake multiples in data!	tde
03/02/2010 20:20	- 56.5239	-27.493	1808.85	23.8	268.91	Deploy xbt6 south of Zavodovski Island.	tde
03/02/2010 20:30	- 56.5241	-27.523	1778.58	21.63	255.56	jr206_xbt6.asvp loaded into EM120 logging to line 82, survey jr206_e.	tde
04/02/2010 12:05	- 57.3542	-26.999	2875.55	19.8	181.11	End survey jr206_e at line 98. Start survey jr206_f. Beams in to 63 degrees.	tde
05/02/2010 19:35	- 57.5317	-26.697	2219.89	8.15	335.5	Deploy xbt 7.	tde
05/02/2010 19:49	- 57.5065	-26.72	2130.75	5.75	334.67	jr206_xbt7.asvp loaded into EM120 logging to line 33, survey jr206_f.	tde
07/02/2010 00:39	- 57.6556	-26.278	1703.27	21.1	191.29	Stop swath at line 61, survey jr206_f.	tde
08/02/2010 07:53	- 58.2671	-26.421	1914.83	10.86	245.91	Swath on, logging to line 62, survey jr206_f.	tde
09/02/2010 13:23	- 58.7435	-26.381	1578.51	18.7	122.26	Deploy xbt 8.	tde
09/02/2010 13:35	- 58.7545	-26.339	1589.36	18.38	80.46	jr206_xbt8.asvp loaded into EM120 logging to line 116, survey jr206_f	tde
09/02/2010 18:18	- 58.3686	-26.141	1145.31	18.65	171.81	Swath off.	tde
10/02/2010 03:05	- 58.3569	-26.154	956.98	21.58	177.48	Swath on, logging to line 121, survey jr206_f.	tde
10/02/2010 04:37	- 58.5198	-26.053	1992.96	20.07	166.98	Swath off at line 122, jr206_f.	tde
10/02/2010 06:16	- 58.6621	-25.649	1994.64	23.34	192.37	Swath on, logging to line 123, survey jr206_f.	tde
10/02/2010 10:50	-58.783	-26.215	1631.63	22.6	213.45	Stop survey jr206_f. Start jr206_g. At southern extent of Montagu swath.	tde
11/02/2010 16:08	- 59.0277	-26.336	557.68	15.07	287.89	Swath off at line 28, survey jr206_g. CTD trial site II.	tde

11/02/2010 17:49	- 59.0214	-26.314	843.25	9.72	94.81	Swath on, logging to line 29, survey jr206_g.	tde
12/02/2010 12:59	- 59.4248	-26.959	502.74	13.97	179.37	Possible long survey line 46, jr206_g.	tde
13/02/2010 12:46	- 59.4441	-26.952	334.08	19.43	154.46	Swath off at line 70, jr206_g: tight turn through previous swath.	tde
13/02/2010 12:48	- 59.4474	-26.949	357.15	18.94	154.66	Swath on at line 71, survey 206_g.	tde
13/02/2010 15:02	- 59.4392	-27.074	268.75	20.05	37.7	Deploy xbt 9 in caldera near Cook Island.	tde
13/02/2010 16:14	- 59.4822	-27.071	417.82	21.56	68.16	Swath off.	tde
13/02/2010 17:10	- 59.5812	-26.979	1488.52	21.64	171.26	Swath on, logging to line 76, survey jr206_g.	tde
13/02/2010 21:51	- 59.3389	-26.994	2412.75	21.8	359.6	Swath off at line 81, survey jr206_g.	tde
14/02/2010 01:23	-59.303	-26.989	1371.09	18.38	215.4	Swath on, logging to line 82, survey jr206_g.	tde
15/02/2010 02:49	- 59.6961	-26.594	2264.88	8.47	223.66	Swath off at line 107, survey jr206_g.	tde
15/02/2010 02:50	- 59.6984	-26.598	2264.41	9.19	223.42	Start logging to line 2, survey jr206_h.	tde
15/02/2010 13:20	- 60.3303	-27.15	1090.16	16.52	22.9	Deploy xbt 10, 50 miles south of Southern Thule.	tde
15/02/2010 13:29	- 60.3172	-27.14	1114.03	17.9	23.22	jr206_xbt10.asvp loaded into EM120 logging to line 13, survey jr206_h.	tde
16/02/2010 15:50	- 59.7026	-27.91	375.23	8.4	56.27	Stop EM120 as no pinging. Restart on line 40, survey jr206_g.	tde
17/02/2010 11:19	- 59.8897	-28.345	2214.25	18.31	351.52	Line 57, survey jjr206_g fails to increment.	tde
17/02/2010 12:57	- 59.7709	-27.904	1046.44	17.56	323.25	Swath off at line 59, survey jr206_g: in previously swathed area.	tde
17/02/2010 22:05	- 59.8855	-28.21	1889	17.18	245.63	Swath on, logging to line 60, survey jr206_h.	tde
19/02/2010 14:00	- 60.2193	-27.546	857.6	25	263.75	Swath off, hove to at start of fire drill.	tde
19/02/2010 14:32	- 60.2205	-27.6	770.36	28.07	262.91	Swath logging at end of fire drill.	tde
20/02/2010 10:55	- 62.5258	-22.444	5002.08	10.83	156.78	Deploy xbt 11 at northern end of Weddell Sea.	tde
20/02/2010 11:10	- 62.5472	-22.427	4989.22	13.97	157.31	jr206_xbt11.asvp loaded into EM120 logging to line 17, survey jr206_i.	tde
21/02/2010 13:52	- 67.4482	-19.581	4900.54	14.84	172.18	Deploy xbt12 in mid Weddell Sea.	tde
22/02/2010 03:11	- 69.6229	-18.639	4676.47	10.11	63.61	Swath off at line 57, survey jr206_i.	tde
22/02/2010 04:49	- 69.6402	-18.653	4672.44	14.99	168.5	Swath on: logging to line 58, survey jr206_i.	tde
22/02/2010 21:02	- 72.1572	-18.493	2837.26	5.81	191.9	jr206_xbt13.asvp loaded into EM120.	tde
23/02/2010 02:44	- 72.4467	-17.713	871.5	8.5	165.92	Swath off at line 83, survey jr206_i.	tde
23/02/2010 03:58	- 72.4511	-17.779	1039.38	8.34	51.04	Swath on, logging to line 84, survey jr206_i.	tde

23/02/2010 04:30	- 72.4428	-17.713	913.86	4.15	119.37	Swath on, logging to line 85, survey jr206_i.	tde
23/02/2010 05:23	- 72.4408	-17.713	943.73	10.9	332.21	Swath off at line 85.	tde
23/02/2010 06:16	-72.445	-17.692	797.79	6.23	115.33	Swath on, logging to line 86, survey jr206_i.	tde
23/02/2010 07:15	- 72.4896	-17.454	254.4	5.86	181.76	Swath off at line 86, survey r206_i.	tde
23/02/2010 12:14	- 72.4816	-17.467	283.48	8.48	295.96	Swath on, logging to line 87, survey jr206_i.	tde
23/02/2010 12:18	- 72.4775	-17.507	332.41	7.91	282.93	Swath off - running over previous data.	tde
23/02/2010 16:21	- 72.4538	-17.661	555.32	7.31	289.46	Swath on.	tde
23/02/2010 16:21	- 72.4537	-17.662	563.91	6.32	289.35	Swath on, logging to line 88, survey jr206_i.	tde
23/02/2010 16:44	- 72.4411	-17.726	989.33	9.58	290.31	Swath off.	tde
25/02/2010 15:10	- 72.3851	-18.285		10.88	164	Swath on, logging to line 94, survey jr206_i.	tde
25/02/2010 19:50	- 72.4873	-17.468		9.08	55.11	Swath off. Line 94, survey jr206_i.	tde
25/02/2010 20:58	- 72.4833	-17.474		8.91	39.85	Swath on: logging to line 95, survey jr206_i.	tde
25/02/2010 22:14	- 72.3685	-17.665		12.67	245.41	Hour previous to this did not record data due to maximum depth setting being set to 500m and seafloor depth exceeding that.	tde
26/02/2010 01:40	-72.453	-18.83		9.16	60.58	Swath off at line 99, survey jr206_i.	tde
26/02/2010 05:20	- 72.4778	-18.979		6.78	300.27	Swath on, logging to line 100, survey jr206_i.	tde
27/02/2010 00:02	- 74.7538	-26.128		4.12	235.37	Swath off at line 188, jr206_i.	tde
27/02/2010 05:28	- 74.7707	-26.098		5.47	238.43	Swath on, logging to line 118, survey jr206_i.	tde
27/02/2010 13:03	- 75.4777	-26.905		13.76	29.95	Swath off: line 127, survey jr206_i. At Creek 3, Halley.	tde
28/02/2010 11:08	- 75.4524	-26.846		22.63	67.52	Swath on: logging to line 128, survey jr206_i. Stooping offshore from Creek3, Halley.	tde
28/02/2010 12:18	- 75.4576	-26.953		12.92	248.28	Swath off.	tde
28/02/2010 12:18	- 75.4578	-26.956		16.72	249.49	Swath on: recording loop offshore from Creek 3, Halley.	tde
28/02/2010 21:08	- 75.4431	-26.793		22.42	106.64	Swath off.	tde
02/03/2010 13:40	- 75.4756	-26.909		7.52	263.09	Started logging to line 133, survey jr206_i	ajtate
03/03/2010 04:22	- 72.9835	-25.998		6.3	80.01	Swath stopped logging at line 148, survey jr206_i as stopped in ice.	ajtate
03/03/2010 05:53	- 72.9883	-26.009		7.27	94.35	Swath started logging to line 149, survey jr206_i	ajtate
03/03/2010 15:37	- 71.8123	-22.666		19.7	37.38	Changed sound velocity profile to jr206_xbt12.asvp as nearing mid Weddell	ajtate

						Sea area.	
05/03/2010 17:07	- 62.1344	-26.4		14.19	3.7	Changed sound velocity profile to jr206_xbt11.asvp as at northern end of Weddell Sea.	ajtate
05/03/2010 23:45	- 60.8338	-27.163		12.02	10.6	Survey jr206_i ended. New survey jr206_j started using sound velocity profile jr206_xbt10.asvp	ajtate
06/03/2010 01:35	- 60.5051	-27.081		15.02	8.22	Topas on but controlled by the SSU.	ajtate
06/03/2010 11:00	- 58.9107	-25.709		23.28	14.43	Change sound velocity profile to jr206_xbt10.asvp logging to line 14.	ajtate
06/03/2010 16:49	- 57.9684	-26.259		26.15	284.61	Swath stopped logging and off at line 19 as crossing previously swathed area to the south of Saunders Island. Topas only survey commences.	ajtate
06/03/2010 19:51	- 57.7176	-27.007		15.95	350.33	Swath on and logging to line 20 at end of Topas only survey approaching shallow seamount.	ajtate
06/03/2010 20:14	-57.627	-26.993		17.85	1.91	Change sound velocity profile to jr206_xbt9.asvp. Note to check this as xbt9 was very shallow drop into Resolution Caldera. More likely (ie should have been) xbt8.	ajtate
06/03/2010 23:07	-57.618	-27.059		11.03	35.97	Swath stopped logging and off as commencing Topas only survey over previously surveyed area to the north of Saunders Island.	ajtate
07/03/2010 02:00	-57.294	-26.623		8.23	37.17	Swath on and logging as Topas only survey finishes. Topas off.	ajtate
07/03/2010 10:53	- 55.9798	-27.156		20.63	294.13	Change to sound velocity profile jr206_xbt6.asvp logging to line 39.	ajtate
07/03/2010 15:37	- 55.4469	-28.357		25.04	260.44	Change to sound velocity profile jr206_xbt5.asvp logging to line 43.	ajtate
07/03/2010 22:41	- 54.5917	-30.096		23.15	316.63	jr206_j ended. Survey jr206_k started after crossing South Sandwich Trench using sound velocity profile jr206_xbt5.asvp	ajtate
08/03/2010 11:30	- 52.8364	-32.915		13.43	319.44	Deploy xbt14	ajtate
08/03/2010 11:45	- 52.8098	-32.953		13.35	316.3	Change to sound velocity profile jr206_xbt14.asvp. Note time approximate as not written down.	ajtate
09/03/2010 11:25	- 49.4523	-37.714		22.11	320.98	Deploy xbt15	ajtate
09/03/2010 11:32	- 49.4407	-37.728		27	317.58	Change to sound velocity profile jr206_xbt15.asvp logging to line 39.	ajtate
09/03/2010 20:18	- 48.2277	-39.568		23.98	308.52	Deploy xbt16	ajtate
09/03/2010 20:33	- 48.1964	-39.612		23.97	308.88	Change to sound velocity profile jr206_xbt16.asvp logging to line 48.	ajtate
11/03/2010 13:05	- 42.2246	-47.909		12.46	322.36	Deploy xbt17	ajtate

11/03/2010 13:17	-42.205	-47.931		3.85	320.35	Change to sound velocity profile jr206_xbt17.asvp logging to line 89.	ajtate
12/03/2010 11:45	- 38.6185	-51.776		17.1	319.53	Deploy xbt18	ajtate
12/03/2010 12:06	-38.575	-51.823		16.71	323.24	Change to sound velocity profile jr206_xbt18.asvp logging to line 112.	ajtate
12/03/2010 13:07	- 38.4163	-51.989		12.85	323.83	Swath stopped logging and off at line 114, survey jr206_k as approaching 200 mile territorial limit.	ajtate
22/02/2010 20:55	- 72.1406	-18.477	2945.38	5.79	193.17	Deploy xbt13	ajtate

Appendix 2: Plotting cruise tracks on the Helmsman display

The steps below detail how complex shapes can be transferred to the EM120 ping display window and by association the Helmsman Display on the bridge. A slightly modified series of steps is shown to transfer the same shapes into the Microplot 7 navigational software. Both processes are required to allow the Bridge Officer the ability to see areas that have already been surveyed.

Shape to Helmsman Display

- 1) Create a line or polygon shape in your favourite GIS or alternatively pick lat/lons vertices from a map and skip to step 2

1a) If only a small number of point (less than 10), use the Sketch Properties tool of ArcGIS and copy/paste longitude/latitude values into Excel or text editor.

1b) If many points export to ArcInfo Generate format using the Data Interoperability Toolbox and import that into Excel or text editor.

- 2) Using Excel or a text editor to produce a file that looks like

```
# 1
-54.249147 -36.330768
-54.249734 -36.329888
-54.249147 -36.325781
-54.245921 -36.330768
-54.249147 -36.330768
# 1
-54.249147 -36.325781 etc.
```

Latitude is followed by longitude and is space delimited. Hashes indicate a new polygon.

- 3) Save the file into the home directory of Neptune. You will need to be logged into Neptune to do this. With only a few points you could create the file directly as Neptune.
- 4) Logged in as Neptune, run the following command

```
mcoast -r 0 "text_file_name" -f "output_coastline_file_name"
```

This program creates two binary files with .cdr and .cdt suffixes. See JCR wiki for further details.

- 5) Moves these two files into:-

5a) /data/cruise/jcr/current/em120/proc/"current survey name" for Neptune applications

5b) /data1/proc/"current survey name" for EM120 acquisition applications. Moving files to this directory is best done using ftp. The EM120 server name is currently em120-101.

Note that the manual suggests that moving the files to the /shared directory should be possible and would be preferable as the polygons would be viewable by all surveys under a cruise leg but this does not appear to work.

- 6) Restarting Neptune and/or closing and restarting the ping display window of the EM120 acquisition software should automatically display the desired polygon as a coastline. Restart the Helmsman display so the bridge can see the updated coastline.

Shape to Microplot

Create the shape as step 1) above followed by

- 2) Using Excel or a text editor to produce a file that looks like

```
Microplot 7 file JR206-SSI_SWATH_04_03_2010.LIN          04/03/10
```

```
Code Colour Width Style/Mark Use      Latitude      Longitude
$
1    12    2    1    1/i  55 10.2252 S    029 23.3586 W
2    12    2    1    1/i  55 21.4192 S    029 02.7698 W
2    12    2    1    1/i  55 32.4171 S    028 48.0870 W
2    12    2    1    1/i  55 32.6715 S    028 43.5086 W
$
```

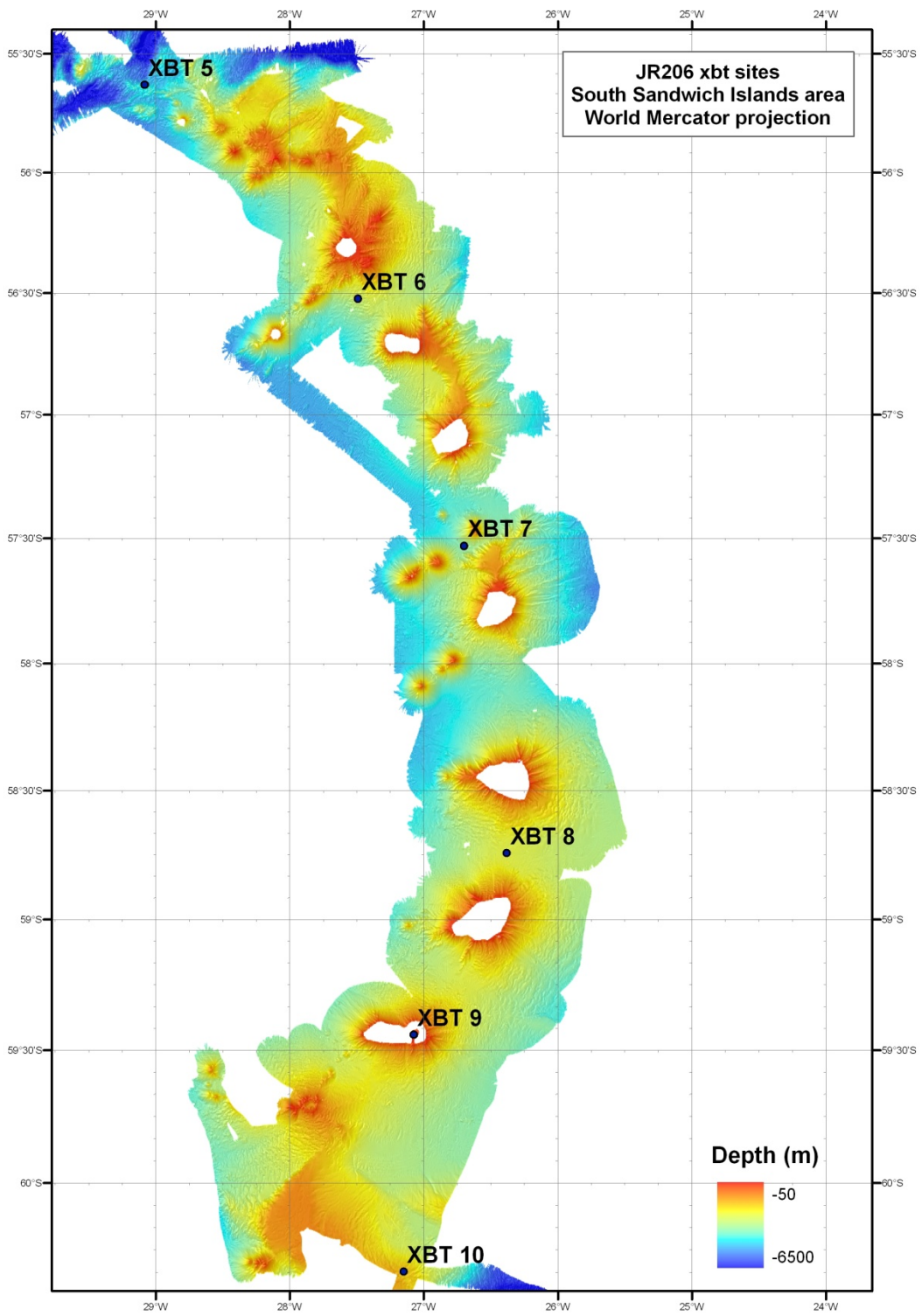
And save as "filename".T_L. All lines except for the one line header are tab delimited. Note that leading and trailing zeroes are required to maintain the latitude/longitude formatting.

- 3) Save to a memory stick or similar and take to the bridge for input into the Microplot 7 software saving the file to C:/MP7/GLOBAL.A
- 4) Using the Microplot software choose Selections > Menus & Apps > M7 Read
- 5) Choose the "Text to MP7" tab, select "line" type and locate the uploaded file. Make MP7 file.
- 6) The newly created binary file should now be available to display on the Microplot.

Appendix 3. XBT locations

Time	Latitude	Longitude	Cruise ID	Filename	Locality
18/01/2010 20:12	-51.88705	-56.77362	JR206 xbt 1	T5_00002.EDF	Off Falklands Islands
19/01/2010 12:49	-53.09269	-51.33883	JR206 xbt 2	T5_00003.EDF	Falkland Trough
20/01/2010 11:40	-54.00044	-43.88909	JR206 xbt 3	T5_00004.EDF	South of Shag Rocks
22/01/2010 12:00	-55.14532	-38.44365	JR206 xbt 4	T5_00005.EDF	South Georgia southern shelf margin
30/01/2010 09:25	-55.63069	-29.08578	JR206 xbt 5	T5_00006.EDF	30 nm north of Protector Shoal
03/02/2010 20:20	-56.52392	-27.49319	JR206 xbt 6	T5_00007.EDF	South of Zavodovski Island at 1600m depth
05/02/2010 19:35	-57.53171	-26.69741	JR206 xbt 7	T5_00008.EDF	North of Saunders Island at 2000m depth
09/02/2010 13:23	-58.74353	-26.38105	JR206 xbt 8	T5_00009.EDF	Between Montagu and Bristol Islands at 1500m depth.
13/02/2010 15:02	-59.43916	-27.07378	JR206 xbt 9	T5_00010.EDF	In caldera near Bellingshausen Island
15/02/2010 13:20	-60.33034	-27.14972	JR206 xbt 10	T5_00011.EDF	50 miles south of Southern Thule
20/02/2010 10:55	-62.52583	-22.4439	JR206 xbt 11	T5_00012.EDF	North Weddell Sea on transit to Halley
21/02/2010 13:52	-67.44818	-19.58053	JR206 xbt 12	T5_00013.EDF	Mid Weddell Sea on transit into Halley
22/02/2010 20:55	-72.14062	-18.47746	JR206 xbt 13	T5_00014.EDF	Southern Weddell Sea near deep mooring. Salinity assumed as Oceanlog
08/03/2010 11:30	-52.83635	-32.91525	JR206 xbt 14	T5_00015.EDF	ger values not obtainable.
09/03/2010 11:25	-49.45233	-37.71364	JR206 xbt 15	T5_00016.EDF	Falklands Fracture zone area
09/03/2010 20:18	-48.22767	-39.56807	JR206 xbt 16	T5_00018.EDF	North of Falklands Fracture zone area
11/03/2010 13:05	-42.22462	-47.90924	JR206 xbt 17	T5_00019.EDF	Argentine basin area
12/03/2010 11:45	-38.61846	-51.77587	JR206 xbt 18	T5_00020.EDF	Approaching South American shelf

Figure A3.1. XBT sites in the South Sandwich arc



Appendix 4. Table of TOPAS lines.

Line No.	Location	Start time (Z) dd.mm.yy 00:00	Start longitude, latitude	End time (Z) dd.mm.yy 00:00	End longitude, latitude	comments
JR206_TOPAS_01		21/01/10 10:21	-39.84891, -54.36448	21/01/10 13:48	-39.13155, -54.72127	
JR206_TOPAS_02		21/01/10 14:13	-39.07528, -54.68632	21/01/10 16:00	-39.48904, -54.50592	Run with EM120
JR206_TOPAS_03		21/01/10 16:15	-39.48332, -54.50527	21/01/10 22:27	-39.5439, - 54.54411	Perpendicular to western fault system
JR206_TOPAS_03a		22/01/10 00:11	-39.63227, -54.61651	22/01/10 01:11	-39.50063, -54.68014	Recorded in transit to line 4
JR206_TOPAS_04		22/01/10 01:43	-39.51126, -54.67722	22/01/10 03:35	-39.29345, -54.53739	
JR206_TOPAS_06		22/01/10 05:06	-39.23407, -54.78163	22/01/10 06:55	-39.02782, -54.64566	Perpendicular to western fault system
JR206_TOPAS_07		22/01/10 07:57	-39.19178, -54.79277	22/01/10 11:24	-38.40368, -55.13102	Parallel to margin through basin
JR206_TOPAS_08		22/01/10 11:47	-38.41215, -55.12666	22/01/10 12:41	-38.56791, -55.22726	
JR206_TOPAS_09		22/01/10 13:04	-38.52194, -55.23162	22/01/10 14:27	-38.84078, -55.08993	Run with EM120
JR206_TOPAS_10		22/01/10 14:44	-38.83714, -55.09932	22/01/10 17:14	-38.52297, -54.82694	
JR206_TOPAS_11	South Georgia – Southern margin	22/01/10 17:43	-38.40324, -54.86861	22/01/10 19:27	-38.6308, - 55.05007	Across basin, intersects margin in heavily scarred area
JR206_TOPAS_12		22/01/10 19:35	-38.6288, - 55.03771	22/01/10 22:15	-37.93938, -55.11124	Across basin and onto trough-mouth fan
JR206_TOPAS_13		22/01/10 22:31	-37.94961, -55.10787	22/01/10 23:18	-37.86976, -55.04497	Up fan slope
JR206_TOPAS_14		22/01/10 23:27	-37.8729, - 55.04687	23/01/10 00:34	-38.05922, -55.00124	Across upper fan
JR206_TOPAS_14a		23/01/10 00:50	-38.04676, -54.99719	23/01/10 01:33	-37.87821, -54.94543	Transit to line 15
JR206_TOPAS_15		23/01/10 01:44	-37.87934, -54.94552	23/01/10 04:34	-38.17232, -55.20047	Down strike of fan
JR206_TOPAS_16		28/01/10 22:00	-39.95055, -54.57452	28/01/10 22:41	-39.82532, -54.66556	Down slope into basin

JR206_TOPAS_17		28/01/10 22:41	-39.82427, -54.66592	29/01/10 01:34	-39.00754, -54.80566	Cross basin, proximal to western faulted area
JR206_TOPAS_18		29/01/10 01:34	-39.00621, -54.90618	29/01/10 03:30	-38.51144, -55.0155	Cross basin
JR206_TOPAS_19		29/01/10 03:30	-38.51144, -55.0155	29/01/10 05:47	-37.84876, -55.06672	Across basin and onto trough-mouth fan
JR206_TOPAS_20		29/01/10 05:47	-37.84876, -55.06672	29/01/10 07:09	-37.50909, -55.21113	Down slope from saddle to eastern basin
JR206_TOPAS_21		29/01/10 07:09	-37.508, - 55.21141	29/01/10 07:09	-36.70853, -55.35293	Run with EM120 across eastern basin
JR206_TOPAS_22		30/01/10 11:54	-28.56947, -55.7984	30/01/10 12:23	-28.48583, -55.84208	Dredge site 193
JR206_TOPAS_23		30/01/10 16:06	-28.4498, - 55.9106	30/01/10 16:20	-28.45057, -55.94833	Dredge site 194
JR206_TOPAS_23a	South Sandwich – Protector Shoal	30/01/10 21:29	-28.29152, -55.87805	30/01/10 22:08	-28.13357, -55.9684	Across possible slump on northwest aspect of Protector Shoal
JR206_TOPAS_24	Shoal	30/01/10 22:25	-28.108, - 55.95215	31/01/10 00:22	-27.9632, - 56.1145	Downslope along Protector Shoal slump feature
JR206_TOPAS_25		02/02/10 15:39	-27.88168, -55.93532	02/02/10 16:45	-28.19785, -56.02822	Across Protector Shoal slump feature
JR206_TOPAS_26		02/02/10 21:46	-28.21878, -56.1307	02/02/10 21:53	-28.22795, -56.12317	Dredge site 199
JR206_TOPAS_27		03/02/10 12:35	-27.40415, -56.25497	03/02/10 15:09	-26.76993, -56.24583	Downslope through Zavodovski sediment waves
JR206_TOPAS_28	South Sandwich	03/02/10 15:20	-26.77897, -56.24297	03/02/10 16:29	-26.83852, -56.43542	Traverses slope at distal end of sediment waves
JR206_TOPAS_29	– Zavodovski	03/02/10 16:38	-26.82457, -56.43532	03/02/10 18:23	-27.28547, -56.326	Upslope through Zavodovski sediment waves
JR206_TOPAS_30		03/02/10 18:23	-27.28575, -56.32597	03/02/10 18:59	-27.46332, -56.34438	Up stepped channel upslope from sediment waves
JR206_TOPAS_31		07/02/10 01:03	-26.29357, -57.6688	07/02/10 03:04	-25.90075, -57.5809	Downslope through gully
JR206_TOPAS_32	South Sandwich – Saunders	07/02/10 03:29	-25.8243, - 57.5989	07/02/10 05:48	-26.3009, - 57.66508	Upslope across broad ridge
JR206_TOPAS_33		07/02/10 06:12	-26.33372, -57.6165	07/02/10 07:52	-25.9986, - 57.54765	Downslope through gully
JR206_TOPAS_34	South Sandwich	07/02/10 17:44	-25.55352, -58.66505	07/02/10 19:29	-25.747, - 58.34387	Across basin to east of Montagu
JR206_TOPAS_35	– Montagu	09/02/10	-26.17105,	09/02/10	-26.15822,	Downslope along ridge

		18:33	-58.34483	20:04	-58.16947	neighbouring line 36
JR206_TOPAS_36		09/02/10 20:18	-26.2157, - 58.16958	09/02/10 21:19	-26.18482, -58.3543	Upslope within gully neighbouring line 35
JR206_TOPAS_37		09/02/10 21:31	-26.13225, -58.34997	09/02/10 22:57	-25.83247, -58.18305	Downslope through sediment waves
JR206_TOPAS_38		09/02/10 23:10	-25.84298, -58.18375	09/02/10 23:51	-25.7835, - 58.29118	Across fan structure at base of sediment waves
JR206_TOPAS_39		10/02/10 00:07	-25.78203, -58.28743	10/02/10 00:36	-25.89462, -58.33875	Upslope through sediment waves
JR206_TOPAS_40		10/02/10 00:47	-25.88812, -58.34488	10/02/10 01:34	-25.952, - 58.2316	Crosses gully upslope from fan structure
JR206_TOPAS_41		10/02/10 01:50	-25.93857, -58.2412	10/02/10 03:00	-26.14978, -58.34937	Upslope on same route as line 37 with settings for greater sediment penetration
JR206_TOPAS_42		10/02/10 03:15	-26.14013, -58.37727	10/02/10 04:06	-26.12368, -58.4698	Run with EM120, crosses gullies on upper slope
JR206_TOPAS_43		10/02/10 04:40	-26.04787, -58.52488	10/02/10 06:12	-25.65572, -58.65177	Downslope through sediment waves ending in basin to southeast of Montagu
JR206_TOPAS_44	South Sandwich	11/02/10 19:27	-26.69513, -59.15887	11/02/10 20:18	-26.86532, -59.10865	
JR206_TOPAS_45	- Bristol	11/02/10 21:07	-26.92538, -59.06225	11/02/10 23:06	-26.55818, -59.18745	Run with EM120, across glaciogenic fan structure
JR206_TOPAS_46		13/02/10 16:23	-27.03717, -59.48268	11/02/10 17:07	-26.98033, -59.57882	Downslope through sediment waves south of Bellinghausen
JR206_TOPAS_47	South Sandwich - Southern Thule	13/02/10 21:53	-26.995, - 59.33443	13/02/10 23:04	-26.89735, -59.1478	Across sediment wave glaciogenic fan boundary
JR206_TOPAS_48		13/02/10 23:11	-26.89567, -59.14725	13/02/10 01:18	-26.98437, -59.29503	Same route as line 47 with settings for greater sediment penetration
JR206_TOPAS_49		14/02/10 17:05	-27.67407, -59.61318	14/02/10 18:45	-27.14178, -59.63345	Run with EM120, across basins and sediment waves south of Southern Thule
JR206_TOPAS_50	South Sandwich - southern arc	14/02/10 18:45	-27.14178, -59.63345	14/02/10 19:06	-27.09323, -59.68167	Run with EM120, within sediment waves south of Southern Thule
JR206_TOPAS_51		15/02/10 12:59	-27.18567, -60.37817	15/02/10 17:12	-26.77312, -59.72987	Run with EM120, across basins and ridges east of Vysokaya bank
JR206_TOPAS_52		17/02/10 13:00	-27.91, - 59.7666	17/02/10 13:28	-28.0059, - 59.69915	Crosses bathymetric high on route to dredge site 200

JR206_TOPAS_53		17/02/10 16:33	-27.95375, -59.68745	17/02/10 17:06	-27.8808, - 59.67225	Recorded on approach to dredge site 201
JR206_TOPAS_54		17/02/10 17:30	-27.88072, -59.67243	17/02/10 17:47	-27.87923- 59.67467	Recorded on drege site 201
JR206_TOPAS_55		17/02/10 19:53	-27.87592, -59.68313	17/02/10 21:05	-27.97482- 59.83305	Crosses caldera and downslope through sediment waves
JR206_TOPAS_56		17/02/10 21:06	-27.97482, -59.83305	17/02/10 22:03	-28.20192- 59.88368	Down slope through sediment waves
<hr/>						
JR206_TOPAS_57		18/02/10 17:16	-27.79748, -59.986	18/02/10 18:25	-27.72257- 59.79293	Run with EM120, crosses boundary between tilted structure and sediment waves
JR206_TOPAS_58		06/03/10 01:36	-27.07917, -60.50057	06/03/10 16:49	-26.26157, -57.96798	Run with EM120 to east of arc
JR206_TOPAS_59	TOPAS lines 06 – 07 March 2010	06/03/10 16:54	-26.2859, - 57.96382	06/03/10 18:19	-26.79093, -57.9388	Run south of Saunders
JR206_TOPAS_60		06/03/10 18:19	-26.7916, - 57.93863	06/03/10 19:49	-27.00527, -57.71985	Across slope to Humpback seamount
JR206_TOPAS_61		06/03/10 23:18	-27.01515, -57.58488	06/03/10 01:57	-26.6301, - 57.29908	Northeast from Humpback seamount

Appendix 5. Details of dredges

Table A5.1. Dredge locality metadata

Table A1 below is a slightly modified version of the dredge locality metadata held in the BAS geological database. For clarity some null fields have been omitted and some column headings have been changed. Start and end dates in this context refer to the dredge reaching and leaving the seabed.

DREDGE NO	START DATE/TIME	END DATE/TIME	START LATITUDE	START LONGITUDE	END LATITUDE	END LONGITUDE	AREA	LOCATION DESCRIPTION	DREDGE STATUS	START DEPTH (m)	END DEPTH (m)	COMMENTS
DR 193	30/01/2010 13:36:25	30/01/2010 14:39:33	-55.82244	-28.51318	-55.81479	-28.52932	Protector Shoal	Floor and NW rim of inner crater of seamount PS7 (informal name in Leat et al. 2010 in review, Marine Geology) in Protector Shoal chain	Good haul. In-situ.	950	861	Variety of in-situ volcanic rocks and pumice-bearing sediment
DR 194	30/01/2010 17:56:06	30/01/2010 18:40:53	-55.92677	-28.42439	-55.92145	-28.42435	Protector Shoal	Upper slope of slide scar on SW face of seamount PS6 (informal name in Leat et al. 2010 in review, Marine Geology) in Protector Shoal chain	Good Haul.	583	450	Mainly scoriaceous volcanic rocks. Dark, sandy sediment. Evidence of biological colonisation, including starfish.
DR 195	30/01/2010 20:29:18	30/01/2010 20:56:59	-55.88269	-28.2979	-55.87958	-28.29791	Protector Shoal	Upper south-facing slope of dome-like feature . Started at top of possible land-slide feature.	Good Haul. In situ	638	434	Fresh rhyolitic pumiceous volcanic rock brought up in bucket. Dredge bag empty. Biological colonisation. No sediment.
DR 196	02/02/2010 11:48:39	02/02/2010 12:32:16	-55.93293	-27.69127	-55.92924	-27.69632	Protector Shoal	SE flank of seamount PS1 (informal name in Leat et al. 2010 in review, Marine Geology) in Protector Shoal.	Moderate Haul.	397	311	Black, fresh, glassy volcanic rocks. Dark, gritty sediment. Biological colonisation, including bivalves, starfish, deep water corals.
DR 197	02/02/2010 14:00:25	02/02/2010 14:40:59	-55.96852	-27.83799	-55.9644	-27.84217	Protector Shoal	SE flank of seamount PS2 (informal name in Leat et al. 2010 in review, Marine Geology) in Protector Shoal.	Good Haul.	645	482	Pumiceous volcanic rocks. Dark, gritty sediment.
DR 198	02/02/2010 17:35:22	02/02/2010 18:04:25	-56.0288	-28.21779	-56.02696	-28.22195	Protector Shoal	SE flank of seamount PS5 (informal name in Leat et al. 2010 in review, Marine Geology) in Protector Shoal.	Good Haul.	795	590	Pumiceous volcanic rocks. Dark, gritty sediment.
DR 199	02/02/2010 20:10:00	02/02/2010 20:37:23	-56.13515	-28.2138	-56.13285	-28.21855	Protector Shoal	Small cone south of Protector Shoal	Poor Haul	2525	2340	Eratics and brown mud only.
DR 200	17/02/2010 15:08:30	17/02/2010 15:55:00	-59.69732	-27.99871	-59.703	-27.9955	Vysokaya Bank	North flank of plateau east of main caldera	Moderate Haul.	599	395	Range of moderately altered and fresh in-situ volcanic rocks. Dark, sandy sediment. High content of bivalve shells, mostly empty and some other faunas.
DR 201	17/02/2010 17:30:00	17/02/2010 18:09:20	-59.67237	-27.88074	-59.67683	-27.87787	Vysokaya Bank	North flank of volcano outside main caldera	Very poor haul. Dredge caught on snag and one of the weak links broke.	535	331	Black, sandy sediment and some volcanic clasts.
DR 202	17/02/2010 19:06:30	17/02/2010 19:31:43	-59.67695	-27.87783	-59.67985	-27.87588	Vysokaya Bank	North flank of volcano outside main caldera. Continuation of track of DR201 upslope.	Moderate Haul.	318	201	Range of moderately altered and fresh in-situ volcanic rocks. Dark, sandy sediment.

Table A5.2. Dredge log

Table A5.2 below shows the dredge event log. Note that values such as depth, wind speed and heading are taken at a particular instance in time and maybe erroneous.

Date/Time	Latitude	Longitude	Depth - EA600	Depth - EM120	Wind Speed (knots)	Heading	Comment
30/01/2010 13:05	-55.8225	-28.5131	966.37	949.45	12.43	289.02	DR193 in water
30/01/2010 13:36	-55.8224	-28.5132	952.85	957.86	8.58	288.49	DR193 at seabed
30/01/2010 14:39	-55.8148	-28.5293	885.01	861.66	11.31	328.05	DR193 leaving seabed
30/01/2010 15:10	-55.814	-28.531	889.67	864.94	18.71	327.95	DR193 out of water
30/01/2010 17:34	-55.9268	-28.4243	578.14	581.8	22.77	347.47	DR194 in water
30/01/2010 17:56	-55.9268	-28.4244	569.45	582.88	25.66	342.91	DR194 at seabed
30/01/2010 18:40	-55.9215	-28.4244	437.8	449.59	22.18	346.17	DR194 leaving seabed
30/01/2010 19:09	-55.9215	-28.4244	0	1322.13	23.85	343.51	DR194 out of water
30/01/2010 20:07	-55.8827	-28.2979	647.1	647.08	21.65	344.37	DR195 in water
30/01/2010 20:29	-55.8827	-28.2979	633.53	636.25	29.26	345.98	DR195 at seabed
30/01/2010 20:56	-55.8796	-28.2979	433.7	431.74	20.97	330.36	DR195 leaving seabed
30/01/2010 21:09	-55.8796	-28.2979	435.11	431.7	21.38	332.21	DR195 out of water
02/02/2010 11:30	-55.9329	-27.6913	471.92	396.5	23.45	284.08	DR196 in water
02/02/2010 11:48	-55.9329	-27.6913	476.43	398.47	24.52	283.64	DR196 at seabed
02/02/2010 12:32	-55.9292	-27.6963	337.41	313.07	20.99	289.18	DR196 leaving seabed
02/02/2010 12:46	-55.9292	-27.6963	338.42	312.12	20.56	288.79	DR196 out of water
02/02/2010 13:37	-55.9687	-27.8378	666.36	651.8	23.52	296.85	DR197 in water
02/02/2010 14:00	-55.9685	-27.838	660.26	637.84	19.43	300.36	DR197 at seabed

02/02/2010 14:40	-55.9644	-27.8422	500.61	482.24	17.68	310.49	DR197 leaving seabed
02/02/2010 14:55	-55.9644	-27.8422	494.13	481.69	18.78	298.91	DR197 out of water
02/02/2010 17:03	-56.0295	-28.2164	0	797.12	18.31	328.58	DR198 in water
02/02/2010 17:35	-56.0288	-28.2178	0	736.17	20.77	332.85	DR198 at seabed
02/02/2010 18:04	-56.027	-28.222	0	583.23	18.38	329.85	DR198 leaving seabed
02/02/2010 18:20	-56.027	-28.2219	0	588.53	19.26	328.15	DR198 out of water
02/02/2010 19:17	-56.1353	-28.2136	2526.11	2525.16	22.34	349.15	DR199 in water
02/02/2010 20:10	-56.1352	-28.2138	2525.4	2531.36	22.45	347.04	DR199 at seabed
02/02/2010 20:37	-56.1329	-28.2186	2357.66	2334.8	27.49	345.23	DR199 leaving seabed
02/02/2010 21:34	-56.1329	-28.2185	2367.95	2337.94	20.38	345.49	DR199 out of water
17/02/2010 14:48	-59.6972	-27.9988	600.3	605.61	18.05	169.26	DR200 in water
17/02/2010 15:08	-59.6973	-27.9987	600.46	600.94	19.69	170.36	DR200 at seabed
17/02/2010 15:55	-59.703	-27.9955	386.78	393.66	16.61	169.76	DR200 leaving seabed
17/02/2010 16:12	-59.703	-27.9955	387.23	397.3	18.69	169.8	DR200 out of water
17/02/2010 17:09	-59.6723	-27.8808	536.05	536.07	19.75	176.54	DR201 in water
17/02/2010 17:30	-59.6724	-27.8807	534.3	468	20.86	178.2	DR201 at seabed
17/02/2010 18:09	-59.6768	-27.8779	320.78	330.64	22.31	190.73	DR201 leaving seabed
17/02/2010 18:25	-59.6768	-27.8779	317.7	331.17	19.13	192.77	DR201 out of water
17/02/2010 18:48	-59.6769	-27.8779	317.71	328.3	18.8	191.46	DR202 in water
17/02/2010 19:06	-59.677	-27.8778	312.92	325.66	19.21	192.4	DR202 at seabed
17/02/2010 19:31	-59.6799	-27.8759	202.71	199.52	18.2	198.13	DR202 leaving seabed
17/02/2010 19:40	-59.6798	-27.8759	203.26	198.87	20.45	198.25	DR202 out of water

Appendix 6. Specimen Register for dredges.

DREDGE SPECIMEN ID		COLLECTOR	SPECIMEN DESCRIPTION	REMARKS	
DR	193	1	SJD	Microgranite xenolith in grey vesicular lava, c. 1 cm across	Photo IMG_1153.jpg
DR	193	2	SJD	Small irregular pale xenolith in grey glassy vesicular lava	Photo IMG_1154.jpg
DR	193	3	SJD	Small clast of banded, likely mingled-magma rock	
DR	193	4	SJD	Grey feldspar-phyric pumice	2 clasts. Photo: IMG_1155.jpg, IMG_1156.jpg
DR	193	5	SJD	Pale altered rocks (originally dacitic?) with ferruginous and siliceous veins	6 clasts. Photos: IMG_1157.jpg, IMG_1158.jpg
DR	193	6	SJD	Pale grey (some flow banded) fresh vesicular rocks (dacitic?)	10 clasts. Photo: IMG_1159.jpg
DR	193	7	SJD	Greenish to red-brown altered pumices and vesicular rocks (dacitic?)	15 clasts. Photo: IMG_1160.jpg
DR	193	8	SJD	Grey to pale brown highly vesicular pumices	6 clasts; similar to pumice granule/sand component of DR193-19. Photo: IMG_1161.jpg
DR	193	9	SJD	Pale grey to brownish vesicular clasts, some near pumiceous (dacitic?)	10 clasts. Photo: IMG_1162.jpg
DR	193	10	SJD	Grey sub-vitreous clasts, zoned from grey cores to darker scoriaceous rims	6 clasts; Photos IMG_1163.jpg (all), IMG_1164.jpg (largest clast) and IMG_1170.jpg (6th clast)
DR	193	11	SJD	Dark grey to reddish-brown vesicular clasts (dacitic?)	19 clasts. Photos IMG_1165.jpg, IMG_1166.jpg
DR	193	12	SJD	large slightly rounded clast; dark grey scoriaceous crust, distinct darker vesicular core	Photo IMG_1167.jpg (also Photo IMG_1169.jpg. 193-12 and 193-13 together)
DR	193	13	SJD	Large angular non-vesicular clast, greenish to brown altered exterior	Photo IMG_1168.jpg (also Photo IMG_1169.jpg. 193-12 and 193-13 together)
DR	193	14	SJD	Dark grey to black, dull to subvitreous moderately vesicular lavas (dacitic?)	52 clasts, many small. Photo IMG_1171 (6 representative larger clasts)
DR	193	15	SJD	Pale grey pumiceous clasts, moderately rounded and with brown surface coating	10 clasts, mostly relatively large (2-10 cm). Photo IMG_1172.jpg
DR	193	16	SJD	Altered pale grey to reddish pumiceous to vesicular dacitic clasts, with coppery surface sheen	5 clasts; more intensely altered than 193-15. Photo IMG_1173.jpg
DR	193	17	SJD	Black, reddish-weathering slate	4 clasts (likely pieces of one clast that broke up during dredging); glacial erratic. Photo IMG_1174.jpg
DR	193	18	SJD	Subangular to rounded clasts of various low-vesicularity volcanic rocks	Possible glacial erratics, but unusual range of rock types for Antarctic. Photo: IMG_1175.jpg
DR	193	19	SJD	Coarse to fine sand grade material; mixed pumice and dark lithic grains dominant	One bag (c. 2 kgs) collected from dredge bucket.
DR	194	1	SJD	Angular clast of grey-green compact rock, possibly veined	possible erratic. Photo IMG_1176.jpg (194-1 and 194-2 together)
DR	194	2	SJD	pink granitic clast (angular)	probable erratic. Photo IMG_1176.jpg (194-1 and 194-2 together)
DR	194	3	SJD	White pumiceous clasts with brown surface alteration	3 clasts (small, 1.5 - 3 cm across). Photo IMG_1177.jpg

DR	194	4	SJD	Altered pale grey to reddish pumiceous to vesicular dacitic clast, with coppery surface sheen	Similar to 193-16. Photo: IMG_1178.jpg
DR	194	5	SJD	Altered pale grey pumiceous clasts, slightly rounded, with brown surface alteration	7 clasts (small, 2 - 4 cm across). Photo: IMG_1179.jpg
DR	194	6	SJD	Grey slightly altered pumice	16 clasts (mostly small; largest 8 cm across). Photo: IMG_1180.jpg
DR	194	7	SJD	Rounded clasts of porphyritic pumice, with dark phenocrysts	2 clasts (small). Photo: IMG_1181.jpg
DR	194	8	SJD	Vesicular to scoriaceous dark grey feldspar-phyric clasts; breadcrust surface on one side of largest clast.	4 large clasts (6 - 10 cm across). Photo: IMG_1182.jpg
DR	194	9	SJD	Scoriaceous dark clast with two vivid green megacrysts or granular aggregates visible	Possible dunite/pyroxenite microxenoliths? One large clast 13 cm x 8 cm x 8 cm. Photos IMG_1183.jpg, IMG_1184.jpg
DR	194	10	SJD	Scoriaceous dark clast with glassy bands	One large clast 10 cm x 7 cm x 6 cm. Photo: IMG_1185.jpg
DR	194	11	SJD	Clasts of black, scoriaceous fresh rock; compact rather than glassy (basaltic rather than dacitic)	332 clasts, 2 - 10 cm across but mostly small. See also 194-12. Photo: IMG_1186.jpg (representative group)
DR	194	12	SJD	Black scoriaceous fresh rocks, as 194-11 but with rust-red surface alteration on some surfaces	11 clasts, up to 12 cm across. Alteration suggests basaltic composition. Photo: IMG_1187.jpg (largest clast)
DR	194	13	SJD	Brownish altered scoriaceous clast, with possible brown/dark phenocrysts	Photo: IMG_1188.jpg
DR	194	14	SJD	Angular grey low vesicularity clasts; rather altered, with reddish surfaces	2 clasts. Photo: IMG_1189.jpg
DR	194	15	SJD	Scoriaceous to angular, dark sub-glassy clasts (dacitic?) with possible small grey phenocrysts	13 clasts, 2 - 8 cm across. Compare DR194-8. Photo: IMG_1190.jpg
DR	194	16	SJD	Black fine-grained sand	One bag (c. 1.5 kgs) collected from dredge bucket.
DR	195	1	SJD	Flow banded, sparsely vesicular near-white porphyritic dacite or rhyolite. Vesicles elongate in plane of banding	5 pieces. Photos: IMG_1191.jpg and (detail of banding in largest clast) IMG_1192.jpg IMG_1193.jpg
DR	195	2	SJD	Near white porphyritic rhyolite or dacite, more vesicular than 195-1	2 pieces. Photo: IMG_1194.jpg
DR	195	3	SJD	Grey, sugary - textured rhyolite or dacite; sparse pyroxene phenocrysts. Moderately vesicular, patches of large interconnected vesicles	9 pieces. Photos: IMG_1195.jpg and (details of interconnected vesicles) IMG_1196.jpg IMG_1197.jpg
DR	195	4	SJD	Grey, highly vesicular rhyolite or dacite with oblate vesicles (compare 195-3), some large (up to 2 cm across)	26 pieces, 10 large. Photos: IMG_1198.jpg (larger clasts) IMG_1199.jpg (smaller clasts)
DR	195	5	SJD	Grey, highly vesicular rhyolite or dacite with oblate vesicles up to 10 cm long. Similar to 195-4	1 large block 20 cm x 20 cm x 15 cm. Photo: IMG_1200.jpg
DR	196	1	SJD	Black to dark, sub-obsidianic (glassy to compact) aphyric lava; angular clasts with some conchoidal fracture surfaces.	92 clasts, 0.5 - 4 cm across; most clasts c. 1 cm across. Photo: IMG_1222.jpg (selected pieces)
DR	196	2	SJD	Black to dark, partly glassy, partly scoriaceous clasts	6 clasts only; rinds of glassy lavas fractured to produce 196-1? Clasts 1 - 3 cm across. Photo: IMG_1223.jpg
DR	196	3	SJD	Black to dark grey, weathered to brown on some surfaces, compact to scoriaceous lava. Apparently aphyric.	46 clasts, 0.5 - 5 cm across. Photo: IMG_1224.jpg (representative group)
DR	196	4	SJD	Mafic gneiss clast c. 8 cm across	Glacial erratic. Photo IMG_1225.jpg (along with 196-5 to -7)

DR	196	5	SJD	Mica schist clast c. 3 cm across	Glacial erratic. Photo IMG_1225.jpg (along with 196-4, -6, -7)
DR	196	6	SJD	Amygdaloidal lava clast c. 3 cm across	Probable glacial erratic. Photo IMG_1225.jpg (along with 196-4, -5, -7).
DR	196	7	SJD	Vesicular, strongly feldspar-phyric weathered lava clast c. 5 cm across.	Probable glacial erratic. Photo IMG_1225.jpg (along with 196-4 to -6).
DR	196	8	SJD	Brown weathered or altered pumice	One large (c. 4 cm across) and 7 small clasts. Similar material abundant in sand (DR196-12). Photo IMG_1226.jpg
DR	196	9	SJD	Fresh grey pumice	One small (1.5 cm across) pumice. Photo IMG_1227.jpg. Placed in same bag as DR196-8 (see photos for distinction)
DR	196	10	SJD	2 cm long solitary coral (hard skeleton only) attached to sub-glassy dark grey lava clast only 1 cm across.	Photo IMG_1228.jpg (with 196-11)
DR	196	11	SJD	Disarticulated bivalve shells, 1 - 3 cm across. 4 well-preserved, one heavily encrusted.	Photo IMG_1228.jpg (with 196-10)
DR	196	12	SJD	Mixed, poorly sorted sand including (dominant) dark angular glassy to vesicular grains, also brown altered pumice grains	sample c. 2kg (wet) in weight
DR	197	1	SJD	Altered pumices with brown to black (manganiferous?) surface coatings.	Large clasts up to 30 cm across; 13 pieces including 2 pieces broken off other clasts during sorting. Photo IMG_1229.jpg SAMPLES IN 4 BAGS
DR	197	2	SJD	Small clasts of altered pumice with brown to black (manganiferous?) surface coatings as DR197-1	33 pieces. Photo: IMG-1230.jpg
DR	197	3	SJD	Pumice clasts with extensive and thick black (manganiferous?) surface coatings that also extend into interior as surface layer. Elongate vesicle fabric in most pieces.	19 pieces, 3 - 15 cm across. Photo: IMG_1231.jpg
DR	197	4	SJD	Moderately fresh grey pumice with patchy brown surface coatings only. Mostly small clasts; larger clasts (up to 15 cm across) notably rounded.	43 pieces. Photo: IMG_1232.jpg (5 largest clasts with distinctly rounded shape)
DR	197	5	SJD	moderately fresh grey pumice with patchy brown surface coatings only, as DR197-4 but with dark angular enclaves.	3 pieces. Photo IMG_1233.jpg (showing enclaves)
DR	197	6	SJD	Small blocky angular clasts of dark non-vesicular volcanic rock (see also DR196-1)	16 pieces, 1 - 3 cm across. Photo: IMG_1234.jpg
DR	197	7	SJD	Angular clasts of compact, low-vesicularity, dark to brown-weathering volcanic rock; indistinct feldspar phenocrysts visible in some clasts	101 pieces, mostly < 3 cm but a few up to 8 cm across. Photo: IMG_1235.jpg (5 representative pieces)
DR	197	8	SJD	Vesicular to scoriaceous dark, brown-weathering volcanic rock. Larger clasts tend to be flat or slabby, suggesting internal microfabric	23 pieces, 2 - 10 cm across. Photo: IMG_1236.jpg (4 representative pieces)
DR	197	9	SJD	Small rounded pebbles of compact, fine-grained (volcanic?) rocks, one with partially dissolved veins.	6 pieces. Probable glacial erratics. Photo: IMG_1237.jpg DR197-9 to -15 all in one bag.
DR	197	10	SJD	Small clasts of green coarse sandstone with prominent quartz grains.	3 clasts. Glacial erratics. Photo: IMG_1238.jpg DR197-9 to -15 all in one bag.
DR	197	11	SJD	Small reddish granular clasts - probable coarse sandstone?	2 clasts. Probable glacial erratics. Photo: IMG_1239.jpg DR197-9 to -15 all in one bag.
DR	197	12	SJD	Laminated to slaty mudstones	8 clasts. Glacial erratics. Photo: IMG_1240.jpg DR197-9 to -15 all in one bag.
DR	197	13	SJD	Flat clast of slightly micaceous dark sandstone, c. 7 cm across	Glacial erratic. Photo: IMG_1241.jpg DR197-9 to -15 all in one bag.
DR	197	14	SJD	Angular clast, c. 5 cm long, of dark grey siliceous rock.	Possibly quartzose siltstone or volcanic rock with siliceous alteration. Probable glacial erratic.

					Photo: IMG_1242.jpg DR197-9 to -15 all in one bag.
DR	197	15	SJD	Angular clasts of strongly indurated greenish quartzitic sandstone	2 clasts (one c. 10 cm across, other ~ 2 cm across). Glacial erratics. Photo: IMG_1243.jpg DR197-9 to -15 all in one bag.
DR	197	16	SJD	Poorly sorted dark sand and silt	sample c. 2-3kg (wet) in weight
DR	198	1	SJD	Slightly vuggy-vesicular pale greenish grey sparsely porphyritic rock, probable rhyolite, with dark manganiferous surface coating and surface layer alteration.	8 pieces, most of which appear to fit together to form parts of a single block that disintegrated in the dredge. Photo: IMG_1244.jpg
DR	198	2	SJD	Pale grey fresh (brown surface alteration only) vesicular to pumiceous rock, probable rhyolite, larger clasts with weak flow banding and strongly elongate vesicles	32 mostly small pieces (note counting error on slip in photo). Photo: IMG_1245.jpg
DR	198	3	SJD	Pale grey vesicular to pumiceous rock, probable rhyolite as DR198-2, but with dark manganiferous surface coatings and surface layer alteration on some surfaces	54 mostly small (<4 cm across) pieces. Photo: IMG_1246.jpg (representative pieces).
DR	198	4	SJD	Varied but distinctively greenish - altered pumiceous to platy low-vesicular clasts, probable rhyolite	12 pieces; 9 small, 2 - 6 cm across (Photo: IMG_1247.jpg) and 3 larger (Photo: IMG_1248.jpg)
DR	198	5	SJD	Intensely altered, moderately vesicular pumiceous clasts with strongly developed black manganiferous crusts	40 pieces (many more dumped because of alteration - dominant rock type in dredge). Photo: IMG_1249.jpg (representative clasts)
DR	198	6	SJD	As DR198-5, but more strongly and coarsely pumiceous.	11 pieces (many more dumped; second most common rock type in dredge). Photo: IMG_1250.jpg
DR	198	7	SJD	Blocky, low vesicularity to scoriaceous dark lava clasts	11 small clasts. Too dense to float (along with DR198-1); likely part of local edifice under drape of pumices. Photo: IMG_1251.jpg
DR	198	8	SJD	Large block of veined and jointed black siltstone	Glacial erratic. Photo: IMG_1252.jpg
DR	198	9	SJD	Small and varied clasts including rounded pebbles, a granitic gneiss clast, and a veined altered rock (sandstone?)	Probable glacial erratics. Photo: IMG_1253.jpg
DR	198	10	SJD	Sieved sand to granule grade material, mostly 1-5 mm grain size. Pumiceous, dark volcanic and red scoriaceous clasts	Sieved using 1 mm mesh sieve to remove abundant mud.
DR	199	1	SJD	Cohesive greenish to grey green mud, intensely distorted by dredging, with sand filling small burrows in mud.	2 cakes extracted from dredge bucket and stored in plastic box
DR	199	2	SJD	Dark fine grained compact rock (volcanic?)	2 clasts 5 and 2 cm across. Probable glacial erratics, extracted from remainder of mud in dredge bucket. Photo: IMG_1254.jpg In one bag with DR199-3
DR	199	3	SJD	Greenish - grey dark compact crystalline rock (dolerite?)	1 clast 2 cm across. Probable glacial erratic, extracted from remainder of mud in dredge bucket. Photo: IMG_1254.jpg In one bag with DR199-2
DR	200	1	SJD	Strongly feldspar-phyric porphyry clasts: subhedral white feldspars (1-5 mm) in grey groundmass. Non-vesicular and compact to moderately vesicular; partial black (manganiferous?) surface coatings	1 large block 25 cm x 15 cm x 10 cm, and 15 smaller pieces 4 - 12 cm across. Photos: IMG_1797.jpg to IMG_1800.jpg (1799 is detail of cleanest clast)
DR	200	2	SJD	Angular compact to amygdaloidal fine grained volcanic rocks with greenish groundmass under well developed black surface coatings. Some clasts appear to have sparse dark phenocrysts	18 clasts (largest 12 cm x 6 cm x 6 cm, smallest < 2 cm). Photo IMG_1801.jpg
DR	200	3	SJD	Vesicular to scoriaceous volcanic rocks, with thick black (manganiferous?) coatings	Need to be split or sawed for identification. 13 clasts, largest 8 cm across, most 2 - 5 cm. Photo: IMG_1802.jpg
DR	200	4	SJD	Red oxidized scoria	One clast only, 8 cm x 4 cm x 4 cm. Photo IMG_1803.jpg

DR	200	5	SJD	Compact angular fine-grained volcanic rocks, with thick black (manganiferous?) coatings	Need to be split or sawed for identification. 8 small clasts, 1.5 - 4 cm across. Photo: IMG_1804.jpg
DR	200	6	SJD	Reddish to dark-coated volcanic rocks, with moderately vesicular or scoriaceous surfaces, compact cores. Reddish colour suggests altered, more mafic compositions	6 clasts, largest 8 cm x 7 cm x 6 cm. Photo: IMG_1805.jpg
DR	200	7	SJD	Micro(grano)diorite to granitic rocks with greenish hue, partial black (manganiferous) surface coatings. Subrounded to angular clasts.	5 clasts; largest 20 cm x 10 cm x 10 cm, others 2 - 8 cm across. Glacial erratics. Photos: IMG_1806.jpg and IMG_1807.jpg
DR	200	8	SJD	Disarticulated bivalve shells, 2- 4 cm across. Some fresh and well-preserved, others brown - coated with borings. Appears to be a monospecific assemblage.	22 valves in sample; many more live and dead, disarticulated shells discarded from dredge. Photo: IMG_1808.jpg
DR	200	9	SJD	Coarse sand (mostly lithic, with a few shell fragments); brown mud washed out of weave sample bag	c. 3 kg of material
DR	201	1	SJD	Small clasts of black vesicular to scoriaceous volcanic rock, apparently fresh (not coated). Aphyric.	17 clasts, largest only 4 cm across (several < 1 cm). Photos: IMG_1809.jpg and IMG_1810.jpg (detail of largest clast)
DR	201	2	SJD	Greenish, fine-grained, microvesicular volcanic rocks of notably low density	3 clasts, < 1 cm to 3 cm across. Photo: IMG_1811.jpg
DR	201	3	SJD	Leucogranite with greenish dioritic enclave	Glacial erratic. Angular clast 4 cm across. Photo IMG_1812.jpg (with 201-4)
DR	201	4	SJD	Reddish weathered black shale or slate (see also DR193-17)	2 flakes, few cm across. Glacial erratic. Photo IMG_1812.jpg (with 201-3)
DR	201	5	SJD	Black coarse sand (sieved from bucket sample)	c. 250 g only.
DR	202	1	SJD	Dark scoriaceous to compact, blocky very fine grained volcanic rocks (some sub-vitreous, others microvesicular). Aphyric and apparently fresh (similar to DR201-1).	45 clasts, 1 - 6 cm across. Photo: IMG_1816.jpg (8 representative clasts)
DR	202	2	SJD	Greenish fine grained, compact to microvesicular to vesicular rocks with well developed dark (manganiferous?) surface coatings. Possibly similar to DR201-2	3 clasts (one flat clast broken in two), all relatively large: 9 x 7 x 5 cm; 7 x 5 x 5 cm; 15 x 10 x 2 cm (in two halves). Photo: IMG_1817.jpg
DR	202	3	SJD	Siliceous, white to greenish banded rock with altered feldspar phenocrysts (silicified flow-banded rhyolite?)	1 small clast, c. 5 cm x 1 cm. Might be glacial erratic or hydrothermally altered volcanic rock. Photo: IMG_1818.jpg
DR	202	4	SJD	Brownish - grey altered obsidianic volcanic glass	1 small clast (2 x 3 cm). Hydrothermally altered? Photo IMG_1819.jpg (with 202-5)
DR	202	5	SJD	Greenish microvesicular pumiceous rock (similar to DR201-2)	1 small clast only (c. 1 cm across). Photo IMG_1819.jpg (with 202-4)
DR	202	6	SJD	Disarticulated bivalve valves, 1 fresh, 1 brown-coated	2 valves, 2 - 3 cm across. Photo IMG_1820.jpg
DR	202	7	SJD	Coarse poorly sorted sand and fine gravel, mostly black lithic grains plus some shell fragments. Brown mud washed out of sample through weave bag.	c. 0.5 kg weight

Appendix 7. Maps showing proposed new feature names in the South Sandwich Islands.

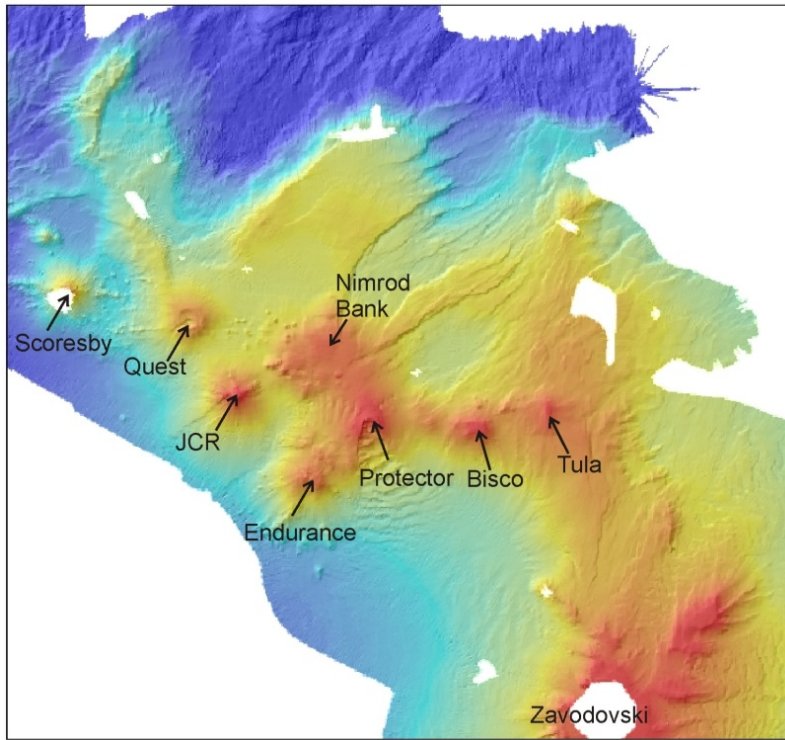


Figure A7.1. Map of Protector Seamounts showing proposed names.

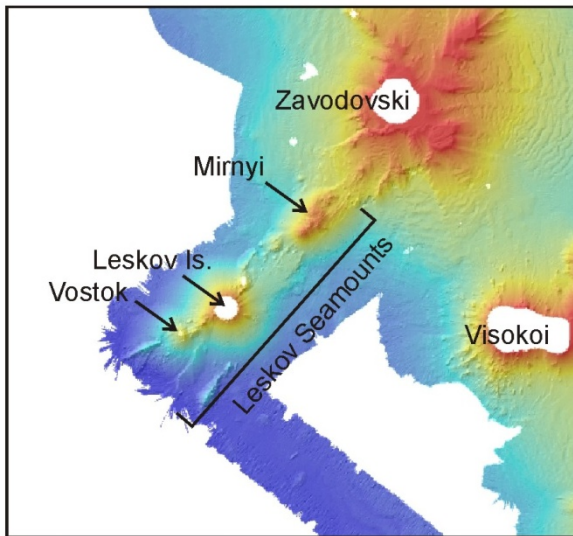


Figure A7.2. Map of Leskov Seamounts showing proposed names.

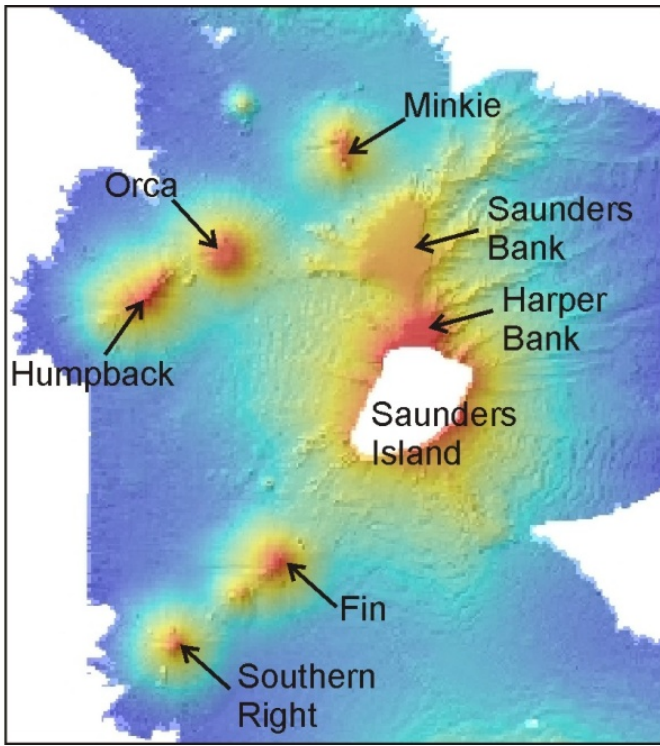


Figure A7.3. Map of the area around Saunders Island showing proposed names.

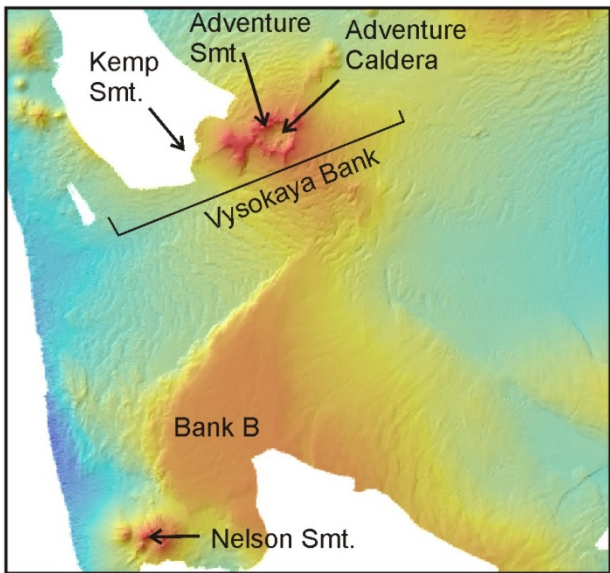


Figure A7.4. Map of the area around Vysokaya Bank showing proposed names.